DEVELOPMENT AND CHARACTERIZATION OF HIGH-PERFORMANCE FUNCTIONALIZED MEMBRANES FOR ANTIBODY ADSORPTION

by

JAYRAJ SHETHJI

STEPHEN M.C. RITCHIE, Ph.D., COMMITTEE CHAIR
PETER E. CLARK, Ph.D.
CHRISTOPHER S. BRAZEL, Ph.D.
YUPING BAO, Ph.D.
DAVID E. NIKLES, Ph.D.

A DISSERTATION

Submitted in partial fulfillment of the requirements
for the degree of Doctor of Philosophy in the
Department of Chemical and Biological
Engineering in the Graduate School of
The University of Alabama

TUSCALOOSA, ALABAMA

2012

ABSTRACT

Capacity and selectivity are the major bottlenecks for the development of affinity membrane adsorbers for protein and antibody purification. The focus of this doctoral research is to develop polyethersulfone (PES) microfiltration (MF) membranes containing multiple highly selective poly(styrene-co-hydroxystyrene) grafts mimicking the key dipeptide Phe-132/Tyr-133 motif of ligand protein A to selectively adsorb immunoglobulin G (IgG) under convective flow conditions.

This research work consists of two phases. In phase 1, homopolymer and block copolymer grafts were synthesized and characterized in the membrane pores using monomers styrene, ethoxystyrene, and chloromethylstyrene. ^{1}H NMR characterization showed successful incorporation of the sequential stages of graft chemistry, including: polystyrene, poly(chloromethylstyrene), poly(ethoxystyrene), poly(styrene-b-ethoxystyrene), and poly(styrene-b-chloromethylstyrene). A study of monomer reactivity showed that chloromethylstyrene reacted approximately 1.3 times slower than styrene and ethoxystyrene during formation of homopolymers and block copolymers. The ion-exchange capacity of sulfonated functionalized membranes was 4.9 meq/g with as many as 125 repeat units per chain.

In phase 2, PES MF membranes tailored with two different graft chemistries including poly(styrene-co-hydroxystyrene) and glycine functionalized poly((styrene-co-hydroxystyrene)-b-chloromethylstyrene) grafts were developed and tested for selective IgG adsorption. ^{1}H NMR characterization confirmed membrane pore functionalization by poly(styrene-co-hydroxystyrene), chloromethylstyrene block addition, and subsequent glycine functionalization

of the chloromethyl block. The dynamic binding capacity (DBC) for IgG was as high as 95 mg/ml, more than 9 times as compared to Sartobind® and Ultrabind® membranes and twice as compared to affinity resin. The DBC was independent of flow rate and there was no significant loss (<5%) in capacity at higher linear velocities (230 cm/h) indicating that the transport of IgG to the adsorptive sites is predominantly by convection. Bind and elute experiments showed that there was no significant loss of DBC over a period of five cycles and the average recovery of antibody was >94%. Competitive sorption using membranes containing negatively charged spacer arms showed that the membrane was ~11 times more selective for IgG than BSA. Additionally, the DBC was 22% higher (115 mg/ml) than without spacer arms indicating that the negatively charged spacer arms moved the grafted chains apart and improved the accessibility of IgG to the binding sites.

ACKNOWLEDGEMENTS

The author wishes to express his solemn gratitude to Dr. Stephen Ritchie for his support, counseling and patience throughout the period of research. The author would also like to thank him for showing faith in abilities and giving independent responsibilities and opportunities to attend professional society annual conferences. The author enjoyed working with him and learning from him, and his editorial help in the preparation of this manuscript is greatly acknowledged. Gratitude is also extended to other members of the supervisory committee, including Dr. Christopher S. Brazel, Dr. David E. Nikles, Dr. Peter E. Clark, and Dr. Yuping Bao, for their supervision, interest and insightful suggestions in this work.

The author is thankful to the faculty, staff and graduate students of Department of Chemical and Biological Engineering for making this research journey an enjoyable experience. The author would also like to thank Dr. Soubantika Palchoudhury for her help and support. Help from Ryan Beam and Lukai Yang from the membrane research group is also acknowledged. The author is also thankful to Ms. Inge Archer and Ms. Susan Noble for completing administrative formalities, placing purchase orders for laboratory work, and making several travel arrangements for technical conferences. Gratitude is extended to Dr. Ken Belmore (NMR facility manager, The University of Alabama) for his help in performing the ^{1}H NMR characterization. Many thanks to Dr. Laura S. Busenlehner and Dr. Patrick A. Frantom for letting me use the HPLC instrument and separation column in their laboratory. Additional thanks to Ms. Leslie Gentry for her assistance with the SEC measurements. The financial support from the National Science

Foundation (NSF award number CBET-0756460) and the Department of Chemical and Biological Engineering is also gratefully acknowledged and appreciated.

Finally, the author expresses gratitude to his parents Kanan Shethji and Kirit Shethji, sister Hemali Bareilia, and wife Nikita Kansara for their continuous encouragement and support.

CONTENTS

LIST OF TABLES

LIST OF FIGURES

CHAPTER 1
INTRODUCTION

1.1 Technological background

Packed bed chromatography is the most common downstream process in the biotechnology industry for purification of proteins and antibodies [1-8]. Although this process provides an excellent degree of purity (>95%) and reproducibility, there are areas which need improvement such as high cost and low-throughput [7, 9-13]. Scale up to large diameter chromatography columns presents numerous problems including process complexity, high cost, and complex process control required to achieve good isolation of biological molecules (enzymes, proteins and antibodies). Therefore, large scale purification of proteins and antibodies is a major challenge faced in downstream processing in the biotechnology industry.

Membrane chromatography is an excellent alternative to lower cost and improve throughput [9, 13-21]. This is due to adsorption sites immobilized in large pores (0.1-1 μm) and dominance of convective mass transport eliminating protein transport diffusion limitations [13-14, 22-24]. This reduces processing times and recovery volumes. Economic comparison of the two technologies showed that the total cost of membrane chromatography is one-third of traditional resin columns [25]. The large and open pore structure also allows the capture of large biomolecules (>150 kDa) such as immunoglobulin G (IgG) due to improved accessibility to protein binding sites. Additionally, scale-up in membrane chromatography is relatively easy and can be achieved by increasing the membrane surface area either by providing stack of membrane or increasing the cross-sectional area for flow [13]. Conventional membrane adsorbers have a low dynamic binding capacity (DBC) due to low internal surface area (1%) relative to affinity chromatography media (porous beads) [6]. To address this problem, many researchers have changed the membrane pore surface chemistry by grafting polymer brushes in membrane pores

to allow multilayer protein adsorption [14-15, 22, 26-33]. The functionalized membranes have relatively large internal surface area for binding due to more adsorption sites per unit area compared to conventional membrane adsorbers and is in the range of 4-30 m^2/g [4]. Additionally, the advantage of functionalized membranes is that the adsorption sites are located on each repeat unit of the grafted chains which increases the sorption capacity by several orders of magnitude compared to protein A ligands.

A wide range of polymeric membrane substrates have been functionalized by activation of the pore surface to develop protein adsorbing membrane adsorbers. Examples include polysulfones, regenerated cellulose, polyethylene, and polyvinylidene fluoride [26, 30, 34-35]. The incorporation of functional groups into the membrane pores via polymer grafting can occur via a variety of functionalization techniques including: radiation-induced grafting (UV radiation, γ-radiation or electron beam), plasma-induced grafting, and chemical grafting (cationic, anionic or free radical polymerization) [30, 34-43]. For example, Husson and coworkers prepared high capacity (130 mg BSA per ml of membrane) anion-exchange membranes by grafting poly(2-dimethylaminoethyl methacrylate) into regenerated cellulose membranes via surface-initiated atom transfer radical polymerization [14]. The negatively charged bovine serum albumin (BSA) molecule binds to the positively charged membrane adsorber (weak anion-exchange). Another example is the preparation of high capacity anion-exchange membranes that were synthesized by immobilization of poly((2-(methacryloyloxy)ethyl)-trimethylammonium chloride) into the entire pore surface of hydrophilized polypropylene membranes via photo-initiated graft polymerization technique. Model proteins pure BSA and tripsin inhibitor used in their work were negatively charged and were adsorbed by the positively charged membrane. They reported binding capacities as high as 80 mg/ml and 120 mg/ml for BSA and tripsin inhibitor, respectively [44].

Another noteworthy example is grafting of glycidyl methacrylate (followed by chemical modifications) into the pore surface of polyethylene hollow fiber membranes by radiation-induced graft polymerization for separation of gelsolin from bovine plasma [45]. The selective site in the membrane bed was positively charged to achieve separation of negatively charged bovine plasma. Adsorbed gelsolin was selectively eluted using calcium chloride. In the present work, a controlled/living sequential cationic polymerization technique was used to develop a novel synthetic polymeric brush containing multiple binding sites analogous to the phenylalanine-132/tyrosine-133 (Phe-132/Tyr-133) dipeptide structure of protein A ligand for IgG adsorption.

Affinity purification of IgGs using synthetic ligands immobilized on porous beads has been reported in literature [46-48]. However, investigation of polymeric membranes containing immobilized synthetic mimetic ligands for purification of IgGs is a relatively novel area of research [12, 49]. For example, A2P, a synthetic ligand obtained from triazine scaffold immobilized on regenerated cellulose membrane has been shown to successfully bind with the Fc region of IgG. Another example is immobilization of TG19318 synthetic ligand onto modified polyethersulfone membrane to capture IgG. However, the binding capacity in this case is relatively low (4-12 mg/ml) [49].

The novel aspect of this research is membrane pores were functionalized with a synthetic polymeric brush containing multiple binding sites analogous to Phe-132/Tyr-133 (Figure 1-1) dipeptide motif of ligand protein A for adsorption of IgG under convective flow conditions. The objective of this research work is to develop a high capacity, highly selective functionalized membrane for adsorption of IgG. Hydrolyzed poly(styrene-co-ethoxystyrene), also called

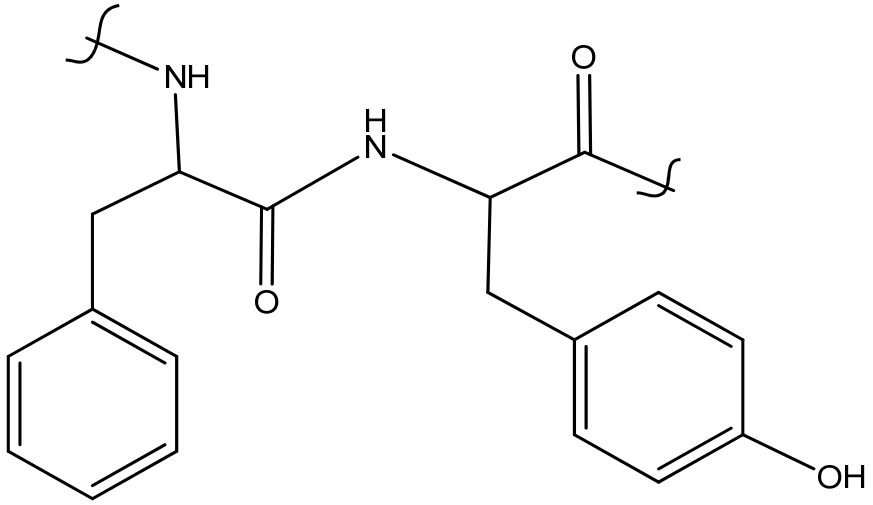

Figure 1-1. Phenylalanine-Tyrosine (Phe-132/Tyr-133) dipeptide structure of protein A ligand with affinity for IgG.

poly(styrene-co-HS), was grafted in the pores of microfiltration (pore size 220 nm) polyethersulfone (PES) membrane by surface-initiated cationic polymerization. The copolymer mimics the Phe-132/Tyr-133 dipeptide structure of protein A ligand which has been shown in the literature to selectively bind with the Fc region of IgG [50-51]. Figure 1-2 (a) shows the PES membrane cross section including the membrane pores and the shaded solid region. The pores of the membrane contain multiple polymeric grafts. Figure 1-2 (b) shows the representative polymeric grafts adjacent to the initiator by zooming in the pores of membrane. Each polymeric graft contains multiple binding sites. Each binding site has heterogeneous functional groups (phenyl, hydroxyl and chloromethyl) derived from the monomers styrene, ES and CMS. The pattern of each binding site shows that the side chain functionalities of the Phe-132/Tyr-133 dipeptide structure were represented by an adjacent hydroxyl substituted phenyl ring and an unsubstituted phenyl ring of the copolymer. The polychloromethylstyrene (poly(CMS)) grafts on each binding site were reacted with glycine to impart an overall negative charge to the grafted chain. The negatively charged membrane will be used during competitive sorption in presence of generic molecule BSA. The negatively charged glycine functionalized chloromethyl spacer arms will keep the grafted chains apart, improve binding site accessibility, and prevent steric hindrance and antibody denaturing.

1.2 List of research objectives

The overall objective of this research is to develop and characterize a microfiltration (220 nm pore size) PES membrane containing poly(styrene-co-HS) grafts for adsorption of IgG. A simple surface-initiated living sequential cationic polymerization technique was used to incorporate polymeric grafts in the membrane pores. This objective was realized in two phases. In phase 1, homopolymer and block copolymer grafts using three separate monomers of styrene

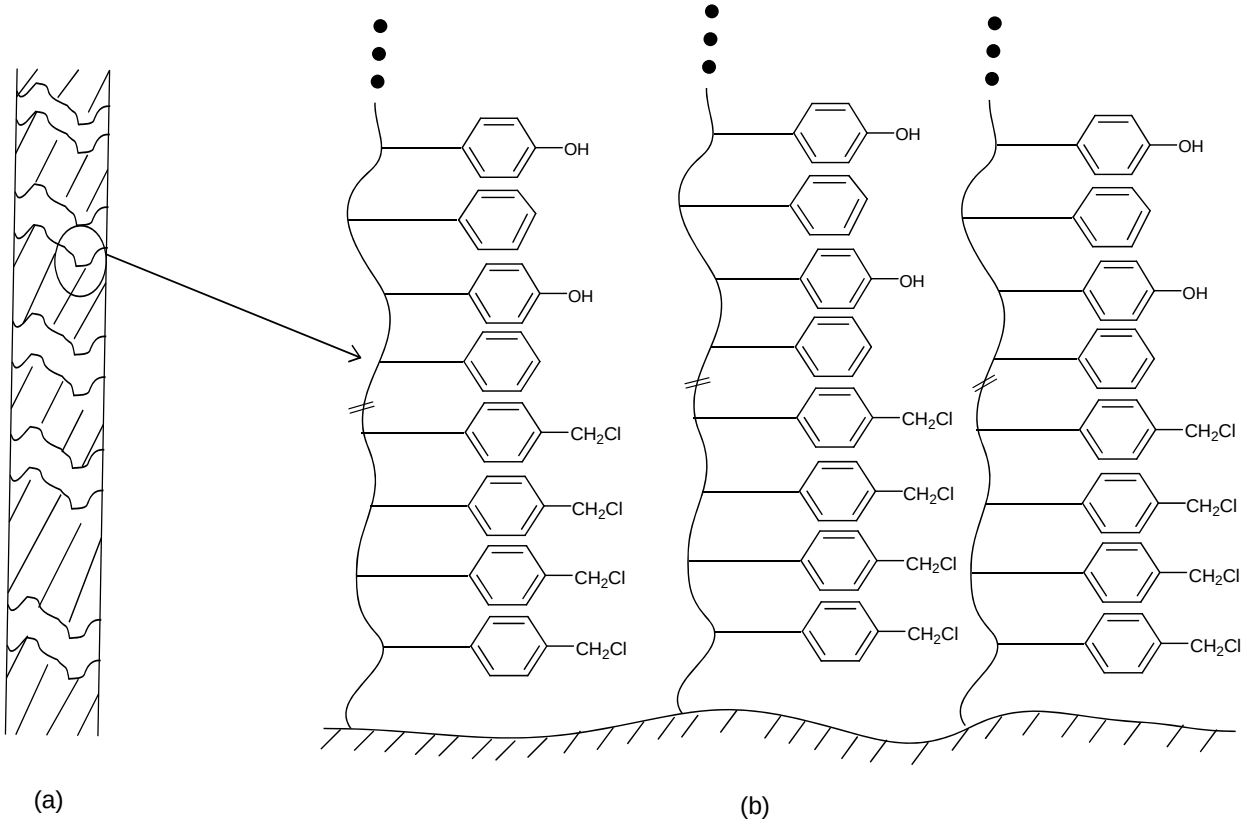

Figure 1-2. Schematic of (a) PES membrane cross-section, and (b) representative polymer graft with multiple binding sites showing ideal pattern of each binding site adjacent to the initiator. The adjacent phenyl ring and hydroxyl substituted phenyl ring will give an analog of Phe-132/Tyr-133. The chloromethylstyrene (CMS) will be reacted with glycine to provide negatively charged spacer arms.

and substituted styrenes (CMS, 4-ethoxystyrene (ES)) were synthesized and characterized in the membrane pores. In phase 2, customized block copolymers grafts of poly(styrene-co-HS) were incorporated in the membrane pores and the performance of the membrane was tested for selective IgG adsorption. These objectives were realized through the following steps.

Phase 1:

- Immobilize initiator sulfonic acid groups for cationic polymerization of styrene and substituted styrene monomers (CMS, ES) in the membrane pores.
- Determine ion-exchange capacity (IEC) of grafted membrane.
- Synthesize poly(styrene), poly(CMS), and poly(ES) homopolymer in the pores of PES MF membranes.
- Synthesize poly(styrene-b-CMS) and poly(styrene-b-ES) block copolymer in the membrane pores by surface-initiated living sequential cationic polymerization technique.
- Study controlled polymer growth. Polymer growth aspects like kinetics of monomer reacted, IEC, and graft length were studied with respect to parameters such as initiator contact time and monomer feed concentration.
- Curve fit experimental monomer reaction kinetic data with the pseudo-first order model and determine model parameters.
- Thorough characterization of composition of homopolymer and block copolymer grafts at each stage of functionalization.

Phase 2:

- Synthesize membranes containing customized poly(styrene-co-HS) grafts mimicking Phe-132/Tyr-133 dipeptide structure of protein A.
- Test the performance of the functionalized membrane for IgG binding capacity.

- Determine DBC with respect to parameters like antibody feed concentration, flow rate, and polymerization reaction time.
- Perform cycles of binding, washing, elution, and regeneration on the same membrane and determine the average recovery.
- Incorporate negatively charged glycine functionalized poly(CMS) spacer arms into the poly(styrene-co-HS) grafted membrane.
- Perform competitive sorption in presence of BSA using the negatively charged membrane and determine the DBC of IgG in presence of negatively charged spacer arms.
- Curve fit experimental antibody adsorption data with the Langmuir adsorption model and determine model parameters.
- Thorough characterization of poly(styrene-co-HS) and subsequent addition of glycine functionalized poly(CMS) grafts into the functionalized membrane.

1.3 Approach

Commercially available microfiltration PES membrane was modified by simple surface-initiated sequential cationic polymerization of styrene and substituted styrene monomers (CMS and ES). Homopolymer and block copolymers were formed in the membrane pores. Permeability studies at each stage were performed to give preliminary evidence of formation of grafts. The ion-exchange capacities of sulfonated and grafted membrane were determined after each stage of modification. The amount of monomers reacted and retained on the membrane were quantified and characterized using analytical techniques like UV-vis and gas chromatography. Finally, polymerization reactions kinetics were studied to understand controlled polymer growth.

The incorporation and composition of block copolymer grafts and moiety stabilities were characterized by proton NMR. Gas chromatography was used to quantify the amount of each

monomer that was reacted and retained on membrane. The functionalized membrane was then used for IgG adsorption. IgG adsorption was determined in terms of DBC from the breakthrough curve. An experimental adsorption isotherm was generated and data were curve fitted with the Langmuir model. Control experiments were performed to understand the influence of flow rate and polymerization reaction time on DBC. DBC (adsorbed and eluted) and average recovery were determined over a period of five cycles of binding, elution and regeneration.

A block of glycine functionalized poly(CMS) was grafted into the functionalized membrane to incorporate negatively charged spacer arms to the grafted chain. The negatively charged functionalized membrane was used to test the selectivity of membrane by performing competitive sorption in presence of BSA. The effect of spacer arms on DBC was also investigated. An overall mass balance on feed and permeate solutions was used to quantify the amount of antibody adsorbed by the membrane using UV-vis spectroscopy. Size exclusion chromatography was used to separate IgG and BSA and measure the concentration of each antibody during competitive sorption studies. The contributions from this research provide insights into applications of synthetic affinity ligand membrane adsorbers for low-cost and large scale purification of antibodies in downstream biotechnology industry.

CHAPTER 2
BACKGROUND AND THEORY

2.1 Introduction

This dissertation describes the development and characterization of high capacity functionalized membranes containing multiple synthetic polymeric binding sites based on the Phe-132/Tyr-133 motif of protein A for adsorption of IgG. The results of this research will improve fundamental understanding of two aspects: first, development of functionalized membrane containing polymeric grafts by surface-initiated living cationic polymerization using different monomers, and second, use of functionalized membranes as membrane adsorbers in membrane chromatography. In order to gain a better understanding of this work, it is essential to know the background of monoclonal antibodies, affinity chromatography, membrane chromatography, affinity membranes, functionalized membranes, polymer brushes, chemical techniques for immobilization of polymeric brushes, and binding chemistry of IgG and protein A. Reviewing the theory and research work published in the literature in all these areas will form a better understanding of this contribution.

2.2 Monoclonal antibodies (MAbs)

2.2.1 Definition

MAbs are monospecific antibodies produced in the laboratory from the same immune cells that are all clones of a single hybrid cell [52]. Immune cells are involved in defending the body against bacteria, viruses, diseases and other foreign invaders like parasites. The first important characteristic of MAbs is they are extremely specific; that is, each antibody binds to and attacks one particular antigen (virus, disease-causing bacteria, and infectious agent). Second, antibodies once formed against a particular disease continue to offer resistance against that particular disease, such as antibodies formed against measles and chickenpox.

2.2.2 Applications of MAbs

MAbs have a variety of applications ranging from academic, medical and commercial uses. MAbs can be used to characterize cell surface proteins which will help in understanding biological functions of membrane proteins. For example, MRK16 (IG_2 isotype) and MRK17 (IG_1 isotype) were used to detect membrane antigens [53]. Antibodies are used in the radioimmunodetection and radio immunotherapy of cancer, and some of the new methods can even target only the cell membranes of cancerous cells. An excellent example is MAbs developed against ovarian cancer. Human monoclonal antibody TC5 (immunoglobulin G1) specifically targets ovarian cancer cells and does not react with normal organs like the liver, heart, lung, or pancreas [54]. MAbs can be used to treat viral diseases like AIDS. A combination administration of two monoclonal antibodies, MAbs 2F5 and 2G12, has been successful in neutralizing HIV virus. MAbs also have successful applications in organ transplants. OKT3, a murine antibody linked to the T-cell antigen receptor cells, is used in clinical applications to prevent and treat acute organ rejection [55]. With such a wide range of applications requiring MAbs doses ranging from milligrams to grams, there is a lot of commercial interest to scale-up MAbs production for therapies requiring larger doses. Hence, large scale purification of monoclonal antibodies has generated great commercial interest.

2.2.3 Downstream purification of MAbs

Purification of MAbs can be divided into two main techniques: precipitation and chromatography. Typically the precipitation technique is used in downstream processing (recovery and purification of biological products) preceding other chromatographic steps to increase product purity. Sodium sulfate or ammonium sulfate salts can be used to precipitate the antibodies. Antibodies can also be precipitated using ethanol or by electrolyte depletion [56].

Chromatographic methods are classified as non-affinity and affinity based. Affinity chromatography is the most common method for antibody purification and its principle and limitations will be described in the following sections. The research in this dissertation is focused on addressing the limitations of affinity chromatography using functionalized membranes as membrane adsorbers in membrane chromatography for large scale purification of MAbs.

2.3 Affinity chromatography

Affinity chromatography is the critical separations component of downstream processing in the biotechnology industry [2-3, 8, 57-59]. This technique is the most common method for separation of proteins and antibodies. Affinity chromatography is effective, but expense and low throughput complicate large scale operation.

2.3.1 Principle

Affinity chromatography is a method of separating proteins and antibodies from biochemical mixtures (e.g. blood serum). It is based on a highly specific chemical interaction between the solute and the ligand. The stationary phase typically consists of a silica or agarose gel containing a surface ligand to bind the protein [60]. The stationary phase should have good chemical and physical stability, flow and packing characteristics, and functionalities for binding a wide variety of compounds. The process starts with a solution (cell lysate or blood serum) containing different types of molecules passed through the stationary phase in an affinity column. The molecules of interest have a specific chemistry that will bind with the ligand on the immobilized (stationary) phase. Specific molecules of interest are eluted from the column.

2.3.2 Applications

The most common use of affinity chromatography is preparative separation of proteins and antibodies [46, 61-63]. The use of affinity chromatography for the removal of unwanted

substances from the blood of living organisms is also being investigated [64]. Another application of affinity chromatography is to substitute natural peptide chains of enzymes with different tailored synthetic peptides [65]. Enzyme solutions are purified and concentrated by affinity chromatography which helps in determining interactions between biological compounds and drugs [65]. A detailed review of clinical applications of affinity chromatography was published by Hage [1]. In this review, applications were grouped based on the type of ligand. For example, boronic acid was used as ligand for determination of glycohemoglobin for the diagnosis of long term diabetes. Another example is the use of lectin as a ligand to bind certain types of carbohydrate residues [1]. In all the applications discussed, the type of ligand plays a very important role and will be discussed in the subsequent section.

2.3.3 Ligands in affinity chromatography

The application of affinity chromatography for large scale production is limited by the low availability of suitable ligands for scale-up. Other challenges include ligand stability, low selectivity, long process times and high cost. These problems have been addressed in recent years by rational and combinatorial approaches to design low cost, stable, and highly selective synthetic affinity ligands [61, 66-68]. Ligand design has been made more feasible and faster by using combined knowledge of advanced computational tools and protein structure with defined chemical synthesis [61]. New synthetic affinity ligands have been synthesized by combinatorial approaches based on libraries of peptides and nucleic acids [67, 69]. In the following sections different types of natural and synthetic ligands for affinity-chromatographic purification of antibodies and their advantages/disadvantages will be discussed.

2.3.3.1 Affinity ligands for immunoglobulins

The immunoglobulins can be divided into five different classes, namely: IgG, IgA, IgE, IgM and IgY. Proteins A or G are the common affinity ligands for purification of IgG and IgM [70-71]. Though these are the most common affinity ligands for purification of the majority of antibodies, there are cases where they have shown ligand leakage (shedding of ligand from support matrix), poor affinity and low binding capacity. Fuglistaller [70] reported ligand leakage with different protein A column matrices using mouse monoclonal IgG3 antibody. It was shown that there was significant leakage at pH 4 in presence of IgGs and at pH 8.9 in absence of IgGs [72]. Proteins A or G do not recognize IgM from sera or cell culture [61]. Alternatively, mannan-binding protein (MBP) has turned out to be a viable option for purification of IgM. Mouse monoclonal IgM purified by this method is 95% pure. However, the binding capacity is limited to 1 mg/ml and the isolation from rat liver is complex, time consuming and expensive [73].

IgA can be purified by fractional precipitation, zone electrophoresis, ion-exchange and other chromatographic procedures [74-75]. A combination of ion-exchange chromatography and immunoadsorption has been successfully used to purify IgA from human serum. Commercially available anion-exchange cellulose was used to isolate IgA. Propionic acid was used as an immune adsorption ligand in sepharose columns. High purity of the product (99%) was achieved but the process required an additional immunoadsorption step to reduce contamination from IgG to less than 1%. Additionally, it has been reported that functionality of IgA may be altered if higher concentrations (1M acetic acid containing 4M urea) of eluants are used to improve recovery [76].

IgE can be purified by immunoaffinity chromatography using anti-IgE antibodies [77]. However, ligand leakage greater than 20 ppm from immunoaffinity columns with glucagon

antibodies has been reported [78]. The ligand leakage from commercially available protein A based affinity medium MabSelect SuRe is less than 3 ppm. Other approaches to purify IgE include ion-exchange and size exclusion chromatography [79]. Studies carried out to investigate binding of proteins A and G for human IgE revealed that protein A showed 12-14% binding with serum polyclonal IgE. However, protein G showed no binding with IgE [80]. IgY, which is typically found in egg yolk, is difficult to isolate because it is present in the water soluble fraction which contains dispersed lipid fraction. Common affinity ligands like Protein A or G showed no binding for IgY [81-82]. In recent years novel synthetic ligands were investigated as an excellent alternative to biological ligands. This is because synthetic ligands are cheaper to produce, their ability to with stand harsh cleaning in place operating conditions (0.1 M NaOH), and ligand leakage is reduced [83].

2.3.3.2 Synthetic (Biomimetic) ligands

One alternative to address the limitations of conventional ligands is the development of synthetic ligands. The advantages include low cost, resistance to chemical and biological degradation, high specificity, high capacity (up to 40 mg protein per ml adsorbent), large scale use (columns > 100 liter) and high sterilizability [84-86]. In recent years, advanced computer-aided molecular design and combinatorial chemical techniques have been used to synthesize and design ligands that mimic their biological counterpart [87-89]. A peptide library comprising 88 ligands was screened to find a ligand which shows binding with pure human IgG [89]. It was found that 3-aminophenol and aminonaphthol substituted on a triazine nucleus was highly effective in binding human IgG showing purity greater than 99%. The binding capacity was observed to be 51.9 mg/g moist gel, and 60% of human IgG from plasma was separated [62, 89].

Protein A mimetic (PAM), also known as TG19318 (Figure 2-1), is another novel synthetic ligand designed by screening of the synthetic peptide library by computational tools. The tetramer of a tripeptide (Arginine-Threonine-Tyrosine), identified after three cycles of screening using computer simulation, showed binding with the Fc portion of IgG. It was then immobilized on preactivated solid supports (enzyme-linked immunosorbent assay format). It was reported that purification of antibody was approximately 95%. Additionally, the ligand was found to be stable and there was no detection of leaks in the purified stream [90]. It is used to purify mouse monoclonal IgE and IgG. The binding capacity can reach up to 5 mg IgE/ml of the support, and 25 mg IgG/ml of the support, respectively [62, 91].

Artificial protein A (ApA) was designed and synthesized to mimic the protein A dipeptide structure Phe132-Tyr133 responsible for IgG binding. Computer aided molecular modeling was used to mimic the dipeptide structure. Stability of the adsorbent was tested with 1M NaOH and the capacity was unchanged following treatment in five cycles. ApA showed a selectivity of 98% for IgG as compared to 94% for biological protein A. Another measure to describe affinity between two molecules is the equilibrium constant that describes bonding affinity between two molecules. The lower value indicates high affinity between molecules. The affinity constant between synthetic ligand ApA and IgG was approximately 10^4 M^{-1} and that between biological protein A and IgG in aqueous solution is 10^7 M^{-1}. The binding capacity between ApA and IgG was found to be 20 mg IgG/g moist gel [87].

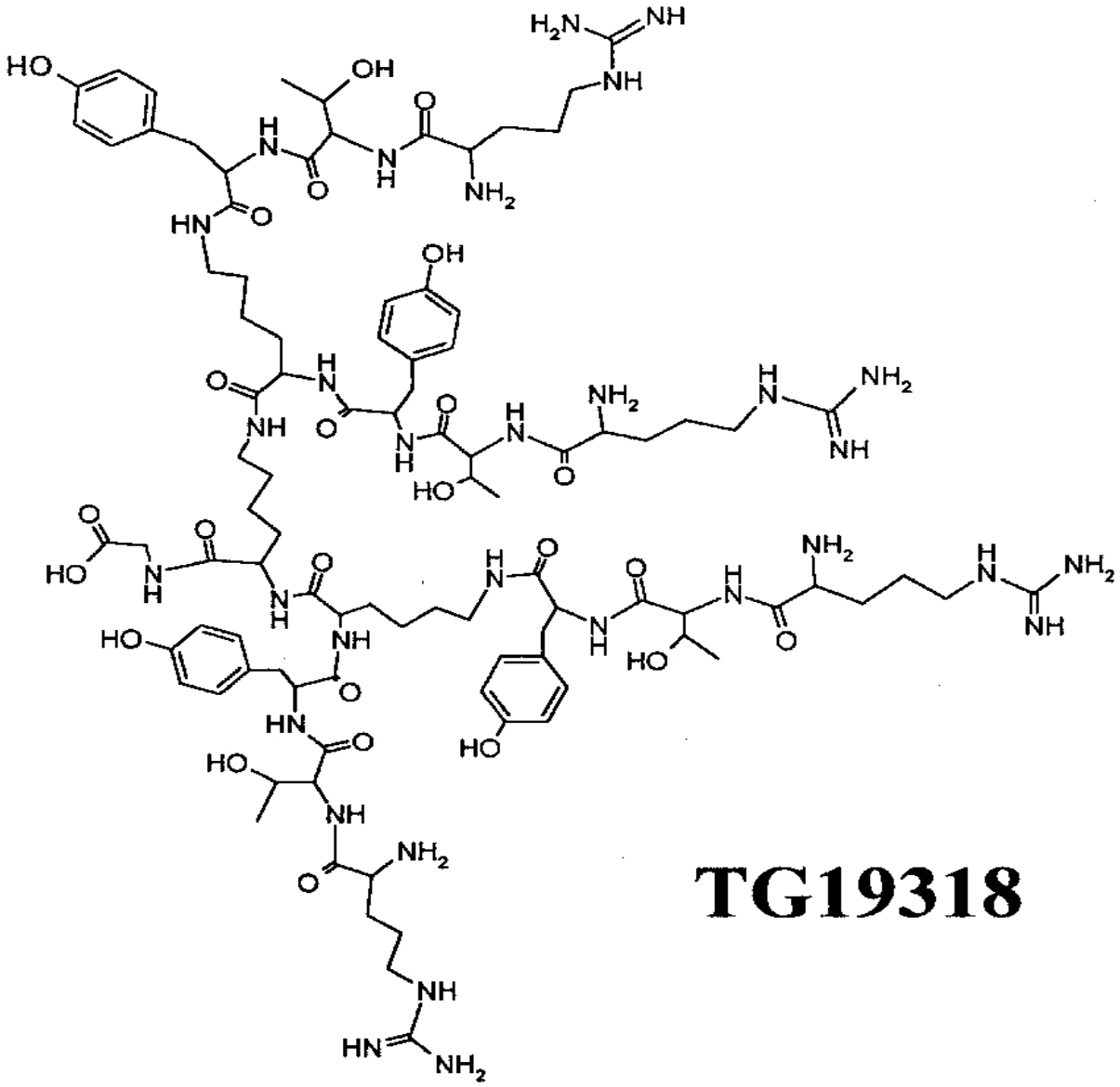

Figure 2-1. Chemical structure of TG19318 [92].

2.3.4 IgG-protein A binding chemistry

The structure of IgG (150 kDa) consists of four peptide chains, two identical heavy chains (50 kDa) and two identical light chains (25 kDa). The heavy chain is connected to the light chain and the other heavy chain by disulfide bonds. Each heavy chain contains one variable domain (V_H) and three constant domains (C_H1, C_H2 and C_H3). The region between the C_H1 and C_H2 domains is the hinge region, where the antibody molecule arms form a flexible Y shape. The antibody hinge region structure controls the biological profile. The fragment antigen binding (Fab) segment contains the antigen-binding site, and the fragment crystallizable (Fc) segment has high affinity for Protein A (Figure 2-2) [51].

The structure of Protein A can be broadly divided into two parts. The first part consists of three alpha helices arranged in an antiparallel bundle. The major part of the whole structure of protein A consists of helices. The second part consists of 72 different chains composed of essential amino acids like leucine, lysine, aspartic acid, phenylalanine, and tyrosine. Among these different chains of amino acids, the particular dipeptide structure of Phe-132/Tyr-133 (Figure 1-1) is very crucial for interaction with IgG [46, 61, 93]. The chemistry of the dipeptide structure is similar to the Fc receptor (protein) which binds specifically to the Fc region of the antibody due to complementary binding sites. The three-helix bundle of protein A does not take part in interaction with IgG. The Phenylalanine-Tyrosine dipeptide residue forms a hydrophobic core (hydrophobic amino acids in internal core region) and is located on the surface twist of a helix in B-domain of protein A. The aromatic side chains of the dipeptide motif are protruded and oriented towards the shallow groove or crevice in IgG. None of the other amino acid residues are close to or accessible to the IgG interaction site, so the contact involves groups

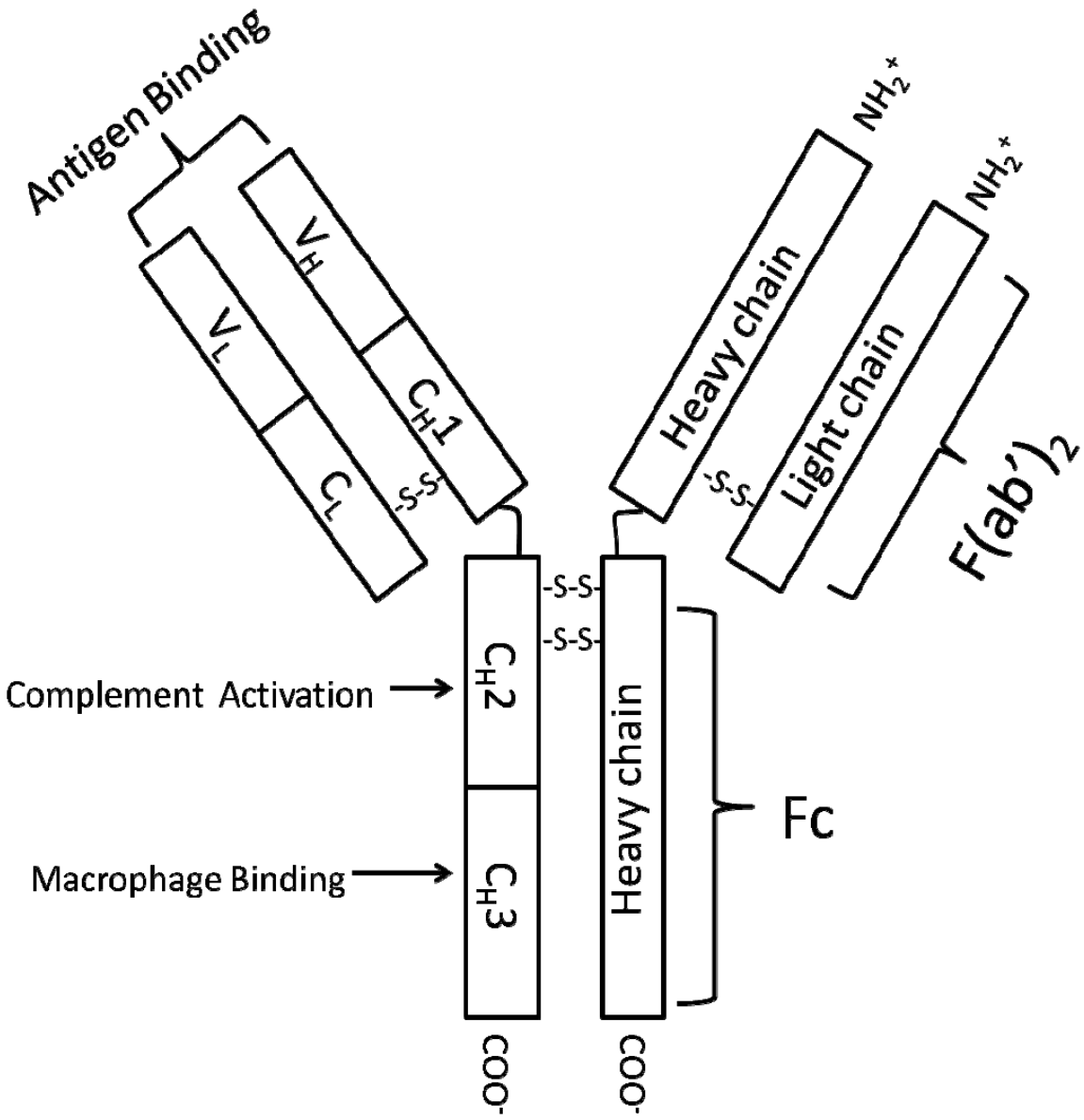

Figure 2-2. Schematic diagram showing the structure of an IgG molecule [51].

between the C_H2 and C_H3 domains (hydrophobic) of the Fc region of IgG and the phenylalanine-tyrosine dipeptide structure. Therefore, binding between IgG and protein A is predominantly characterized by hydrophobic interactions. However, some minor interactions may also be due to hydrogen bonding, ion pair, and van der Waals interactions [87]. In this research, a synthetic analog of phenylalanine/tyrosine dipeptide structure of Protein A was synthesized inside the pores of microfiltration polyethersulfone membrane by sequential cationic polymerization of styrene and substituted styrene monomers.

2.3.5 Limitations of affinity chromatography

Although affinity chromatography is effective and provides excellent resolution and reliability, there are a number of drawbacks. First, the pressure drop across a packed chromatography bed is generally very high, in the range of 20-90 bar [94]. High pressure drop deforms the spherical particles in the packed bed. These particles accumulate and block the bed, further limiting the flow rate [95]. Second, transport of solute particles to their corresponding binding sites takes place by intra-particle diffusion. This results in increased process time and recovery volumes (elution volume). Third, channeling due to cracking of the packed bed causes a tremendous loss in loading capacity (amount of protein bound to substrate) [13]. Fourth, ligands and products are exposed to harsh elution conditions for long times which increases the chances for denaturation. Fifth, separation of macromolecules by affinity chromatography is often a problem since large size protein molecules cannot enter the small pores of particles in a packed bed. Sixth, the most common ligands used in affinity chromatography are still of biological origin. This makes these ligands very expensive and purification steps are required before the ligand is bound to the stationary phase. Finally, mass transfer limitations cause problems with scale-up such that large scale purification (grams per patient per year) of proteins and MAbs is

very expensive. Therefore, there arises a need for new a separation technology which addresses the limitations of affinity chromatography [96-98].

2.4 Membrane chromatography

An alternative viable technology to overcome the limitations associated with affinity chromatography is to use synthetic microporous or macroporous membranes as chromatographic media [98-102]. Membrane chromatography is a more recent purification technique designed to avoid the fundamental limitations of columns packed with beads [13, 103]. The membrane adsorbers used in membrane chromatography contain functional ligands attached in the pores as adsorbent sites.

2.4.1 Advantages over affinity chromatography

Membrane chromatography is dominated by convective mass transport, resulting in high dynamic binding capacity, high productivity and reduced processing times (Figure 2-3). The elimination of diffusional resistance minimizes some of the problems of affinity chromatography like process time (one-tenth the time taken for packed beds) and intra-bed diffusion [99, 104]. The result is exceptional throughput, good resolution (membrane stacks), and higher dynamic binding capacity than packed beds. Furthermore, the cross-sectional area of the membrane bed relative to bed length is much larger as compared to affinity columns. Hence, the pressure drop is drastically reduced resulting in higher flow rates and thus higher productivities [105-109].

The ideal affinity support material should have pore size greater than 30 nm for access to immobilized ligand and protein that are separated. Agarose supports have a pore size of 30 nm and support materials based on silica have large pore size of approximately 400 nm. However, with increase in pore size, surface area per volume of chromatographic media decreases resulting in decrease in binding capacity. So the pore size range of 30-50 nm is a good trade-off for large

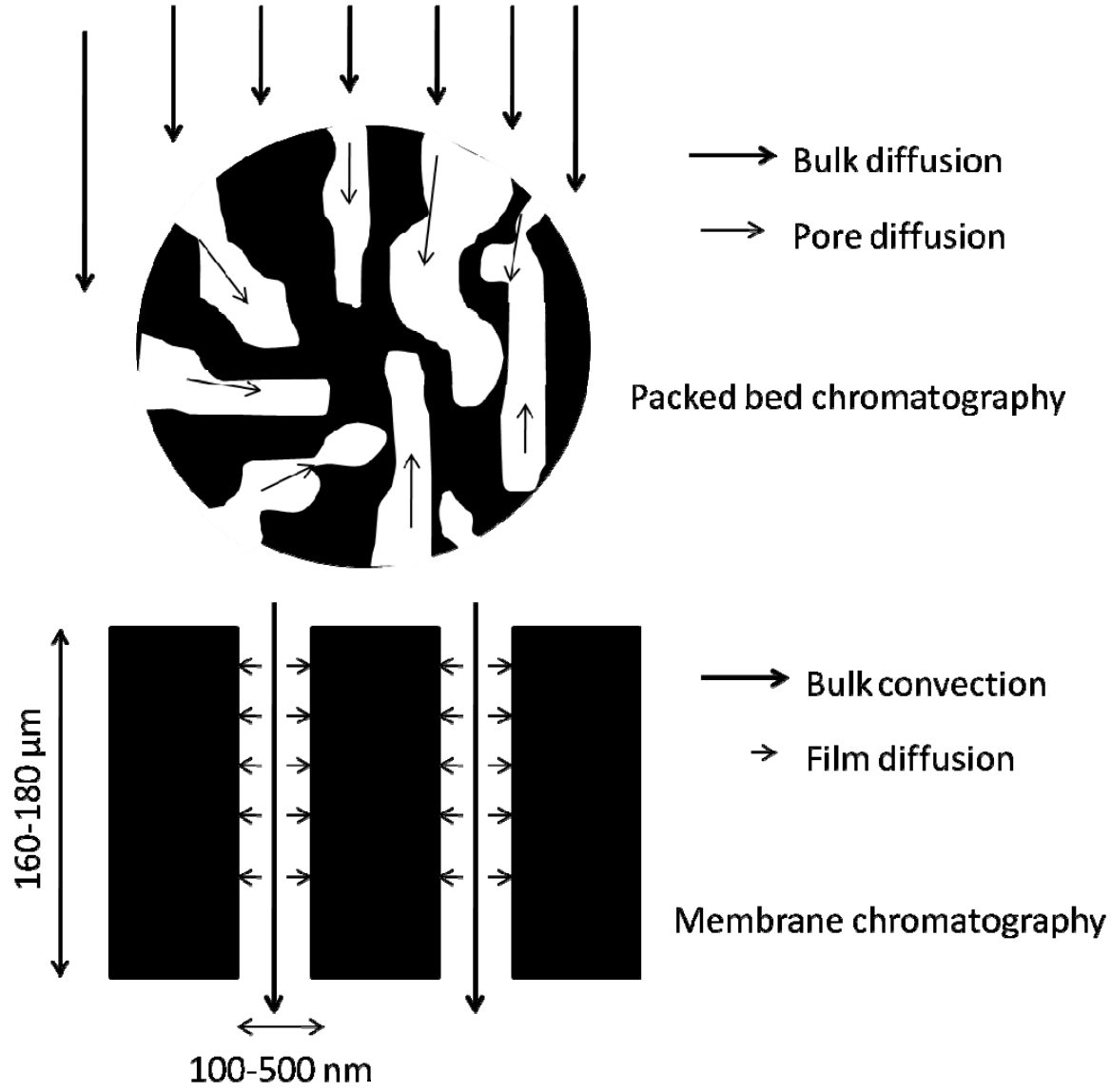

Figure 2-3. Solute transport in packed bed (pore diameter 30-50 nm) and membrane chromatography [13].

surface area. Membrane chromatography can be used for separating large size protein molecules of molecular weight greater than 250 kDa. This is because large size proteins have access to more open pores due to the macroporous support nature [23-24]. In the work of Yang et al. [110], the dynamic binding capacity of thyroglobulin (20 nm diameter) was reported to be 10±2 mg/ml as opposed to 3±0.8 mg/ml for alpha-lactalbumin (3.5 nm diameter) using an anion-exchange membrane (Q membrane). This corresponds to a 160-200% increase in dynamic binding capacity for large size molecules as compared to small size protein molecules. Additionally, low production cost allows development of disposable membrane adsorbers when properties such as binding capacity, selectivity and permeability drop below separation efficiency. Scale-up is a relatively straightforward procedure because capacity is linearly dependent on the membrane surface area (or volume) as well as the size of membrane unit. However, this potential has not been fully capitalized for large scale separation of proteins and antibodies. Lightfoot and coworkers [12] reported that scaling up to larger support diameters reduces the separation efficiency and can cause inefficient flow distribution. Hence, there remain several technical challenges to broader implementation of membrane chromatography.

2.4.2 Affinity membranes for protein purification

Affinity membranes were developed to address the limitations of affinity-based purification with packed beds. Affinity membranes are composed of grafted functional groups (ligands) that are anchored in the pores of a microfiltration membrane. The types of functional groups employed include amino acids, biological ligands, metal affinity ligands, ion-exchange ligands, and antigen and antibody ligands. In subsequent paragraphs, ligands and matrix performance will be discussed.

A hollow-fiber affinity membrane containing phenylalanine or tryptophan ligands was prepared by grafting glycidyl methacrylate onto a porous polyethylene membrane by radiation-induced grafting [111-112]. Bovine γ-globulin saturation capacities of affinity membrane with phenylalanine and tryptophan ligands were 36 and 49 mg/g, respectively. Residence times ranging from 55-220 seconds confirm negligible mass transfer resistance. Protein A and protein G immunoaffinity membranes have also been used to purify IgG at low residence times. IgG was purified in only 10 minutes in a single pass at high flow (150 cm^3/min) and low pressure drop 0.83 bar as compared to 20-90 bar in affinity chromatography [94, 113]. Immunoaffinity membranes immobilized with proteins have shown binding capacities similar to that of a packed column. Protein A was immobilized on hollow fiber membranes composed of modified polysulfone to adsorb IgG [106]. The highest binding capacity studied was comparable to that of bead matrices.

Immunoaffinity membranes have potential use in clinical apheresis (separation of different constituents of blood) applications [114]. The affinity ligand L-histidine was immobilized onto poly (ethylenevinyl alcohol) hollow fiber membranes for selective removal of human IgG from plasma or serum *in vitro*. The pseudobiospecific affinity membrane showed higher capacity than protein A membrane. Additionally, the membrane had higher affinity for IgM as compared to other immunoglobulins (IgA and IgG) studied. So, it has a potential for large scale application due to lower cost (less expensive ligand), high capacity, specificity and stability of histidine affinity membrane.

Immobilized metal ion chromatography affinity membrane also showed improved flow rates as compared to packed beds [115]. S-oxynitrilase was purified from Sorghum bicolor using immobilized iminodiacetic acid (IDA)-copper ion membrane. The membrane showed a 200-fold

increase in flow rate as compared to a gel. However, the binding capacity of 0.15 mg of S-oxynitrilase per cm^2 was slightly lower than the gel.

As discussed above, affinity membranes have clear advantages over conventional packed bed chromatography in terms of cost, residence time, and flow rate. However, there are areas which need improvements for large scale production. The improvement opportunities and how they can be addressed will be discussed in the following sections.

2.4.3 Opportunities for improvements in membrane chromatography

Undoubtedly, separation by membrane chromatography has several advantages over packed bed chromatography. However, some of the major challenges of membrane chromatography include lower equilibrium binding capacity, membrane pore size distribution, selectivity, and uneven membrane thickness. Suen [116] reported that a porosity variation of 3% can result in 11% loss in loading capacity. The pore size in macroporous membranes is usually represented as a range since all the pores are not of the same diameter. This wide pore size distribution results in the feed preferentially being carried through the larger pores, with very little flow through the smaller pores. As a result, utilization and hence the efficiency of the adsorbent is reduced. Variation in porosity also causes channeling leading to loss in loading capacity. Membrane thickness often ranges from several hundred to thousands of microns in a stack and hence due to this wide range there is often nonuniformity in thickness. The adsorbent utilization may be reduced as a result of uneven membrane thickness; flow is usually greater where the membrane is thinner due to the lower pressure drop. Suen [116] reported that a 10% change in membrane thickness results in 10% loss in loading capacity. Binding capacity of membrane adsorbers is lower due to lower surface area to bed volume ratio as well as non uniform inlet flow distribution. The loss of internal surface area generally results in a decrease in

the equilibrium binding capacity. Functionalized membranes synthesized in this research have polymeric grafts with multiple binding sites extending into the pore; therefore, sorption capacity was increased by more than 9 times compared to commercial membrane adsorbers.

Although membrane chromatography appears to be an ideal candidate for large-scale purification and recovery of proteins and enzymes, its potential has not been fully utilized in biotechnology industry. Proper distribution of inlet flow is one area which needs to be investigated in detail. Clearly, the equilibrium binding capacity, pore size distribution, selectivity and flow distribution must be improved if membrane chromatography is to meet the future separation needs of the biotechnology industry.

2.5 Functionalized membranes

2.5.1 Principle

One advance that has resulted in improved equilibrium binding capacity is the development of functionalized membranes. These are membranes where polymers containing adsorptive sites are immobilized in the pores. The grafts may be formed by polymerization from the monomer, or by attachment of large chain molecules, such as enzymes and polyamino acids [39]. In most cases, functionalization results in the addition of a polymer brush in the pores of the membrane, where active sites for adsorption are located in the membrane flow path. The surface chemistry of the membrane is altered to carry out polymerization, affecting its intrinsic properties such as permeability, separation capability, and conductivity. In most cases, the membrane backbone matrix acts as a stable skeletal support for grafted polymers. In the case of porous polymer membranes, the porous structure gives an opportunity for polymer graft stability by providing sufficient interaction between the membrane and the grafted polymer.

2.5.2 Introduction to polymer brushes

Polymer brushes are defined as layers or assemblies of chains end-tethered (grafted, anchored) to a surface or interface [117-119]. The interface to which polymer brushes are grafted may be a solid substrate surface, the interface between liquid and air, or the interface between two liquids. Tethering of polymer on a solid substrate can take place either chemically or by physical adsorption. There are three methods for synthesizing polymer brushes. These include grafting to, grafting from and grafting through. Among these, grafting to and grafting from are the most common. In grafting to method, polymer chains with functional end groups diffuse through the surface which has complimentary functional groups. A reaction then takes place between the functional groups on the surface and polymer. As a result, polymer chains will be tethered on the surface. In grafting from method, an appropriate initiator is attached first and then monomer is diffused through a solid surface at appropriate polymerization conditions. Monomer reacts with the initiator and polymer chains grow from the surface. The advantage of grafting from is that multiple grafts can be formed which increases the binding capacity, and the growth of the grafts can be controlled to create a customized structure.

2.5.3 Classification of polymer brushes

Polymer brushes based on chemical composition can be classified into homopolymer, mixed polymer, random copolymer and block copolymer brushes (Figure 2-4). Homopolymer brushes (Figure 2-4 (a_1 -a_4)) consist of one type of monomer molecule. In mixed polymer brushes (Figure 2-4 (b)), two or more different monomers are grafted to the same substrate [120]. Random copolymer brushes (Figure 2-4 (c)) consist of two different monomer molecules randomly distributed along the polymer chain [121]. Block copolymer brushes (Figure 2-4 (d)) consist of two or more monomer chains linked by covalent bonds [122]. Homopolymer brushes

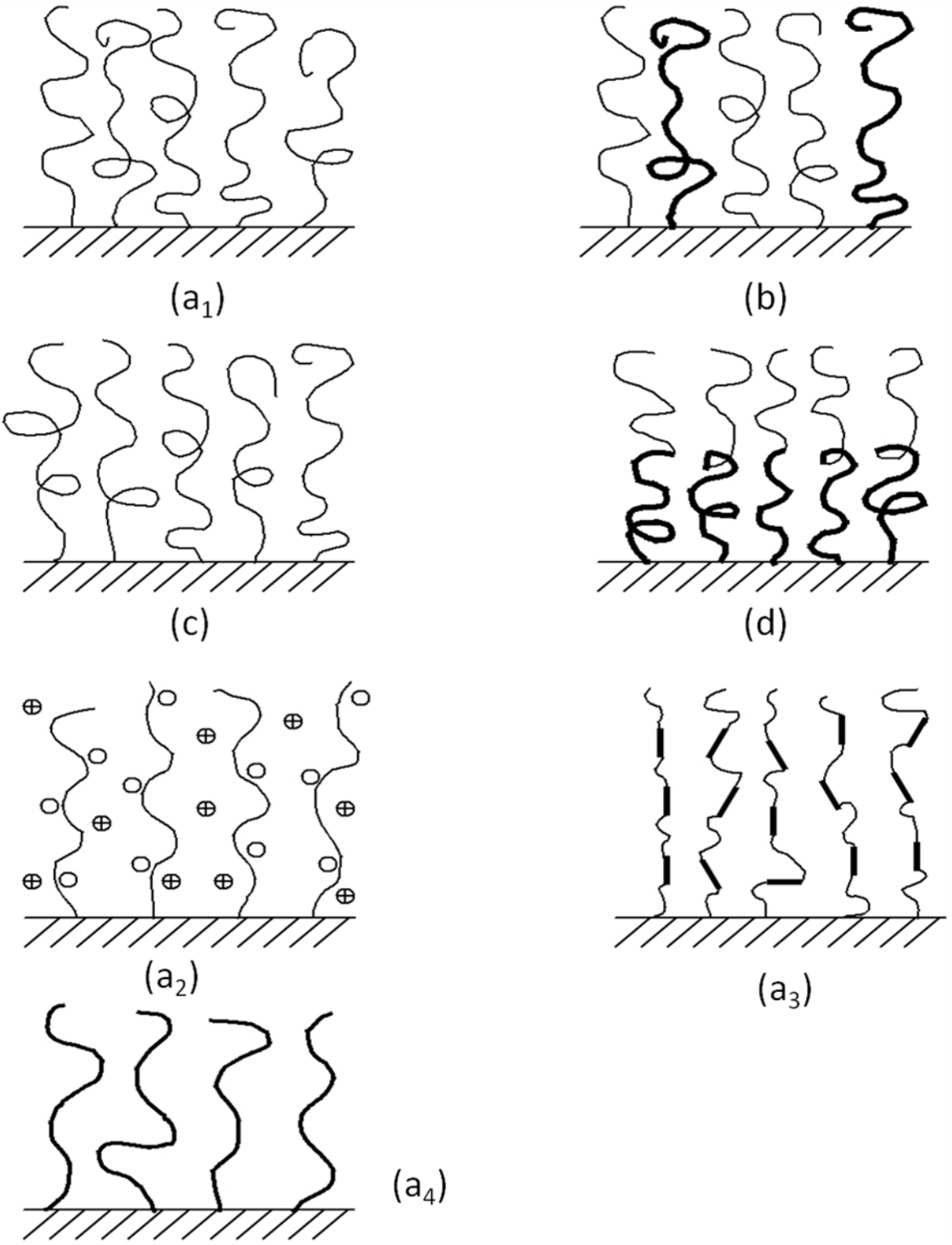

Figure 2-4. Classification of linear polymer brushes: (a_1 -a_4) homopolymer brushes, (b) mixed polymer brush, (c) random copolymer brush, and (d) block copolymer brush [123].

can also be classified based on their polarity and these include neutral and charged polymer brushes (a_2). Another way of classifying homopolymer brushes is in terms of stiffness of the polymer chain and that includes flexible/semi-flexible (a_1, a_4) and liquid crystalline polymer brushes (a_3).

2.5.4 Graft polymerization by chemical techniques

Many methods for graft polymerization of different monomers on polymers have been developed. These techniques include chemical, photochemical, radiation induced, plasma induced and enzymatic grafting. Chemical grafting techniques will be discussed in the subsequent paragraphs. The discussion of other techniques is beyond the scope of this dissertation. Grafting by chemical means can be classified into two types: free radical and ionic. In grafting through free radical polymerization, free radicals are produced from the initiator and transferred to the substrate to react with the monomer to form the graft copolymer. Grafting through ionic polymerization can further be classified into cationic and anionic polymerization.

The initiators for cationic polymerization are electrophilic agents which are electron acceptors; the common examples are sulfuric acid and hydrochloric acid. Additionally, the compounds which generate carbenium ion can also be used as initiator [124]. Anionic polymerization is a form of addition polymerization that involves the polymerization of vinyl monomers with electronegative groups. This polymerization is carried out through a carbanion active species. The polymerization through ionic mode can be living which means polymerization occurs until all the monomer molecules are exhausted or until a desired molecular weight is achieved for particular application.

Functional groups such as carboxyl, phenyl, sulfonic acid, hydroxyls, amines, halogen, and double bonds may be attached to the living active centers [125-127]. The versatility of the

method allows placing these functional groups at any position, either at the beginning, middle or end of polymers, between blocks or evenly spaced along polymer chains. Castro and coworkers introduced vinyl groups chemically by grafting polyvinyl-pyrrolidone brush on porous silica membranes. Ritchie and coworkers [128-129] have successfully immobilized multiple reactive groups (COO^-, NH_3^+, and SH) on cellulose or silica based membrane by chemical techniques. In this work, the functionalization of polymer grafts is accomplished by cationic polymerization of styrene and substituted styrene monomers (CMS and ES). Sulfonic acid groups ($R\text{-}SO_3^-$) immobilized in the pores of the microfiltration membrane act as initiator for cationic polymerization.

2.6 Cationic polymerization

Cationic polymerization is a type of chain growth polymerization in which the active end of a growing polymer molecule is a positive ion. Protonic acids, for example sulfuric acid, can be used as initiators in cationic polymerization. The proton from an acid (HA) is transferred to a monomer molecule (M) giving HM^+ cation and A^- counterion. The newly formed cation will further react with other monomer molecules, each time forming a cation. Molecular weight increases with formation of polymeric grafts. This process is repeated until all the monomer molecules are used up, and thus cationic polymerization is a living polymerization provided the termination rate is negligible. Figure 2-5 illustrates the propagation step of the reaction mechanism for styrene polymerization in a membrane.

In this work styrene and substituted styrene monomers will be used to form polymer grafts. Styrene proceeds by cationic polymerization through electrophilic addition to the growing carbocation and the phenyl ring stabilizes the newly developed cation [130-131]. PES has been sulfonated using sulfuric acid for initiator immobilization [132-133]. Styrene monomer

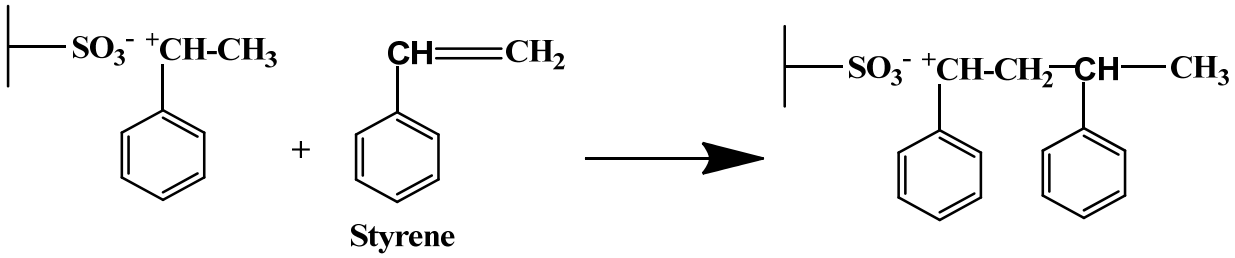

Figure 2-5. Propagation step for cationic polymerization of styrene.

undergoes polymerization reaction from these sites and polymer grafts are formed in the pores of membrane (Figure 2-6).

This research work deals with developing and understanding of polymeric functionalized membranes by sequential cationic polymerization of styrene and substituted styrene monomers (CMS and ES). A variety of functionalities (phenyl, sulfonic acid, chloromethyl, and ethoxy) have been incorporated for attaching the grafts. Homopolymer and block copolymers are formed in the pores of microfiltration membrane. These block copolymers will be the first step in creating a synthetic analog of ligands used in affinity chromatography for antibody separation.

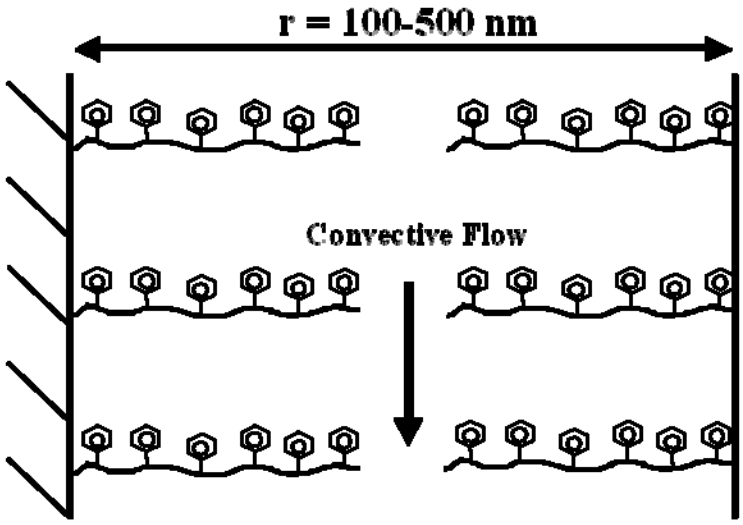

Figure 2-6. Polystyrene grafts in a membrane pore.

CHAPTER 3
EXPERIMENTAL SECTION

3.1 Introduction

In general the functionalized membranes in this work were prepared by a three step procedure. These steps include sulfonation of the raw membrane, polymerization of a copolymer mixture of styrene and ethoxystyrene in the pores of the sulfonated membrane, and hydrolysis of the poly(styrene-co-ES) grafted membrane to remove the ethoxy group and introduce hydroxyl group. Two extra steps were added for membranes with spacer arms that includes introduction of chloromethyl groups by polymerization of CMS and subsequent glycine functionalization. The performance of the functionalized membranes with and without spacer arms was then tested for adsorption of IgG. In phase 1, methods for forming homopolymer and block copolymers using three separate sets of monomers (styrene, ES, and CMS) are described. In phase 2, methods for detailed characterization of polymeric graft composition and moieties, as well as performance testing of the membrane for IgG adsorption, are described. In this chapter, the materials, instruments used for analytical studies, calibration methods, and procedures for experiments are described in detail.

3.2 Materials

Microfiltration PES membranes with 0.22 μm average effective pore diameter, 165 μm thickness, and 47 mm diameter were purchased from Millipore Corporation (Catalogue #GPWP04700), Bedford, MA. The chemical structure of PES is shown in Figure 3-1. The following chemicals, solvents, and antibodies were purchased from Fisher Scientific (Pittsburgh, PA) or VWR (West Chester, PA) unless otherwise stated, with purities given in wt.%: sulfuric acid (96.4%); styrene (99.5%); 4-ethoxystyrene (ES) (97%); 4-chloromethylstyrene (CMS)

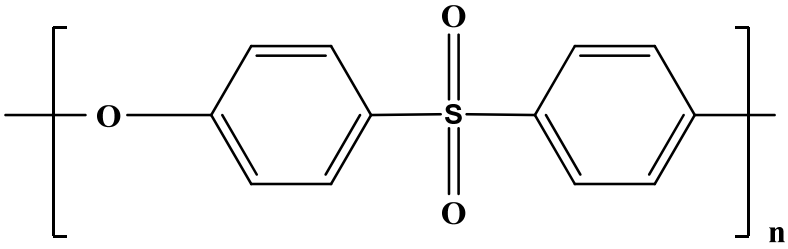

Figure 3-1. Repeat unit structure of polyethersulfone.

(96%); glycine (99.5%); sodium hydroxide, solid beads (95-100%); sodium hydroxide solution (0.5N); toluene (99%); methanol (99%); lyophilized bovine IgG (≥95%, 156 kDa); lyophilized BSA (≥96%, 67 kDa); deuterated dimethylsulfoxide-d_6 (DMSO); deuterated chloroform ($CDCL_3$); sodium phosphate, dibasic, anhydrous (99.5%); sodium citrate dehydrate (99%); phosphate buffered saline (pH 8); and orthophosphoric acid, aqueous solution (85%). All the monomers and antibodies were stored at 5^{o}C until needed. The solvents were used as received without further purification except where noted. Buffer solutions were prepared using analytical grade chemicals and distilled water.

3.3 Laboratory experimental setup

The membranes used in this research were prepared by a simple, three step procedure. First, the initiator was immobilized in the pores of membrane using 0.5N sulfuric acid, a solution of styrene in toluene was permeated to create a homopolymer brush structure, and this was followed by permeation of CMS or ES to form diblock copolymer brush. Figure 3-2 shows a schematic of the customized experimental laboratory setup.

The first step was to wash the whole apparatus with distilled water. This was done by flushing distilled water from the top of the tank and allowing the water to flow through the membrane holder by keeping the valves (upstream and downstream of membrane holder) open. The pH of the water collected from bottom was checked and the apparatus was washed until the pH reached 7. The microfiltration membrane, in the form of white circular disc, was kept in a stainless steel membrane holder. The valves upstream and downstream of membrane holder were closed and the reaction solutions were fed into the stainless steel feed cell. The feed tank was then pressurized with pure nitrogen (zero grade to prevent contamination) at 21 psig and kept constant with a regulator on the nitrogen cylinder. The tank pressure was indicated by a pressure

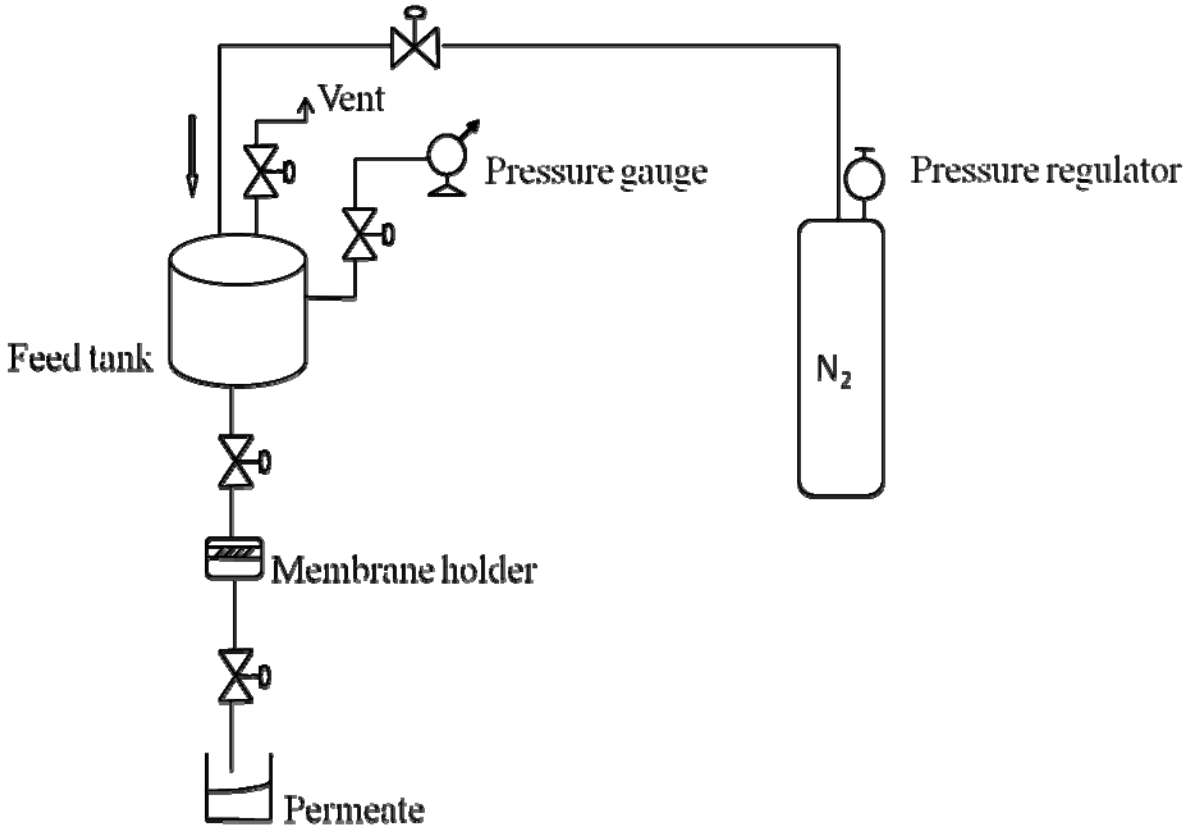

Figure 3-2. Schematic of the experimental laboratory setup.

gauge attached at the top of the tank. Next, the valves were opened to allow the reaction solutions to permeate through the membrane. Permeate was collected at atmospheric pressure from the bottom. All experiments were performed at room temperature. It should be noted that, since the membrane is microfiltration with large pore size, the flow rate of solution through the membrane was very high. Hence, a valve downstream of membrane holder was kept half open to maintain a flow of 1 ml/min. Additionally, pure water flux was measured after each stage of modification to quantify changes in permeability.

3.4 Phase 1: Synthesis and characterization of homopolymer and block copolymer grafts in the pores of PES MF membranes

3.4.1 Initiator immobilization

The feed tank was filled with 250 ml of 0.5N H_2SO_4 and the solution was permeated through the membrane over the course of 3 hours. After permeation, the membrane was taken out of the membrane holder and rinsed multiple times with distilled water until the water pH reached 7. The membrane was then dried in air (~2 hours) until the mass was constant. The apparatus was washed with distilled water after acid treatment to remove all sulfuric acid and allowed to dry.

3.4.2 Synthesis of homopolymer brush in the membrane pores

Styrene, ES and CMS monomers were used to create homopolymer brushes by treating the sulfonated membrane with the desired monomer. The sulfonated membrane was wetted with pure toluene for a few seconds and immediately placed in the membrane holder prior to the polymerization step to prevent membrane cracking. In all cases, a 5 vol% of monomer in toluene (100 ml of styrene/CMS-toluene and 25 ml of ES-toluene) solution was permeated at constant pressure drop of 21 psi across the membrane for 120 minutes. The permeate was collected from

the bottom and the volume was measured. The membrane was washed with pure toluene by permeating toluene through the membrane to remove the unreacted styrene. Unreacted styrene in the toluene was measured by UV-vis spectroscopy at the characteristic peak wavelength of 291 nm using methanol as a solvent.

3.4.3 Synthesis of block copolymer brush in the membrane pores

Block copolymers were formed by polymerization of styrene, followed by sequential polymerization with CMS or ES to create grafts of poly(styrene-b-CMS) or poly(styrene-b-ES), respectively. After styrene polymerization, the feed tank was washed thoroughly with toluene to remove residual styrene (~2 washes). Next, the block copolymer was formed by permeating 100 ml of 5 vol% of CMS/toluene or 25 ml of 5 vol% ES/toluene through polymerized membrane at a constant pressure drop of 21 psi. The permeation was continued for 120 minutes. The permeate was collected and the volume was measured. The membrane was allowed to dry in air and the mass of the membrane was measured.

3.4.4 Membrane permeability measurements

The feed tank, membrane holder and connecting pipes were rinsed with distilled water. The feed tank was next filled with distilled water. The membrane was placed into the membrane holder. The valves upstream and downstream of membrane holder were closed. The tank was then pressurized by adjusting the pressure to 5 psig using the pressure regulator on the nitrogen cylinder. The valves were then opened and the system was allowed to come to steady state (~ 5 minutes) until the flow rate was constant. The permeate was collected at 2 minutes intervals and three readings were taken. The process was repeated with a full tank at incremental pressures of 10, 15, 20, 25 and 30 psig.

3.4.5 ^{1}H-NMR characterization

The composition of homopolymers and block copolymers were characterized by ^{1}H-NMR. ^{1}H-NMR spectra were recorded using Bruker spectrometer operating at a resonance frequency of 500 MHz. Dimethylsulfoxide (20 ml) and deuterated chloroform (10 ml) were used as solvents. Raw and modified membranes were dissolved in solvents (~30 min) and 0.8 ml of sample was used in NMR tube to generate each spectrum.

3.4.6 Atomic absorption spectroscopy

The IECs of the raw and functionalized membranes were quantified by elemental analysis of regenerated sodium ions (λ = 589 nm) in sulfuric acid solution using atomic absorption spectroscopy (Varian 220 FS). In each case, the membrane was treated with 0.1N NaOH (100 ml) by convection for approximately 180 minutes at a pressure drop of 21 psi. The membrane was then rinsed with deionized water to remove any non-specifically bound sodium in the membrane pores. Finally, the membrane was retreated with 0.5N H_2SO_4 (250 ml) for 180 minutes to regenerate sodium ions from the pores. Figure 3-3 illustrates the standard calibration curve prepared by dilution of a 2 mg/l of Na^{+} (reference standard 1 mg/ml) ions in de-ionized water. IEC capacity is calculated as total millieqivalents of sodium ions available for exchange per gram dry weight of sulfonated membrane. The amount of sodium recovered is used to determine the number of available sulfonic acid groups in the membrane.

3.4.7 UV-Visible spectroscopy analysis

Samples of styrene-toluene and CMS-toluene were diluted 1:1250 and 1:416, respectively, with pure methanol. Styrene and CMS monomer concentrations were quantified in the feed and permeate samples after polymerization by UV-vis spectrophotometry at characteristic peak wavelengths of 291 and 295 nm, respectively (Figure 3-4). The characteristic

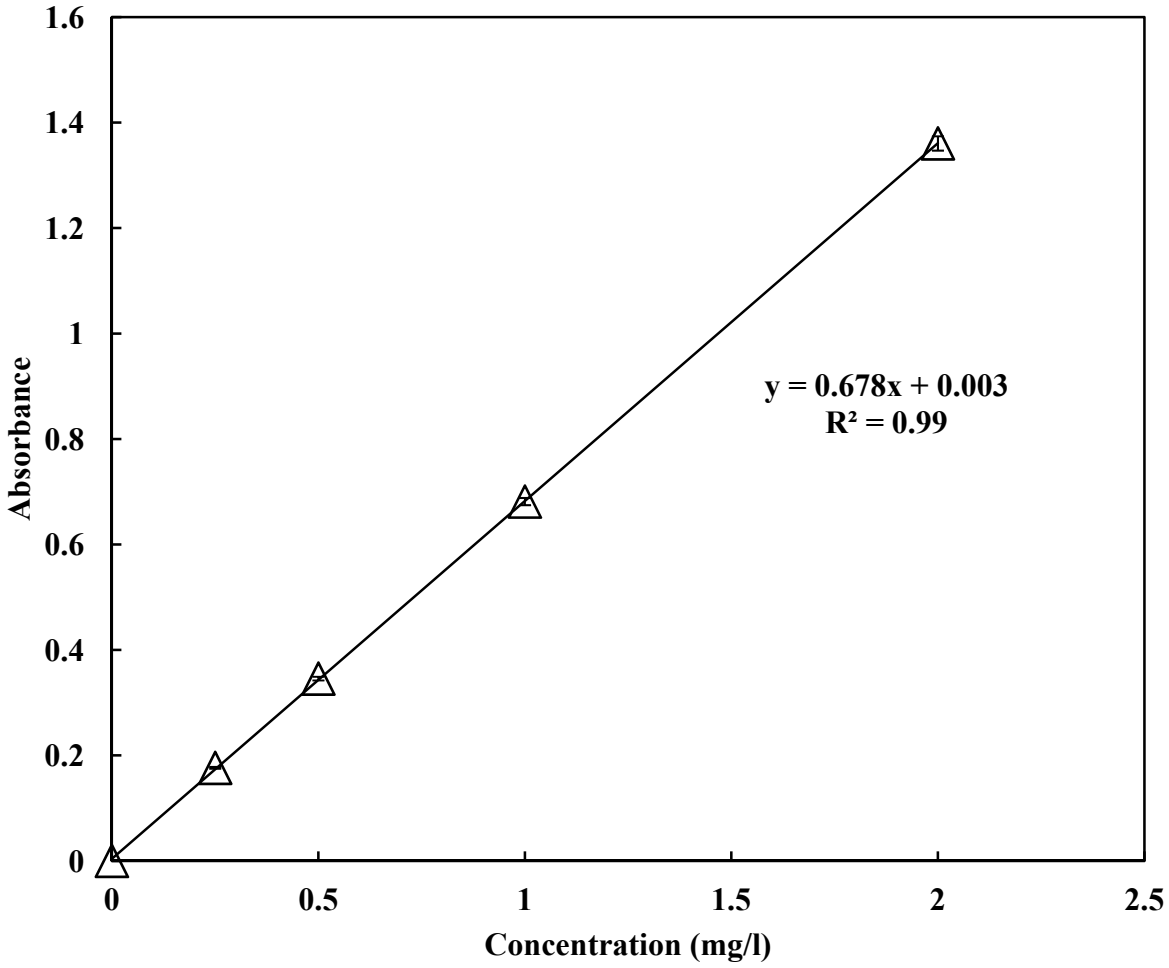

Figure 3-3. Standard calibration curve for IEC analysis by atomic absorption spectroscopy using sodium ion (λ = 589 nm).

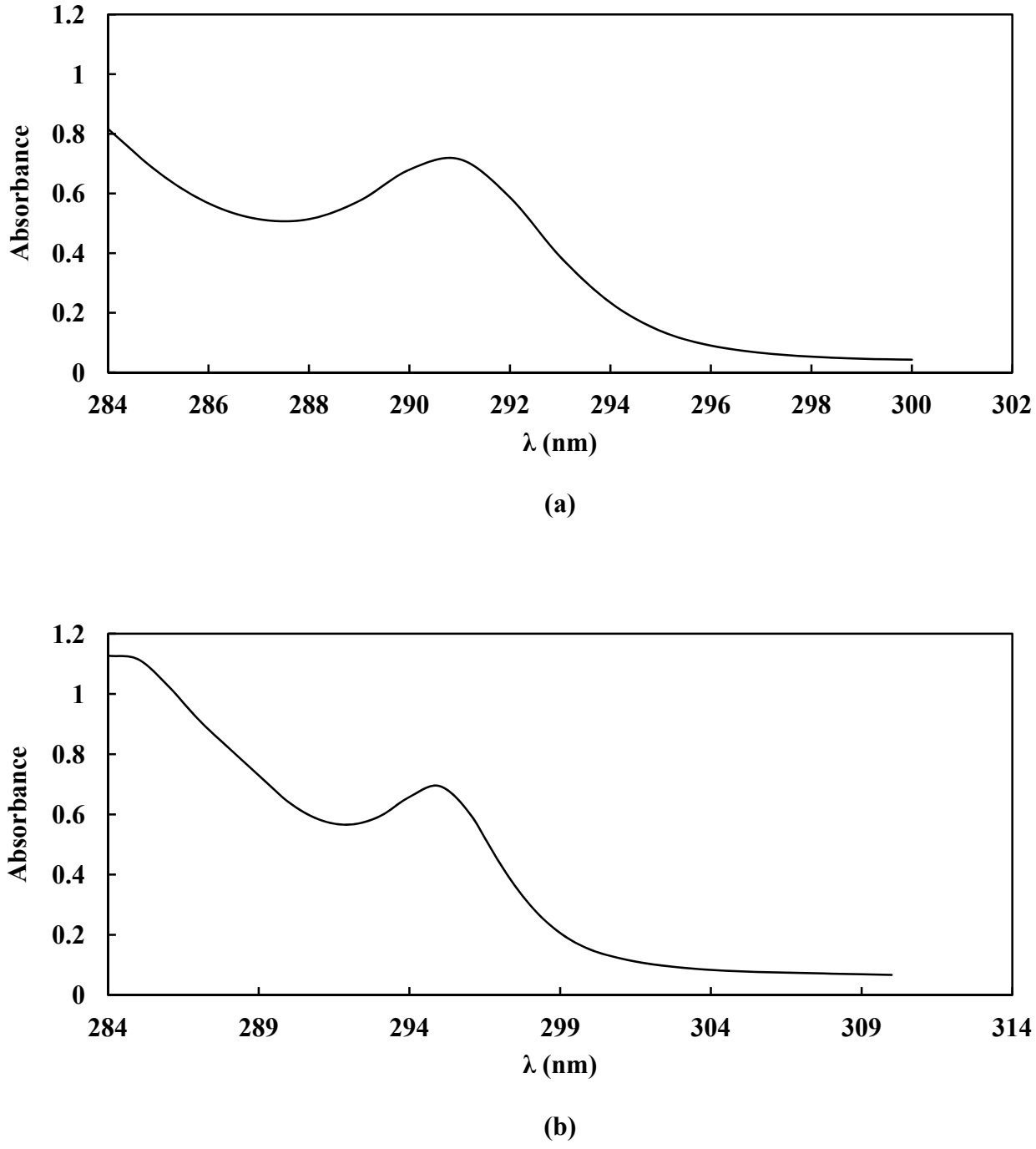

Figure 3-4. UV-spectrum of (a) pure styrene showing characteristic peak at 291 nm, and (b) UV-spectrum of pure CMS showing characteristic peak at 295 nm.

peak wavelength of toluene was at 278 nm (Figure 3-5), so there was no interference. Spectral data was obtained using a Shimadzu UV-2401 spectrophotometer. The standard calibration curves for styrene (Figure 3-6) and CMS were obtained by analysis of different concentrations in the photometric mode.

3.4.8 Gas chromatography analysis

Samples of ES-toluene were diluted 1:1 with pure methanol. ES concentrations were determined in the feed and permeate solutions using gas chromatography at an elution time of 1.56 minutes. The elution times of methanol and toluene are 0.1 and 0.2 minutes, respectively, so there was no interference. All reaction samples were analyzed using a Shimadzu GC-14A gas chromatograph equipped with a flame ionization detector. A 30m X 0.53mm i.d capillary column (Rtx-624, Restek Corporation) containing a 6% cyanopropylphenyl and 94% dimethyl polysiloxane based stationary phase was used for analysis. The gas chromatograph parameters are shown in Table 3-1. Helium was used as the carrier gas. Hydrogen and compressed air gases were used to ignite the flame. The GC range was kept at 3 in order to avoid flat top peaks and get good resolution. Figure 3-7 illustrates the standard calibration curve for ES obtained by analysis of different concentrations. The results from the extensive experiments carried out to synthesize and characterize these functionalized membranes will be discussed in the next chapter.

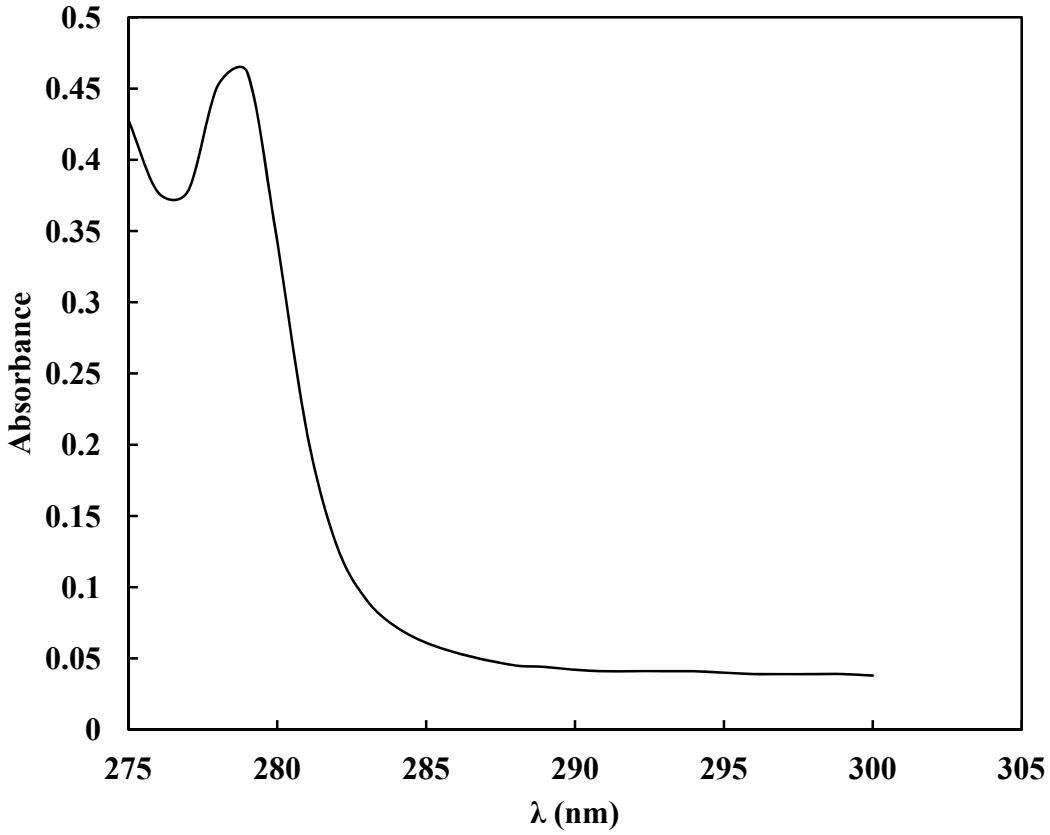

Figure 3-5. UV-spectrum of pure toluene showing characteristic peak at 278 nm.

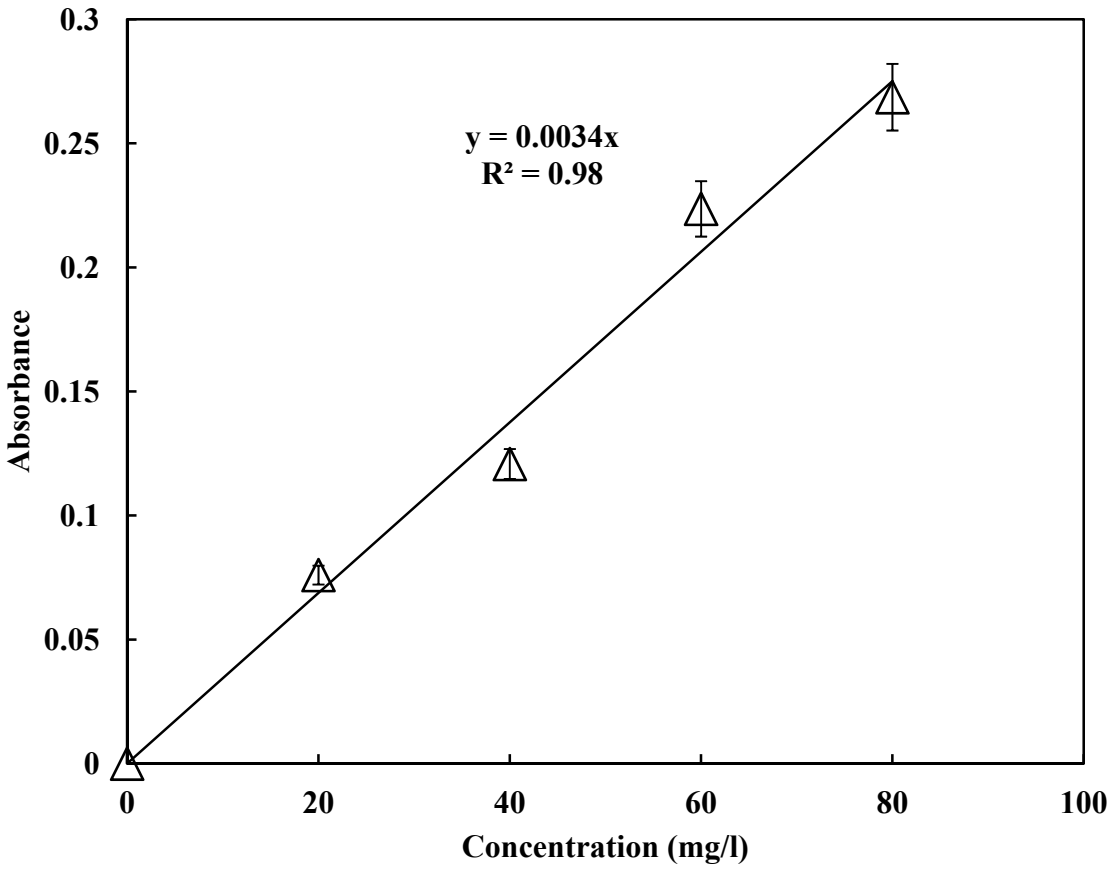

Figure 3-6. Standard calibration curve for styrene analysis at 291 nm by UV-spectrophotometry.

Table 3-1. Gas chromatograph column parameters.

Parameter	**Value**
Helium pressure (kPa)	470
Hydrogen pressure (kPa)	110
Air pressure (kPa)	120
Oven temperature (^{o}C)	125
Run time (min)	5
Range	3
Sample size (μl)	1

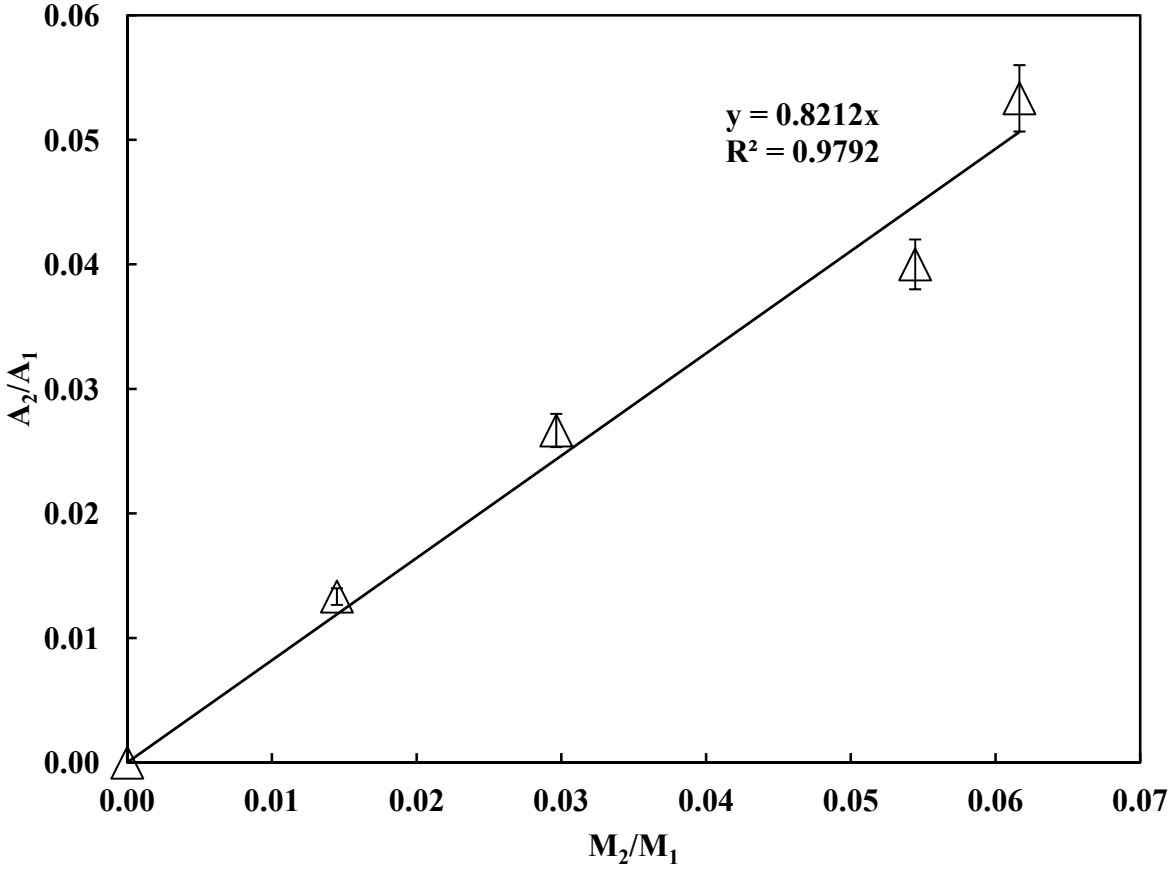

Figure 3-7. Standard calibration curve for ES analysis by gas chromatography.

A_2- Area under the curve for ES

A_1- Total area under the curve for toluene and methanol

M_2- % Concentration of ES

M_1- % Concentration of toluene and methanol

3.5 Phase 2: Development and characterization of functionalized membranes containing customized poly(styrene-co-HS) grafts and testing the performance of membranes for IgG adsorption

3.5.1 Preparation of functionalized membrane containing poly(styrene-co-HS) grafts

The pore surface functionalization of the commercially available PES membranes was achieved by cationic polymerization of styrene and ES by a three-step procedure. The first step was to immobilize the initiator sulfonic acid groups by permeating 250 ml of 0.5N H_2SO_4 solution for 3 hours. The membrane was then rinsed multiple times with water and air dried for 1 hour. In the second step, a 150 ml of 5 volume % mixture each of styrene and ES in toluene was permeated through the initiator functionalized membrane. Polymerization was carried out for 2 hours. Feed and product samples were collected for analysis by gas chromatography. The feed tank was washed with distilled water until all the traces of styrene, ES, and toluene were removed. Finally, 0.5N NaOH solution was permeated through the polymerized membrane for 3 hours. The reactions were carried out at room temperature and the flow rate was maintained at 1 ml/min by varying the pressure using the nitrogen cylinder regulator.

3.5.2 Functionalized membrane characterization by ^{1}H NMR spectroscopy

The composition of copolymers at different stages of functionalization was characterized by ^{1}H-NMR. The functionalized membrane was dried in air (approximately 1 hour) until the mass of the membrane was constant. The membrane was dissolved in a solvent mixture (volume ratio 1:1) of deuterated DMSO and $CDCl_3$, and 0.8 ml of the sample was transferred to a 5 mm dedicated NMR probe. ^{1}H-NMR spectra were recorded at a frequency of 500 MHz and ambient temperature by a Bruker spectrometer (Bruker AV500). Mnova 7, analytical chemistry software

developed by Mestrelab Research, was used to process the spectra and for analyzing and reporting the data.

3.5.3 Quantification of styrene and ES loss by gas chromatography analysis

The amount of styrene and ES reacted and retained on the membrane was determined by performing material balances on the feed and permeate solutions. The GC and column used were the same as described in section 3.4.8. The column parameters were the same as shown in Table 3-1 except that the helium pressure was changed to 450 kPa, the run time was 3 minutes, and the oven temperature was 120 ^{o}C. The elution times for toluene, styrene, and ES were 0.22, 0.36, and 1.95 minutes, respectively. Figure 3-8 and Figure 3-9 show the standard calibration curves prepared for analyzing unknown concentrations of styrene and ES in the copolymer mixture, respectively. Samples of known amounts of each monomer (1:1) in toluene were transferred to GC vials and kept in the sample compartment. EZStart software was used to generate and analyze the chromatogram. The x axis shows the percentage ratio of each monomer in toluene and the y axis shows the area ratio of each monomer to area of toluene at their corresponding elution times.

3.5.4 Quantification of IgG adsorbed by UV-vis spectroscopy

Feed and permeate concentrations of IgG samples were analyzed using a Shimadzu UV-2401 spectrophotometer at a characteristic wavelength of 280 nm (Figure 3-10). Baseline correction was performed by placing binding buffer (50 mM, pH 7.4) in the reference compartment, keeping the sample compartment empty, and recording the spectra. Samples (~0.5 ml) were transferred to a UV quartz cuvette for analysis. A calibration curve (Figure 3-11) was prepared for known concentrations ranging from 0.5 to 3 mg/ml for analyzing the unknowns.

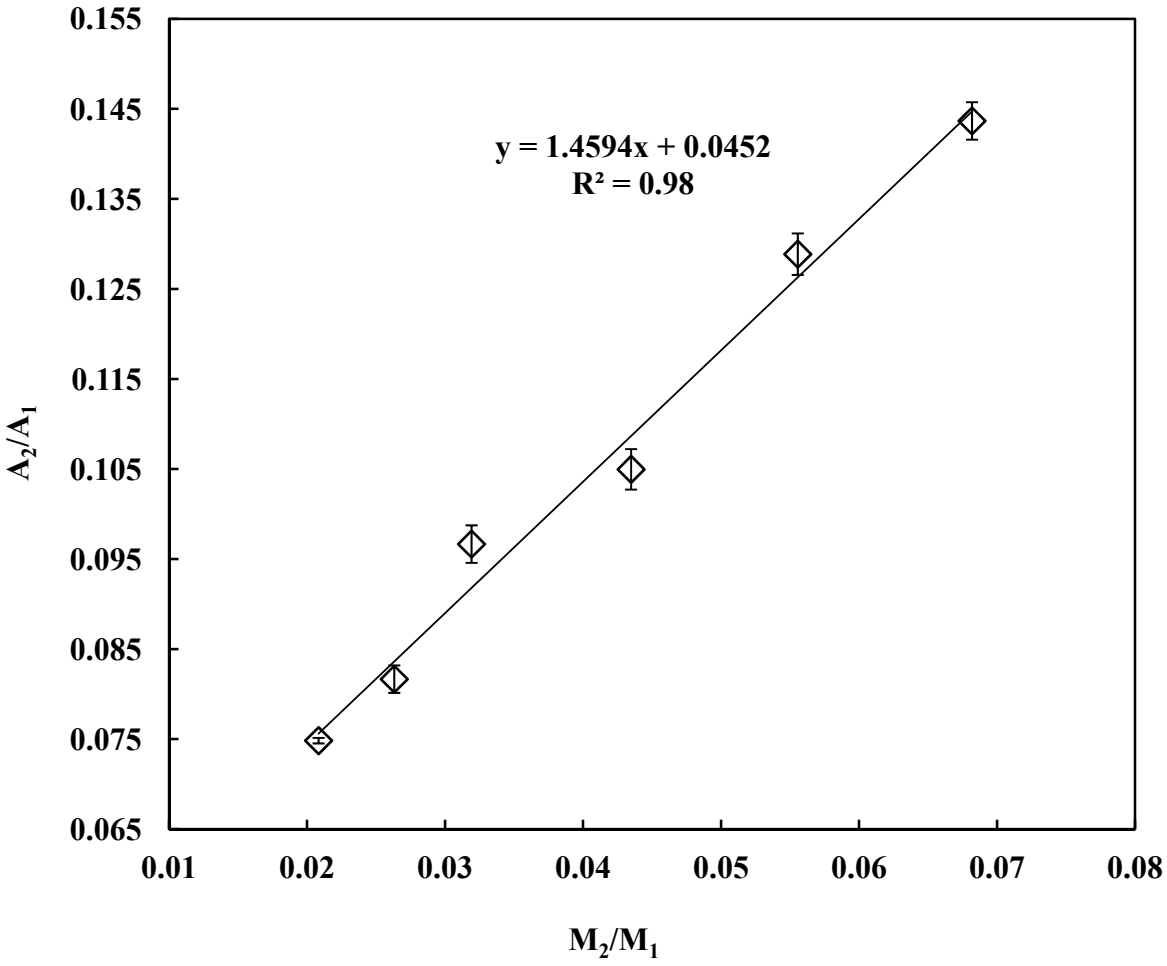

Figure 3-8. Standard calibration curve for ES analysis in copolymer mixture of styrene and ES by gas chromatography. Toluene was used as a solvent.

A_2- Area under the curve for ES

A_1- Total area under the curve for toluene

M_2- % Concentration of ES

M_1- % Concentration of toluene

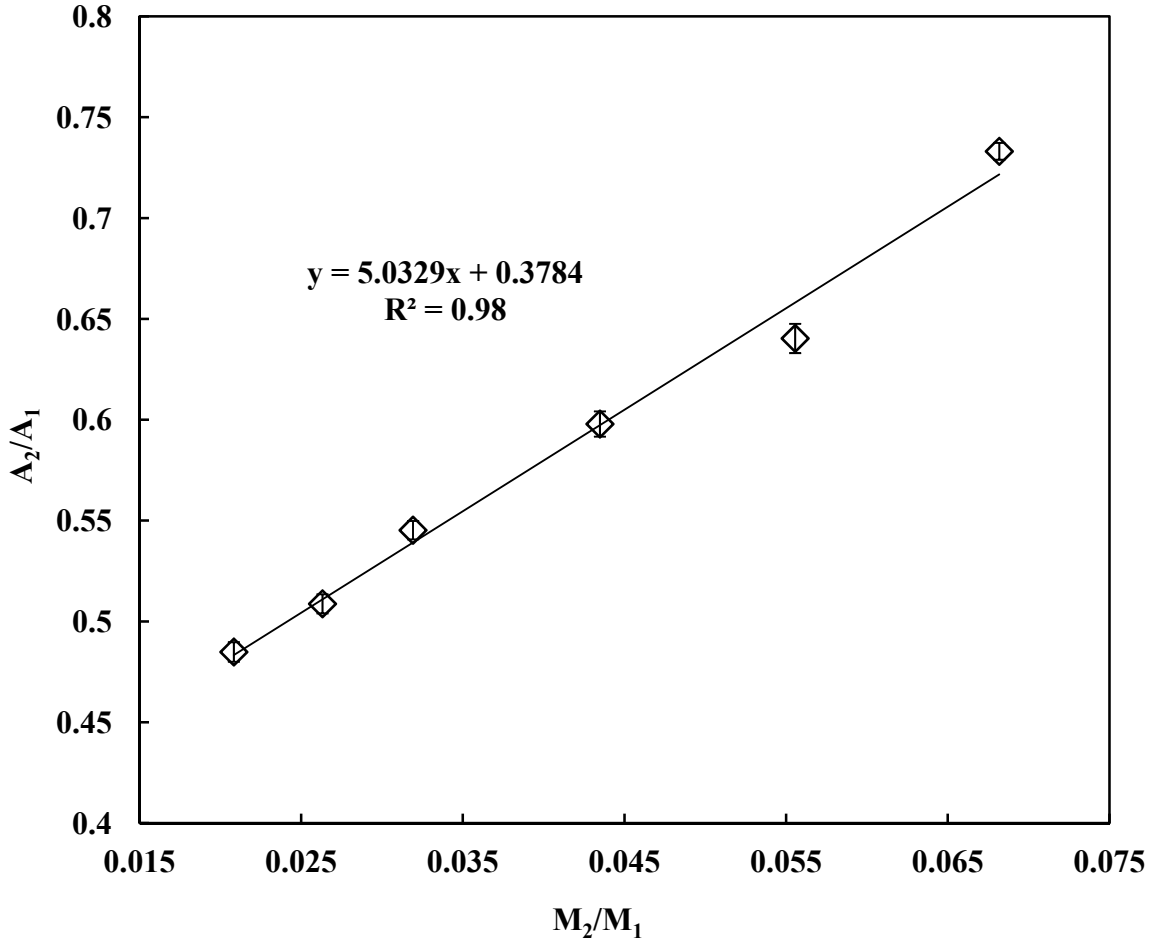

Figure 3-9. Standard calibration curve for styrene analysis in copolymer mixture of styrene and ES by gas chromatography. Toluene was used as a solvent.

A_2- Area under the curve for styrene

A_1- Total area under the curve for toluene

M_2- % Concentration of styrene

M_1- % Concentration of toluene

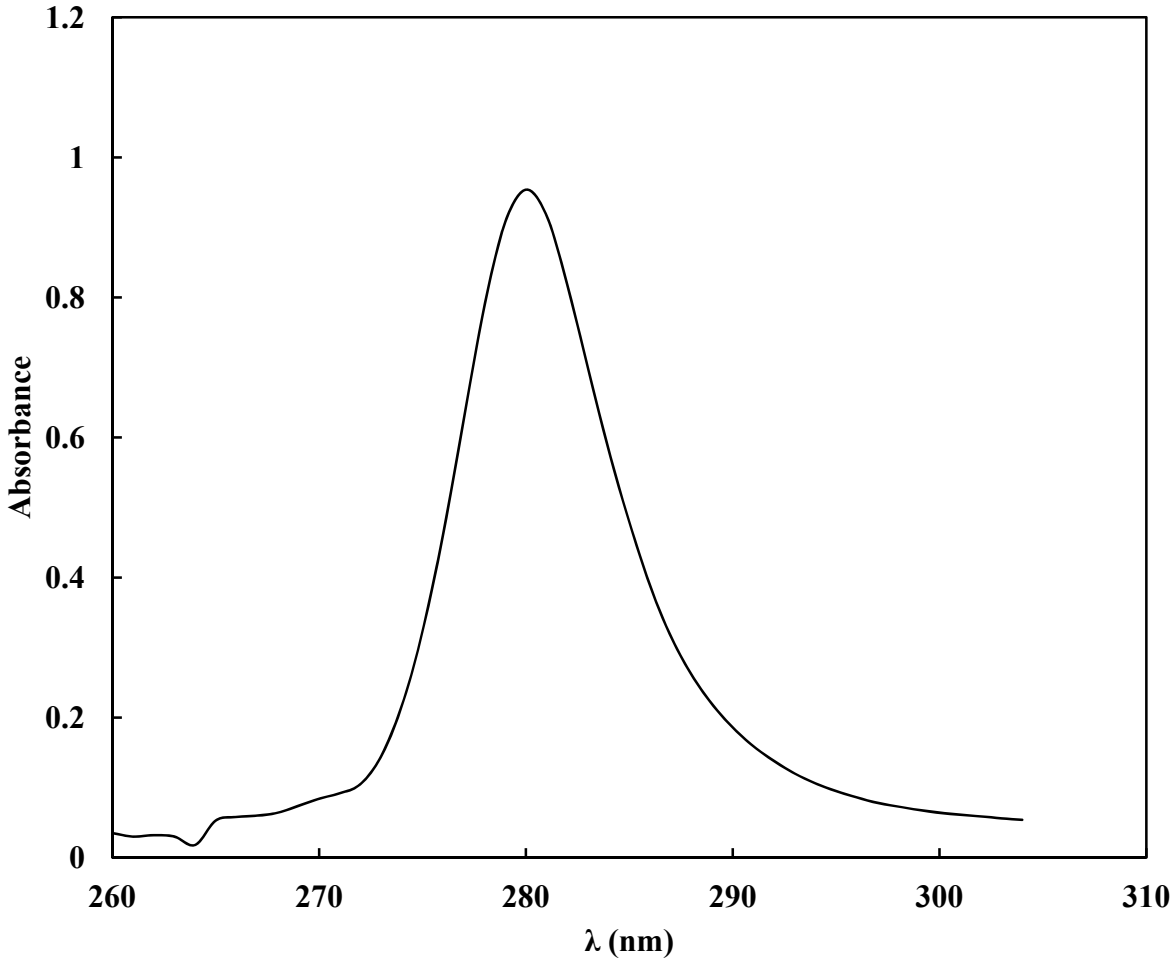

Figure 3-10. UV-spectrum of pure IgG (2 mg/ml) in binding buffer (sodium phosphate, 50 mM, pH 7.4) showing characteristic peak at 280 nm.

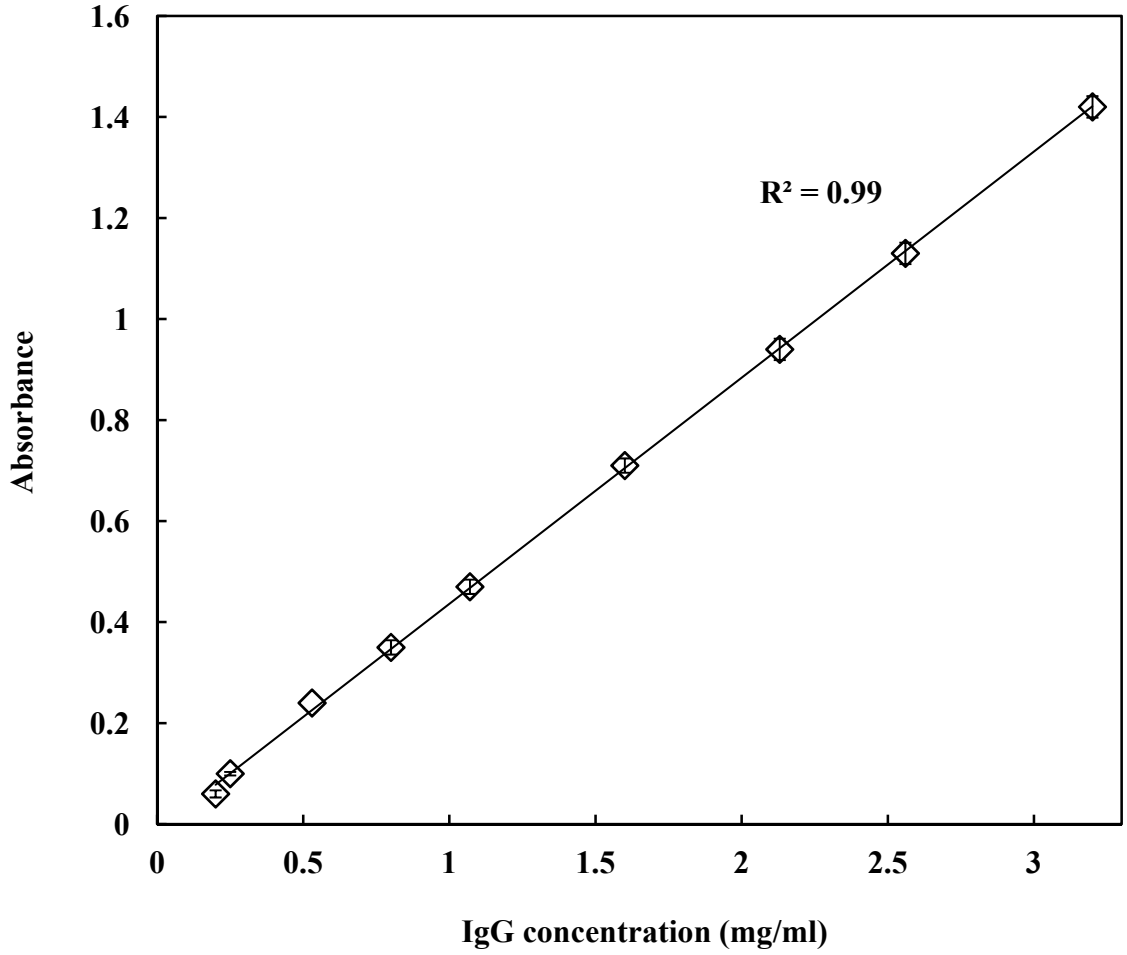

Figure 3-11. Standard calibration curve for IgG analysis at 280 nm by UV-spectroscopy.

The UVPC software was used to determine the peak wavelength of IgG, generate the spectrum, and perform data collection and analysis.

3.5.5 Size exclusion chromatography (SEC)

SEC was used to separate and quantify the amount of IgG and BSA adsorbed during competitive sorption where each biomolecule was present as 1:1 ratio in binding buffer. SEC measurements were performed using an AKTApurifier^{TM} UPC 10 instrument (GE Healthcare Life Sciences) equipped with monitoring of UV absorbance set at 280 nm. The column used was a Superdex^{TM} 200 10/300 GL column from GE Healthcare Life Sciences. The MWCO separation range for the column was between 10 kDa to 600 kDa. UNICORN v5.2 software was used for data collection and analysis. The flow rate through the column was maintained at 0.4 ml/min and temperature and pressure were kept constant at 7.9^{0}C and 0.67 MPa, respectively. The column was equilibrated with two column volumes of fresh buffer before injecting the samples. The column equilibration was confirmed by tracking the baseline UV absorbance of eluted buffer. Antibody stock solutions containing individual as well as 1:1 mass ratio of IgG and BSA in phosphate buffer (50mM, pH 7.4) were prepared to determine the elution times of each biomolecule. Concentrations of IgG and BSA were measured at elution times of 30.61 and 34.81 minutes, respectively. Sample volumes of 100 μL were manually injected into the instrument using a syringe. A calibration curve of absorbance versus concentration was generated using samples containing 1:1 ratio of IgG and BSA with the concentrations ranging from 0.5-3 mg/ml.

3.5.6 Functionalized membrane performance testing

3.5.6.1 Adsorption isotherm

Functionalized membrane containing poly(styrene-co-HS) grafts was placed in the membrane holder of the experimental setup. IgG solutions with concentrations ranging from 0.5

to 3 mg/ml in phosphate buffer (50 mM, pH 7.4) were permeated through the functionalized membrane for 1 hour. Additionally, the antibody solutions were permeated through raw and functionalized membranes containing poly(styrene-co-ES) (pre-hydrolysis) grafts to measure adsorption for comparison with the isotherm obtained for the functionalized membrane containing poly(styrene-co-HS) grafts. Feed and product samples were collected at regular intervals for each concentration. The concentrations of IgG were measured using UV-vis spectrometry at a characteristic wavelength of 280 nm using a calibration curve. Each breakthrough curve was generated and the DBC was calculated by integrating the differences between feed and product concentrations on the breakthrough curve, and dividing the mass of antibody adsorbed (mg) by the membrane volume (0.21 ml). The bound antibody was eluted by permeating citrate buffer having an ionic strength of 100 mM and pH 3.5. The membrane was then regenerated by permeating 150 mM phosphoric acid solution having a pH of 1.5. This protocol was repeated at different concentrations and a plot of DBC versus concentration was generated. Three experiments were performed and the DBC was reported as the average of three measurements.

3.5.6.2 Influence of polymerization reaction time on binding capacity

The initiator functionalized membrane was exposed for different polymerization reaction times ranging from 30 to 180 minutes. The membrane was then hydrolyzed with 0.5N NaOH solution for 3 hours. After each polymerization and hydrolysis step the antibody solution containing 3 mg/ml of IgG in binding buffer was permeated through the membrane. The DBC for each of these membranes polymerized with different polymerization reaction times was calculated from the breakthrough curve. For all reactions, initiator reaction time was 180 minutes and monomer feed concentration was 5 volume percent each for styrene and ES in toluene. Three

experiments were performed for each polymerization reaction time followed by hydrolysis and antibody binding.

3.5.6.3 Influence of flow rate on binding capacity

Functionalized membrane containing poly(styrene-co-HS) grafts was used to study the effect of flow rate on binding capacity. After functionalization the membranes were taken out of membrane holder and kept immersed in water for 3 hours. This increased the mechanical strength of membrane to withstand higher flow rates and prevented the membrane from cracking. Antibody solution containing 3 mg/ml of IgG in binding buffer was permeated through the membrane at different flow rates. The flow rates were varied from 1 to 50 ml/min by pressurizing the system until 30 psig and keeping the ball valve downstream of membrane holder to full open position. The DBC was determined at each flow rate by performing an overall material balance on feed and product solutions. Two measurements of DBC were taken for each flow rate and the average values were reported.

3.5.6.4 Bind and elute

Functionalized membrane was equilibrated with 50 mM sodium phosphate buffer (100 ml) containing 150 mM sodium chloride at pH 7.4. The permeate solution was collected and analyzed for graft loss using UV-vis spectrophotometry at characteristic wavelengths of 291 and 283 nm for styrene and ES, respectively. Then 3 mg/ml of antibody solution was permeated through the membrane for 1 hour at a flow rate of 1 ml/min. The permeate was collected at regular intervals, and then concentration was measured using UV-vis spectrometer at a peak wavelength of 280 nm. This was followed by permeating washing buffer (same as binding buffer) for 1 hour to elute out the unbound antibody. The washed permeate was again analyzed using UV-vis spectrometer for IgG at the characteristic wavelength of 280 nm. Thereafter, the

bound antibody was eluted by permeating 100 mM citrate buffer at pH 3.5 for 1.5 hour. The permeate solution was analyzed to measure the concentration of eluted antibody using the calibration curve. All solutions were permeated for 1 hour at a flow rate of 1 ml/min and a pressure of 21 psig unless otherwise stated. Next, the membrane was regenerated by permeating 150 mM of phosphoric acid solution, pH 1.5, to remove the strongly bound antibody molecules. This procedure was followed each time for a period of five cycles of equilibration, binding, washing, elution, and regeneration. The amount of eluted antibody was calculated by multiplication of the concentration of the eluted antibody with volume of solution. The average percentage recovery was estimated as the average of percentage ratio of IgG eluted to IgG adsorbed over a period of five cycles.

3.5.6.5 Competitive sorption

A 5 volume % chloromethylstyrene in toluene solution was permeated through the poly(styrene-co-HS) grafted membrane at a flow rate of 1 ml/min for 2 hours. The membrane was then rinsed with two washes of pH 8 PBS buffer. Next, a 500 mg/L of glycine in PBS buffer (pH 8) was permeated through the membrane for 3 hours at a flow rate of 1 ml/min. Then the membrane was washed with phosphate buffer (50 mM, pH 7.4) until no absorbance was seen on UV spectrum. The peak wavelength for styrene and chloromethyl styrene are 291 and 295, respectively. Thereafter, 3 mg/ml each of IgG and BSA in binding buffer was permeated through the membrane for 1 hour. The permeate samples were collected at regular intervals and the concentrations of BSA and IgG were measured by SEC. Figure 3-12 shows the SEC chromatogram with elution times for IgG and BSA were 30.61 and 34.81 minutes, respectively. Calibration curves were generated for each of BSA and IgG by measuring the peak absorbance at

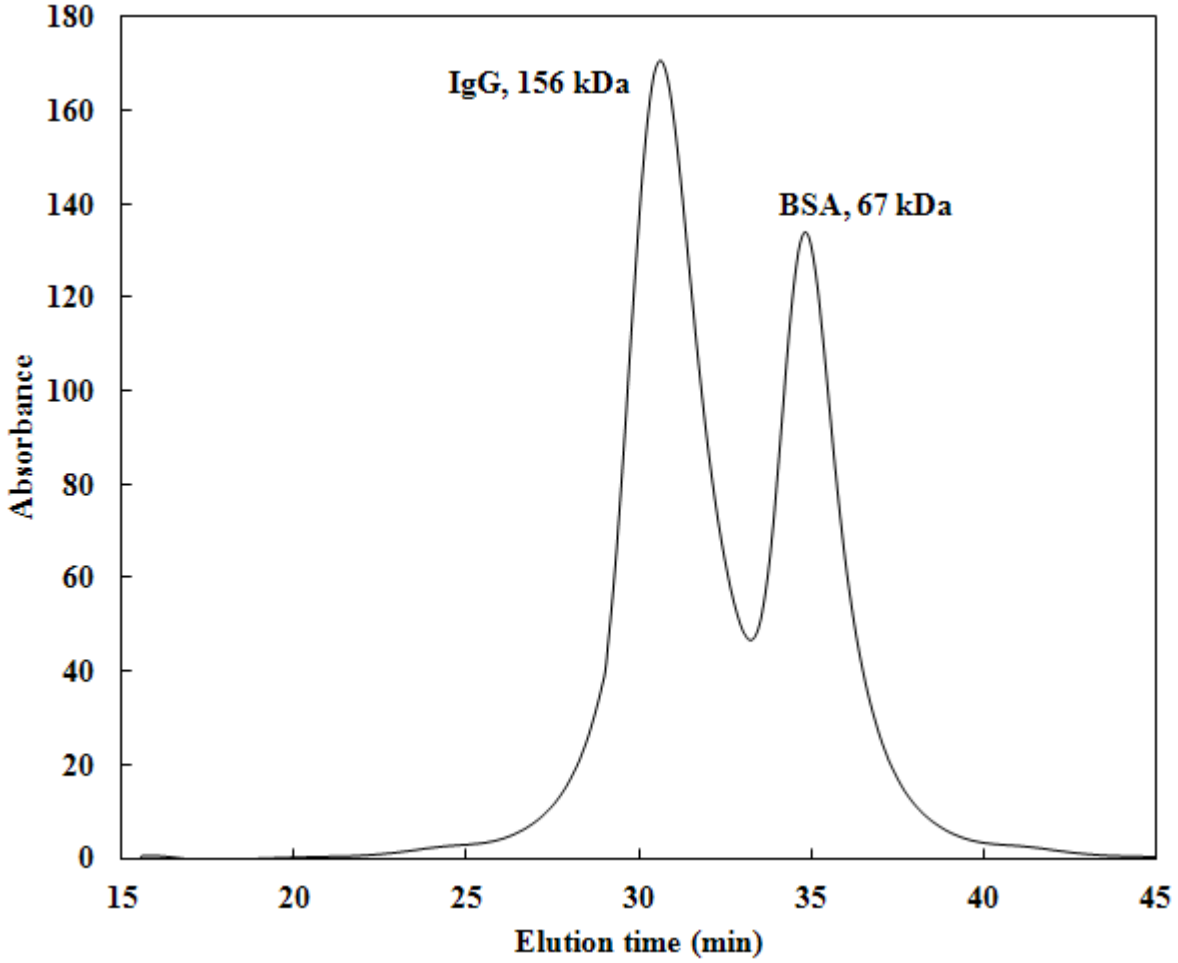

Figure 3-12. Analytical size-exclusion chromatogram of IgG (156 kDa) and BSA (67 kDa) in binding buffer (sodium phosphate, pH 7.4, 0.5M NaCl). Absorbance was recorded at 280 nm.

their respective elution time for different concentrations. A graph of absorbance versus concentration was plotted to determine the concentration of unknown samples.

CHAPTER 4
RESULTS AND DISCUSSION

4.1 Introduction

This chapter describes detailed results and discussion involved in the development and characterization of a functionalized membrane containing multiple adsorptive sites mimicking ligands in affinity chromatography. Modifications to the functionalized membrane have been characterized and quantified at each stage. In phase 1, functionalized membranes were studied in terms of synthesis and quantification of initiator immobilization and polymerization reactions. This includes formation of homopolymer and block copolymer grafts, and determination of ion-exchange capacity, average graft length and membrane permeability. Furthermore, influences of initiator contact time and monomer feed concentration on polymer growth have been studied and discussed. In phase two, using the knowledge of phase 1, customized copolymer grafts mimicking the Phe-132/Tyr-133 dipeptide structure of protein A were grafted in the membrane pores. Functionalized membranes were then tested for selective adsorption of IgG. Detailed discussions on performance properties of these membranes in terms of DBC and selectivity are also reported in this chapter. The influence of parameters like polymerization time, antibody feed concentration, and flow rate on DBC have been studied and discussed in depth. ^{1}H NMR characterization clearly showed grafting of polymers grafts and stable side moieties at different stages of functionalization. These membranes have high dynamic binding capacity, selectivity, can be regenerated and are expected to be effective for large scale purification of MAbs.

4.2 Phase 1: Synthesis and characterization of homopolymer and block copolymer grafts in the pores of PES MF membranes

4.2.1 Membrane permeability studies

Permeability studies were carried out in a batch mode. A flat sheet membrane disc made from PES was used in all experiments. The PES membranes were sealed with a 4.1 cm inner diameter o-ring. Therefore, 4.1 cm was considered as the membrane effective diameter for calculating the flux. The membrane effective area was 13.2 cm^2. Pure water permeation flux is directly proportional to pressure drop, and the slope of the straight line gives the membrane permeability.

Permeability studies were carried out on raw, sulfonated, styrene grafted and styrene-b-ES grafted membranes to compare the effects of polymer graft formation on membrane flux. Polymer growth in the pores of the membrane should reduce the effective pore size in each case, and therefore a decrease in permeability was expected. Figure 4-1 illustrates the effect of each treatment on water flux of the membrane. The permeability of the raw membrane was computed to be 1.98 $ml/cm^2/min/psi$. The permeability decreased by 58% after sulfonation. An increase in $SO_3^-H^+$ group density decreased the permeability of the pure water. This is most likely due to the sulfonation reaction forming hydrogel in the pores that would constrict the membrane pores reducing the effective pore size. A film of hydrogel might have formed around the periphery of the pores that resulted in narrowing of pore diameter and therefore drop in permeability. Similar results have been reported in the literature where SEM micrographs have confirmed formation of hydrogels due to sulfonation of aryloxy or arylamino groups linked to polymers like phosphazenes [134]. Sulfonation was followed by polymerization of styrene which resulted in further reduction of the permeability by 3.3 times. This is because polystyrene grafts were

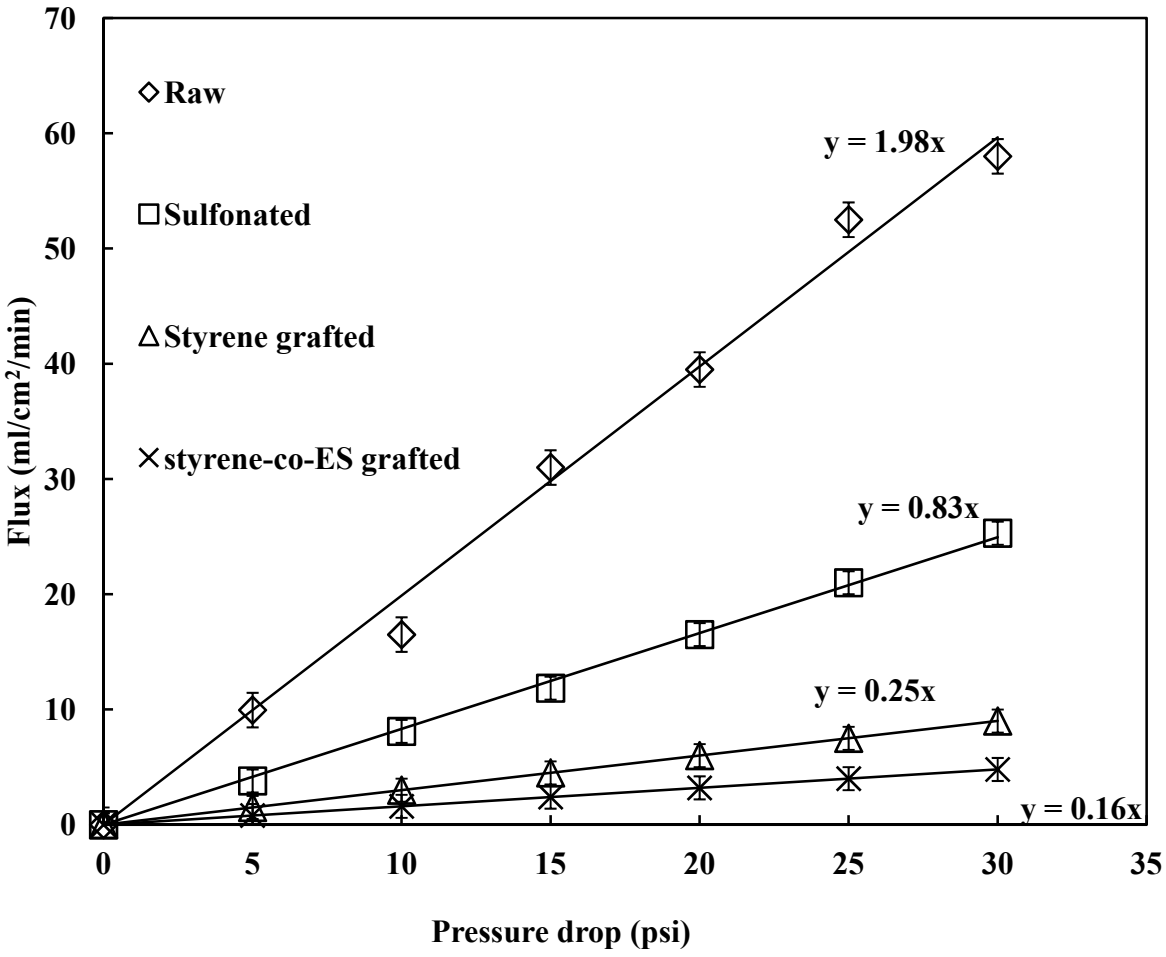

Figure 4-1. Polymer growth effect on membrane permeability.

formed in the membrane flow path, reduced the effective pore size, and consequently decreased the permeability. Styrene polymerization was sequentially followed by ES polymerization. The decrease in permeability in this case leads to further reduction of 1.5 times as compared to the styrene grafted membrane. This is because the longer polymer grafts increased resistance to flow. The results are consistent with results reported by other researchers where they have observed a drop in permeability after functionalization showing evidence of polymer grafting [34, 128, 135]. It should be noted that the permeability of styrene-b-ES grafted membrane is 0.16 ml/cm^2/min/psi which is higher than the permeability of a 300 kDa MWCO PES UF membrane (0.02 ml/cm^2/min/psi) based on the manufacturer reported test criteria. Therefore, although the pore size is reduced, these materials are still microfiltration membranes and are not plugged by formation of polymer grafts.

4.2.2 Characterization

Figure 4-2(a) shows the ^{1}H-NMR spectrum of poly(CMS) grafted in the pores of a PES membrane. The sharp signal at δ = 1.57 ppm was assigned to water. The peak at 1.7 and multiplets from 1.25 to 1.48 ppm represent the methine and methylene protons attached to the benzene ring, respectively [136-137]. Integration of the peaks yielded a relative ratio of 1:2 which further confirmed the assignment of peaks to methine and methylene. The characteristic signal for the chloromethyl group can be seen at 4.5 ppm [137-139]. The integral values of peaks for the chloromethyl groups of CMS and poly(CMS) were the same, indicating that the chloromethyl moiety was stable and had not undergone any side reactions. Peaks at 5.3, 5.8 (=CH-) and 6.75 (=CH_2) were assigned to unreacted vinyl protons of the monomer (CMS) [139]. However, by comparing the integral values it was observed that these peaks make a very small contribution to the spectrum and hence can be neglected. This indicated that the double bond of

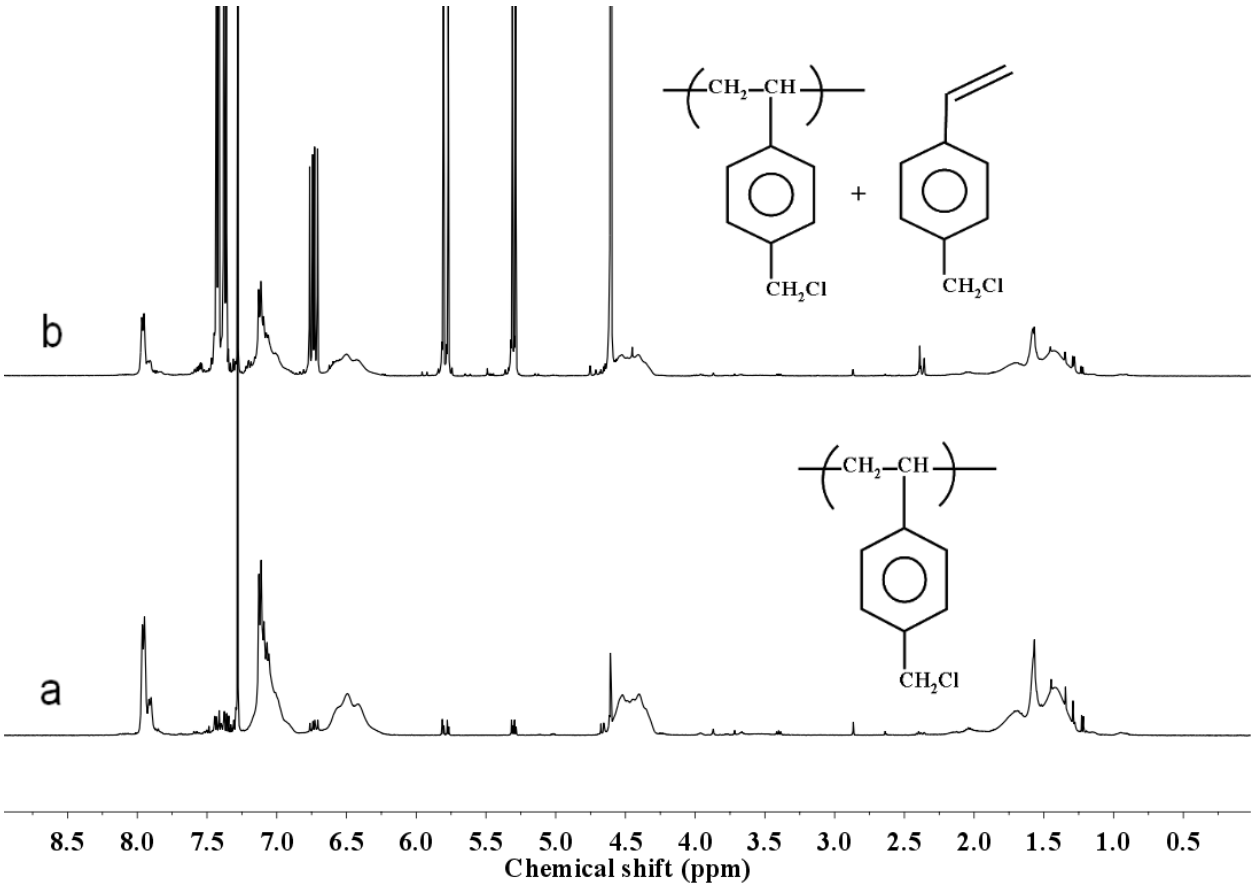

Figure 4-2. ^{1}H NMR spectra of (a) poly(CMS), and (b) poly(CMS) spiked with pure CMS.

the vinyl group (-CH=CH_2) is changed to single bond (-CH-CH_2-) after reaction with the PES backbone. The multiple peaks between 7 and 8 ppm corresponded to aromatic protons on the two phenyl rings of each PES repeat unit [140-141]. The signal at 7.28 ppm was from the solvent. The aromatic protons of pure CMS showed signal at 7.38 and 7.42. After polymerization reaction these protons were shifted to 6.4-6.8 with a broad signal which was characteristic of the polymer. Figure 4-2(b) shows the NMR spectrum of a sample of poly(CMS) spiked with pure monomer. The intensity of signals at 5.3, 5.8 and 6.75 which are the characteristic signals for protons on the vinyl backbone increased with addition of pure monomer. The intensity of aromatic protons of pure CMS at 7.38 and 7.42 also increased. This further gave evidence that double bond of vinyl group was broken and poly(CMS) was synthesized.

Figure 4-3(a) shows the NMR spectrum of poly-ES grafted in the pores of PES membrane. The quartet at 3.98 ppm was assigned to the -CH_2- protons of the ethoxy group (-OCH_2-CH_3). The triplet between 1.29 and 1.33 ppm was assigned to the –CH_3 protons of the ethoxy pendant group. The multiple peaks between 6.8 and 8 ppm were characteristic of the protons on aromatic rings of poly-ES and the PES repeat unit. The signal at 2.5 ppm was from the DMSO solvent. Figure 4-3(b) shows the NMR spectrum of a sample of poly-ES spiked with pure monomer. It can be seen that new peaks at 5, 5.5 and 6.5 appear on the spectrum. These peaks are characteristic of the protons on the vinyl backbone. The breaking of the double bond on the vinyl backbone causes these peaks to disappear in Figure 4-3(a), and peaks between 1 and 2.4 were assigned to protons on methine and methylene groups arising from cleavage of the double bond.

Figure 4-4 and Figure 4-5 show the NMR spectra of poly(styrene-b-CMS) and poly(styrene-b-ES), respectively. As seen during the formation of homopolymers, the chemical

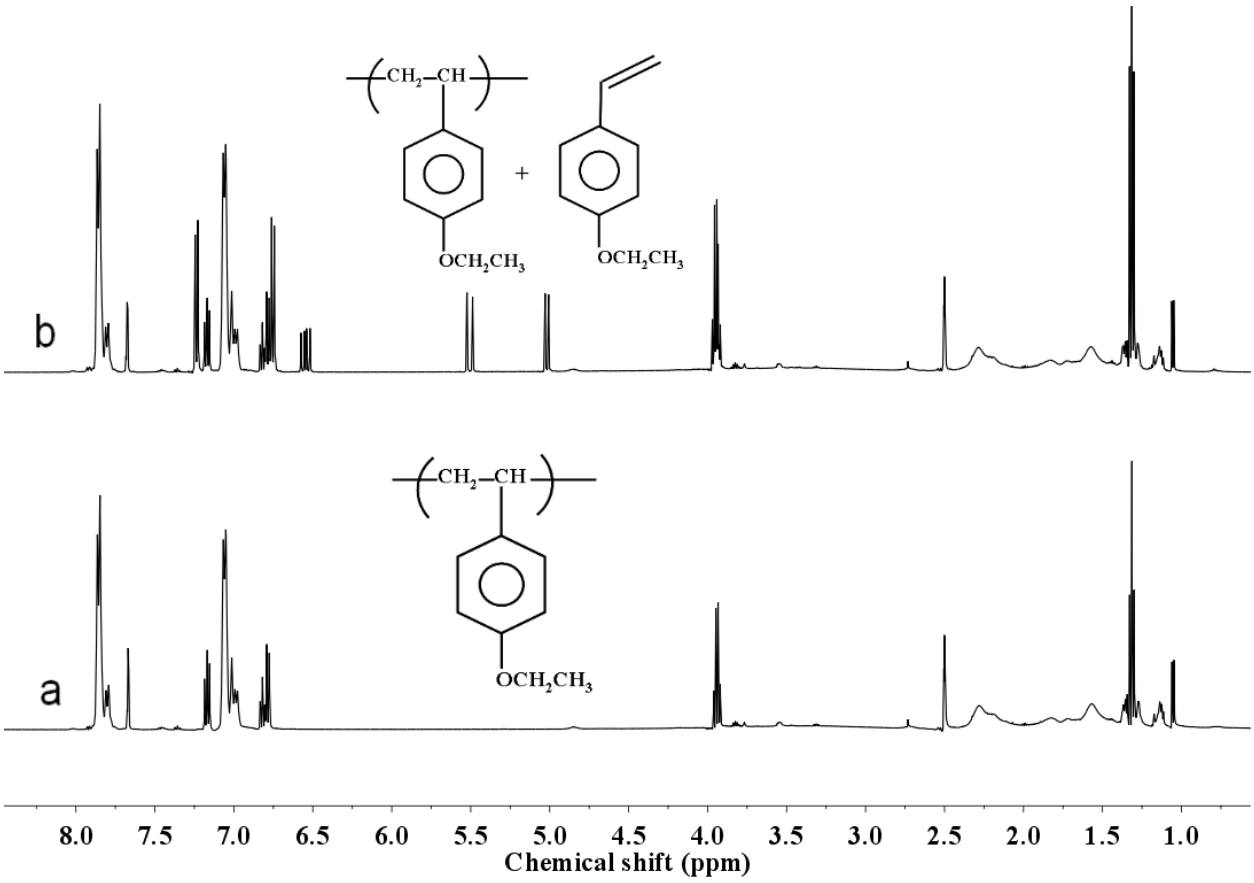

Figure 4-3. ^{1}H NMR spectra of (a) Poly-ES, and (b) Poly-ES spiked with pure ES.

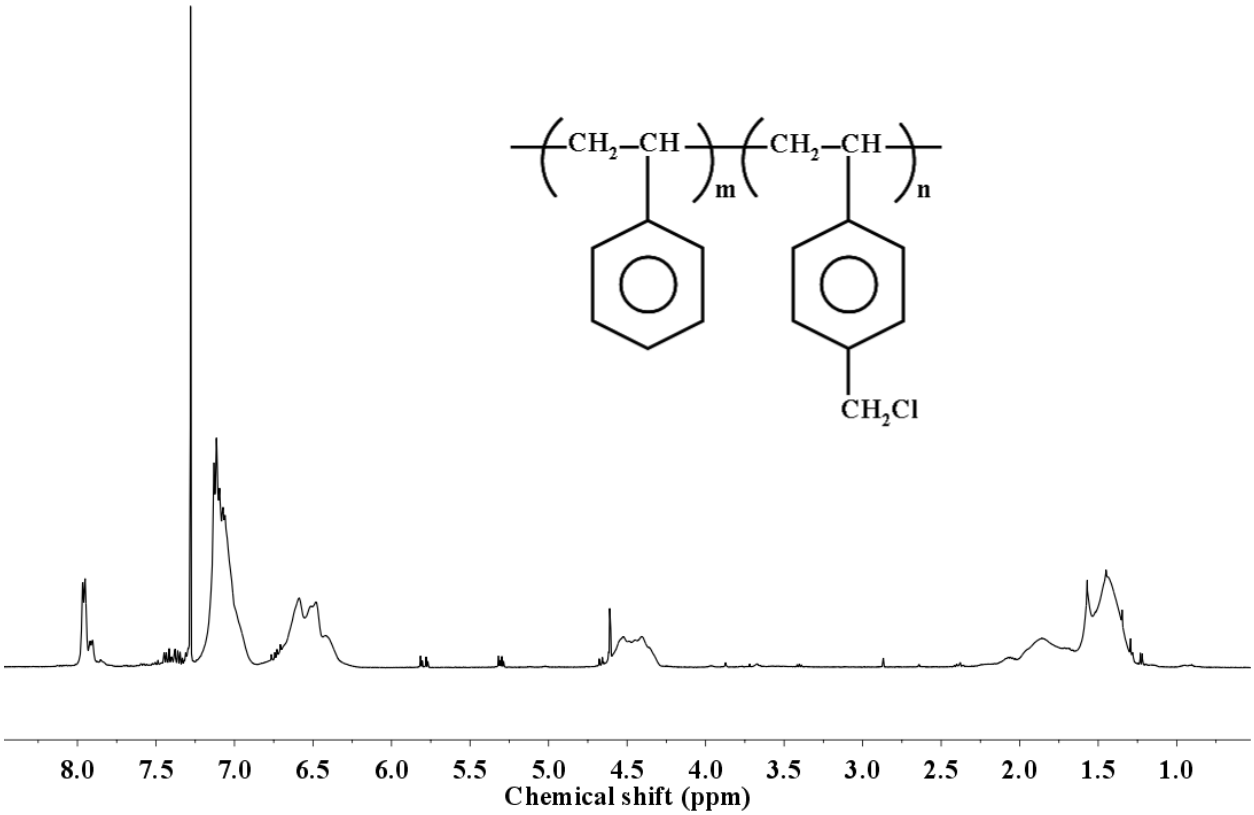

Figure 4-4. ^{1}H NMR spectra of poly(styrene-b-CMS).

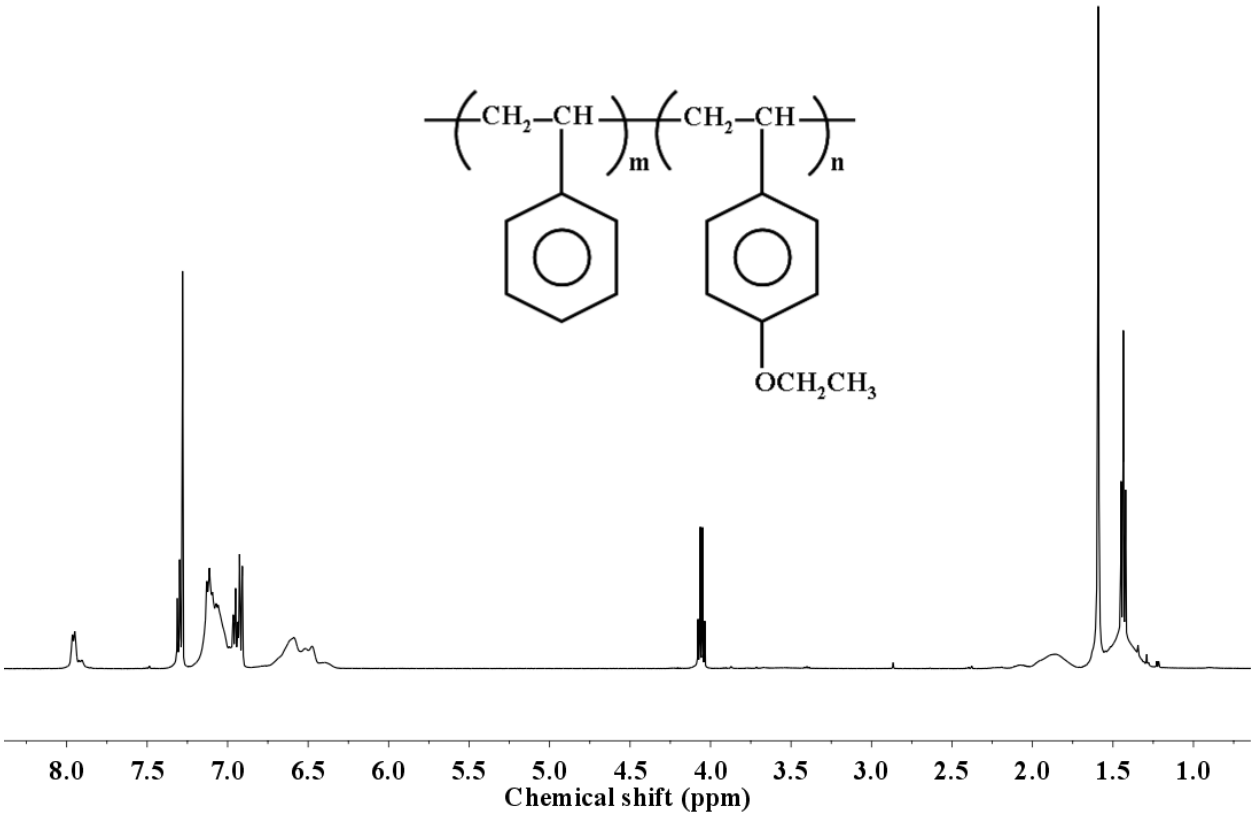

Figure 4-5. ^{1}H NMR spectra of poly(styrene-b-ES).

shift at 4.5 ppm was characteristic of the chloromethyl (–CH_2Cl) moiety on CMS monomer. The signals at 4.1 and 1.4 ppm were assigned to –CH_2– and –CH_3 group of ethoxy moiety. The broad signals from 6.4 to 8 ppm were from the aromatic protons on the phenyl ring of polystyrene, poly(ES), and poly(CMS). The signals from 1.2 to 2.2 are from the methine and methylene groups on the polymer backbone.

4.2.3 Quantification of initiator immobilization

The raw PES membrane was sulfonated to immobilize sulfonic acid groups as initiator for cationic polymerization. The sulfonic acid concentration was quantified by ion-exchange studies. IEC is the parameter that quantifies the number of ionizable groups in the membrane. IEC was determined in terms of milliequivalents of sodium ion exchanged per gram of membrane (dry weight).

The IEC of the raw membrane was determined experimentally to be 0.013 meq/g dry membrane. Ionizable groups were present due to mild surface modification performed by the manufacturer to improve membrane hydrophilicity. Sulfonated PES membrane has a maximum theoretical IEC of 0.32 meq/g. This value is based on an average pore size of 0.22 μm and 70% membrane porosity, yielding a total internal surface area of 30.75 m^2/g based on parallel, cylindrical pores with length equal to membrane thickness [40]. The IEC of the sulfonated membrane was experimentally determined to be 0.15 meq/g. This represents 46% of the maximum theoretical IEC. The higher IEC of the sulfonated membrane relative to the raw membrane was attributed to immobilized sulfonate groups in the membrane. The raw membrane represented less than 10% of the IEC of the sulfonated membrane. In addition, the internal surface area was >99.9% of the total membrane area, and therefore sulfonate groups are mostly in the pores of the membrane and not on the external surface area. The results are consistent with

work done by Ritchie and coworkers who demonstrated successful introduction of sulfonic acid group onto PES [40].

4.2.4 Styrene, CMS and ES graft quantification

Decreases in styrene and CMS concentrations, and thus retention in the membrane, were observed and quantified by decreases in the absorbance at the characteristic peaks of 291 and 295 nm, respectively, by UV-Visible spectroscopy (UV-vis). It was observed that approximately 0.65 mmol of styrene and 0.4 mmol of CMS were retained on the membrane. Negligible decreases in absorbance were observed for either monomer when permeated through the raw membrane. This confirms that there was negligible graft formation in the pores of the membrane by cationic polymerization in the absence of initiator sulfonic acid groups. Additionally, when permeate samples were diluted in methanol to perform UV analysis no precipitation or cloudiness was observed. This confirmed that there was no loss of polystyrene grafts and were retained in the pores of membrane.

The characteristic peak for ES by UV-vis was observed to be 283 nm. This was very close to the characteristic peak for toluene at 281 nm, and therefore some amount of overlapping was seen on the spectrum. However, gas chromatography showed very clear and distinct separation between peaks for ES, toluene and methanol. Consequently, the decrease in ES permeate concentration was quantified using gas chromatography at an elution time of 1.56 minutes which is far from methanol (0.1 minutes) and toluene (0.2 minutes). It was observed that 0.52 mmol of ES was retained on the membrane.

4.2.5 Kinetics of each monomer reacted

The amount of monomer retained on the membrane was measured at definite intervals of time over 120 minutes. The membrane volume was calculated to be 0.21 ml based on an

effective diameter of 4.1 cm and a thickness of 165 μm. Concentration was measured in terms of mmol of styrene reacted per ml of membrane. Figure 4-6 shows the plot of concentration versus time. It was observed that reaction of monomer was initially rapid and then gradually slowed down. This is most likely due to initial availability of active sites for polymerization. The growing grafts form a diffusion barrier that gradually slows down the reaction rate.

The pseudo-first-order kinetic expression shown in Equation 1 was used to model the experimental data [142-143]:

$$Q_t = Q_e(1 - e^{-kt}) \quad (1)$$

where Q_e and Q_t (mmol·ml^{-1}) are the amounts of monomer retained on the membrane at equilibrium and at time t (min) respectively, and k (min^{-1}) is the pseudo-first-order rate constant. The parameter Q_e was treated as an adjustable parameter in the above expression. The value of Q_e was determined by performing regression analysis using the method of least squares to best fit the model with experimental data. The linearized form of Equation 1 is shown in Table 4-1. The values of the rate constant, k, were determined from the slope of the straight line obtained by plotting $\ln(Q_e-Q_t)$ versus t. The values of k, Q_e and correlation coefficients (R^2) are shown in Table 4-1.

It was observed from the R^2 values that the model correlates well with the experimental data. By comparing the rate constants for different monomers it was observed that styrene and ES reacted approximately at the same rate while CMS reacted nearly 25% slower than styrene and ES. Furthermore, the slope between 100 and 120 minutes is still positive and not showing a plateau. This indicates that although the rate is gradually slowing down, the amount of monomer retained on membrane has not reached a maximum value and may increase if reaction is carried out beyond 120 minutes. This result is correlated with the model which shows a computed value

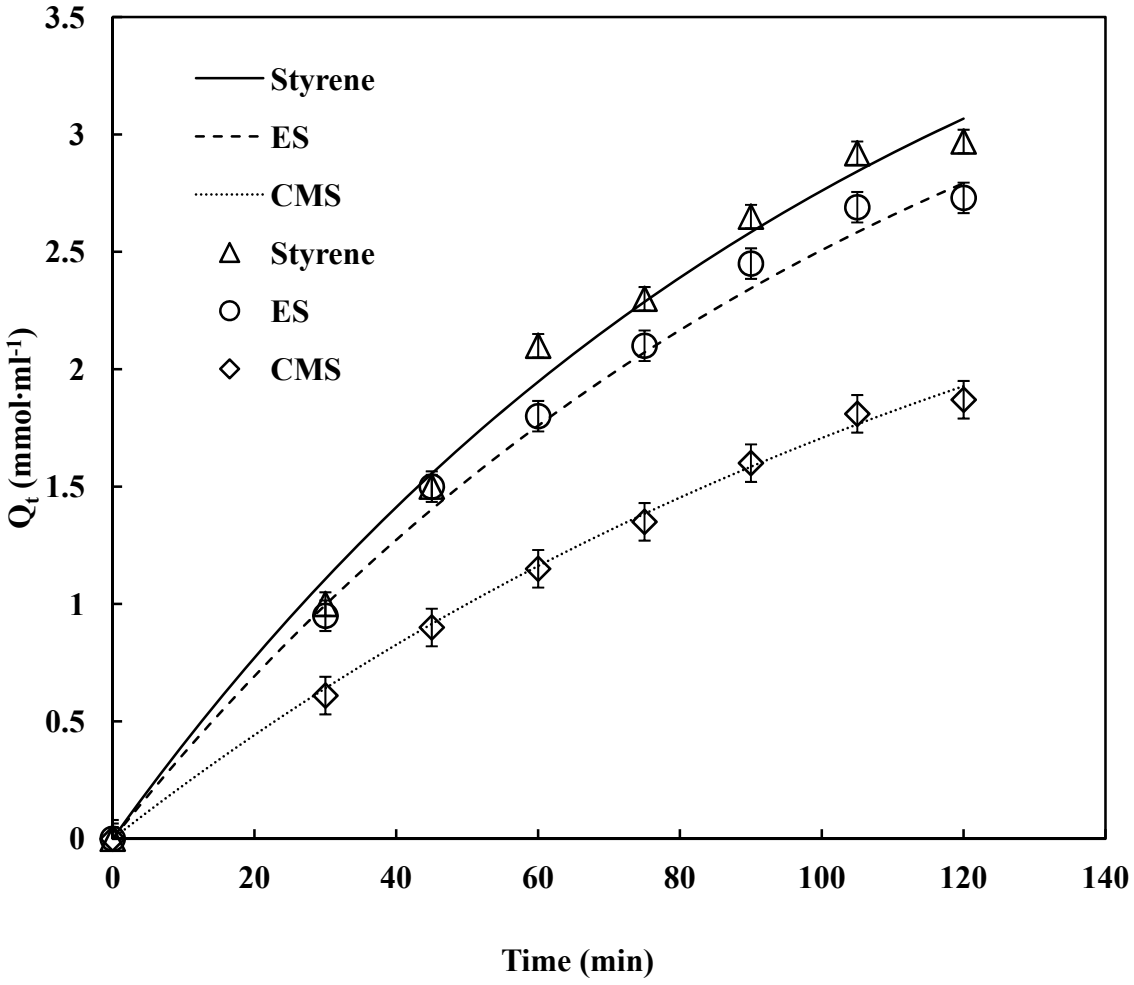

Figure 4-6. Kinetics of each monomer reacted. The smooth curves represent the pseudo-first-order equation fit and the data points represent experimental observations.

Table 4-1. Pseudo-first-order model parameters.

$$\ln(Q_e - Q_t) = \ln Q_e - kt$$

Monomer	k (min^{-1})	Q_e ($mmol \cdot ml^{-1}$)	R^2
Homopolymers			
Styrene	0.0092	4.6	0.9883
ES	0.0088	4.3	0.9914
CMS	0.0069	3.4	0.9974
Block copolymers			
Poly (styrene-co-CMS)	0.0059	2.2	0.9968
Poly (styrene-co-ES)	0.0075	3.8	0.9929
Different monomer feed concentration			
5 vol% styrene	0.0092	4.6	0.9883
10 vol% styrene	0.020	5.6	0.9613
15 vol% styrene	0.024	9	0.9721

of Q_e greater than predicted at 120 minutes of polymerization reaction time. Hence, the model holds well until 120 minutes of polymerization reaction time. However, the validity of the model needs to be investigated for reaction times beyond 120 minutes. The amounts of monomer reacted each for styrene, ES and CMS were 2.97, 2.73 and 1.87 $mmol \cdot ml^{-1}$, respectively, at 120 minutes of reaction time. This indicated that CMS is the least reactive and styrene and ES showed approximately similar reactivity.

The low reactivity of CMS is due to the strong electron-withdrawing chloromethyl substituent. Chlorine is highly electronegative and moves electron density away from the ring due to the negative inductive effects. The presence of an electron-withdrawing substituent inhibits the reactivity of monomer because cationic polymerization is limited to electron-donor substituents. Additionally, one of the two lone pairs of electrons on the oxygen forms a pi orbital overlap (resonance effect) which gives the oxygen an overall positive charge pushing the monomer towards the negatively charged initiator. Therefore, the higher reactivity of ES relative to CMS was reasonable. The results are consistent with those reported by Kamigaito and co-workers [136]. In their work, CMS showed low reactivity relative to styrene during homopolymerization and copolymerization by cationic polymerization using alcohol as an initiator and boron trifluoride etherate as an activator. Their work also showed that methoxy styrene was more reactive than CMS. This confirms that a monomer with an electron-donor group (alkoxy) is more reactive than a monomer with an electron-withdrawing group (chloromethyl).

4.2.6 Kinetics of CMS/ES during formation of block copolymer grafts

Figure 4-7 shows amounts of CMS and ES retained on the membrane after polymerization with styrene. The pseudo-first-order rate expression discussed in section 4.2.5

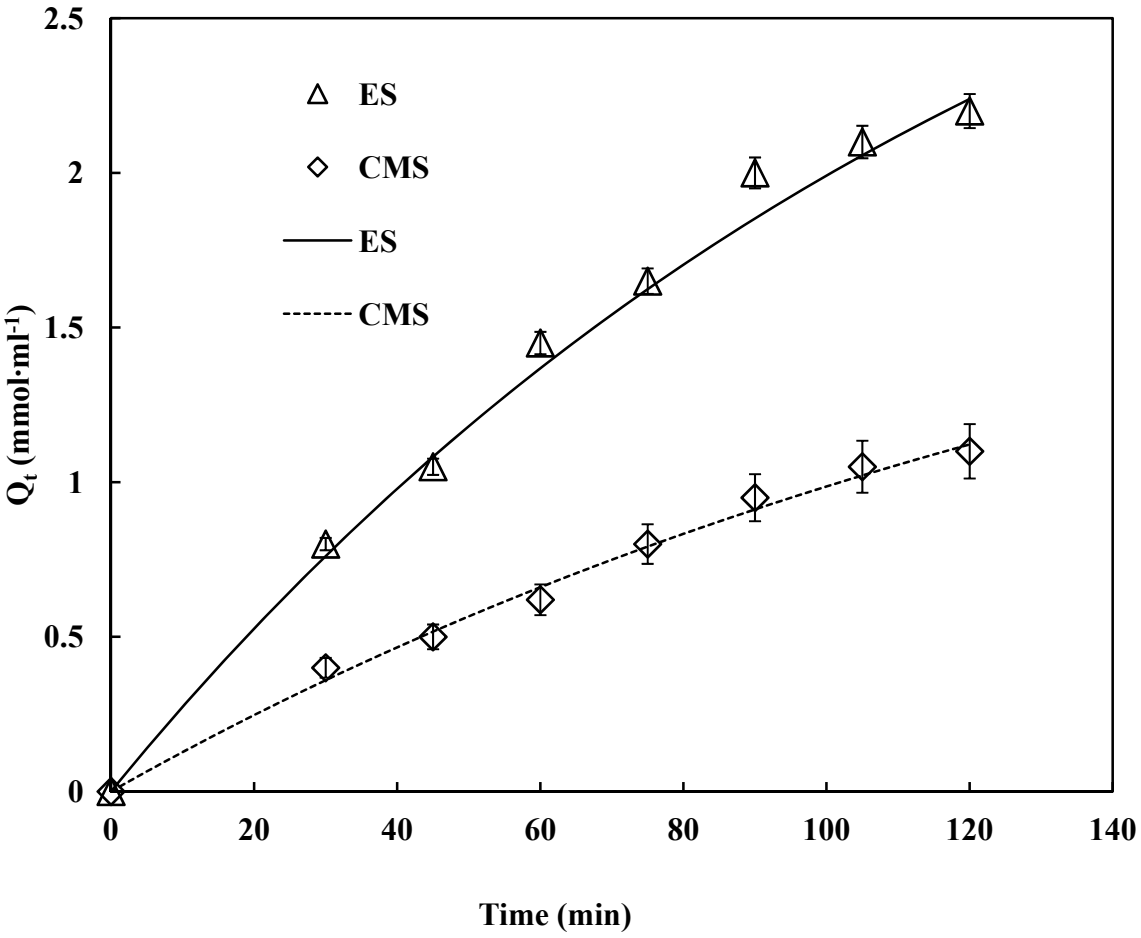

Figure 4-7. Kinetics of CMS and ES reacted after polymerization with styrene. The smooth curves represent the pseudo-first-order equation fits and the data points represent the experimental observation.

was used to model the experimental data. Correlation coefficients show reasonably good fits of the experimental data with the model. The values of k are reported in and indicate that formation of styrene-b-ES block copolymer was roughly 1.25 times faster than styrene-b-CMS block copolymer. The amounts of CMS and ES retained on the membrane during formation of block copolymer were 60 and 80%, respectively, of the amount retained during formation of homopolymer. This was most likely due to lower site accessibility because of the diffusion barrier caused by the already present styrene grafts.

4.2.7 Controlled polymer growth

4.2.7.1 Introduction

In this study, controlled growth of styrene polymer was evaluated through the variation of reaction parameters like monomer feed concentration and initiator reaction time. The study aimed to build an understanding of the process of polymer growth and the reaction mechanism so that data could be used in the future for further optimization of specific applications like antibody adsorption. The kinetics of polymer growth, average graft length, and IEC were evaluated as a function of these reaction parameters.

4.2.7.2 Influence of monomer concentration on kinetics of polymer growth

Styrene reaction kinetics were studied for different feed concentrations. The plot of styrene retained versus time is shown in Figure 4-8. The pseudo-first-order rate expression (Equation 1) was used to fit the experimental data. The values of k, Q_e and R^2 were obtained by the same method as described in section 4.2.5, and are reported in Table 4-1. The experimental data matched reasonably well with that predicted from the model. The reaction proceeded rapidly and then gradually slowed down. However, it should be noted that it did not show a plateau within 120 minutes of polymerization reaction time. It was observed from experimental data that

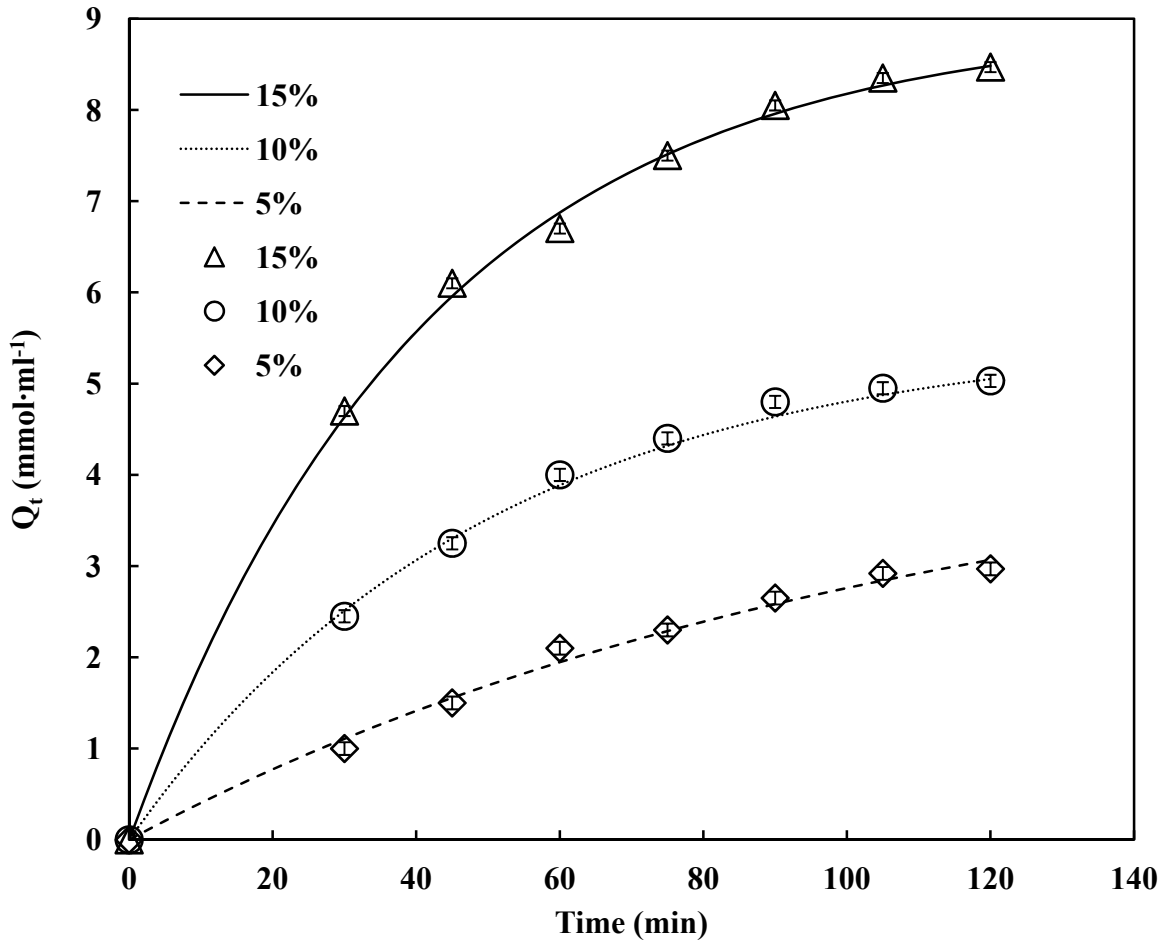

Figure 4-8. Kinetics of styrene reacted for different feed concentration. The smooth curves represent the fit with pseudo-first-order equation and the data points represent the experimental observation.

the amount of monomer retained on membrane at 120 minutes of reaction time increased approximately linearly with monomer feed concentration. By comparing the value of rate constants it was observed that the rate of reaction for 15% monomer feed concentration was roughly 1.2 and 2.6 times higher than 10 and 5% feed concentration, respectively. Furthermore, it was observed that the value of Q_e almost doubled as the monomer feed concentration increased from 5 to 15%. This indicated that a higher feed monomer concentration increased the driving force for mass transfer through the grafts.

4.2.7.3 Influence of monomer concentration on graft length

Graft length as a function of monomer concentration was measured in terms of the average number of repeat units per chain. It was calculated by determining the ratio of the number of styrene molecules reacted to the number of initiator sites. This determination assumed that all the styrene retained on membrane undergoes polymerization and that unreacted styrene remains in the permeate. The assumption was justified because reacted styrene becomes part of the carbocation that interacts with the immobilized initiator (sulfonic acid groups). Also there was no evidence of styrene monomer absorption by the membrane. The bulk of the polymer grafts were formed in the membrane pores because the external surface area is 0.1% of total available area. As illustrated in Figure 4-9, it was observed that the number of repeat units per graft was a linear function of monomer feed concentration. The polymerization reaction time was 120 minutes. Polymer grafts with as many as 125 repeat units per chain were grafted with 15% monomer concentration in the feed. However, it should be noted here that significant membrane swelling and cracking was observed for a feed concentration of 20% monomer.

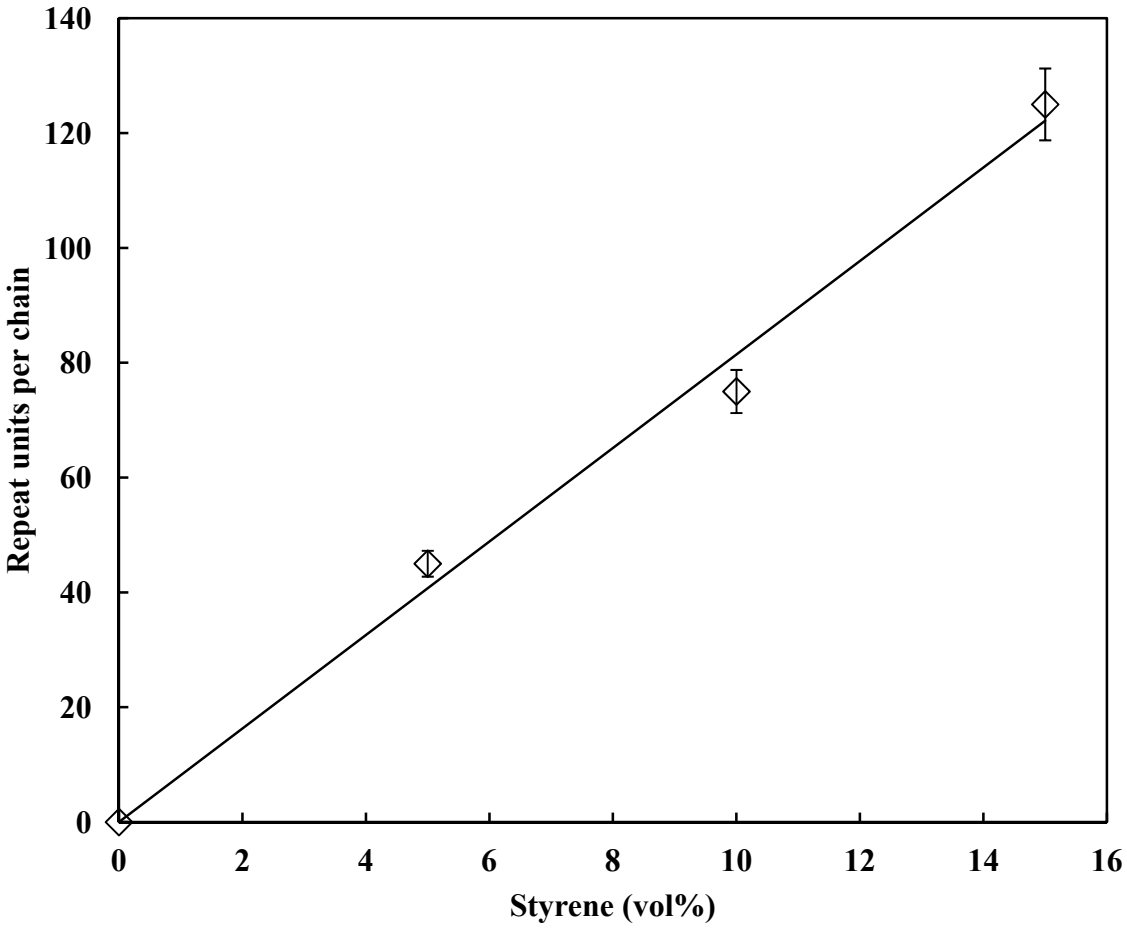

Figure 4-9. Influence of monomer feed concentration on graft length. Polymerization reaction time was 120 minutes.

4.2.7.4 Influence of initiator contact time on amount of monomer reacted

The amount of styrene retained was measured and plotted for different initiator reaction times. Monomer feed concentrations were kept constant at 5 vol% and the polymerization reaction time was 120 minutes. It can be seen from Figure 4-10 that the grafting level increased sharply with increase in initiator reaction time from 45 to 135 minutes. This was because more active sites were available for polymerization with increase in sulfonation reaction time. After approximately 135 minutes, however, there was no significant increase in the percentage of styrene retained**.** This was because number of initiator sites reached a maximum, and the polymerization rate reached a corresponding peak. Similar observations were reported with respect to graft length and IEC where both the parameters plateau after approximately 135 minutes of initiator reaction time.

4.2.7.5 Influence of initiator contact time on graft length

It was observed from Figure 4-11 that the graft length, in terms of number of repeat units per chain, dropped significantly and was approximately constant after 135 minutes of initiator reaction time. This indicates that at low initiator contact time relatively long polymer chains were formed as compared to high initiator contact time. This was most likely due to crowding effects at higher initiator surface density where all active sites are not accessible to grow longer chains. The data also indicated that polymer growth was constant above a critical initiator surface density. This was confirmed by normalizing the data shown in Figure 4-10 where there was no significant change in amount of styrene retained after 135 minutes of initiator contact time. The polymerization reaction time was kept constant at 120 minutes.

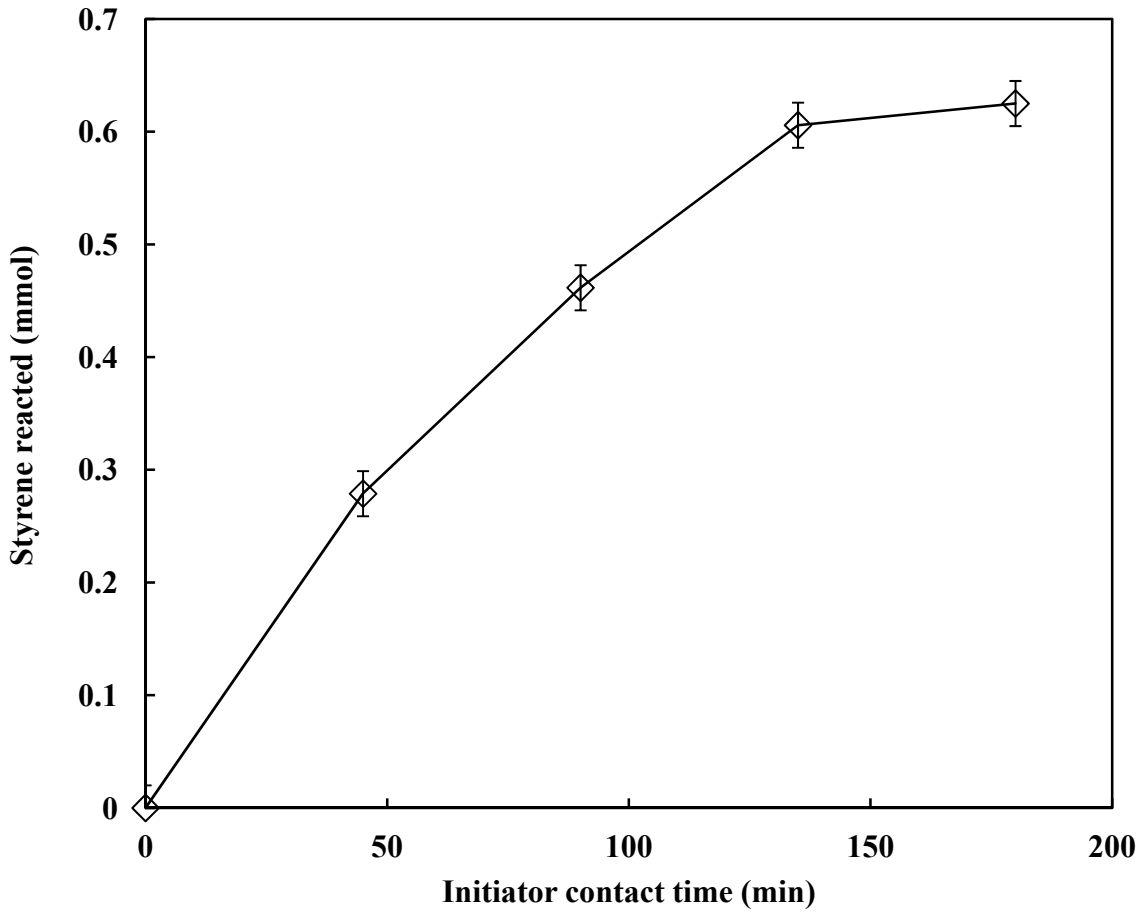

Figure 4-10. Effect of initiator reaction time on amount of styrene reacted.

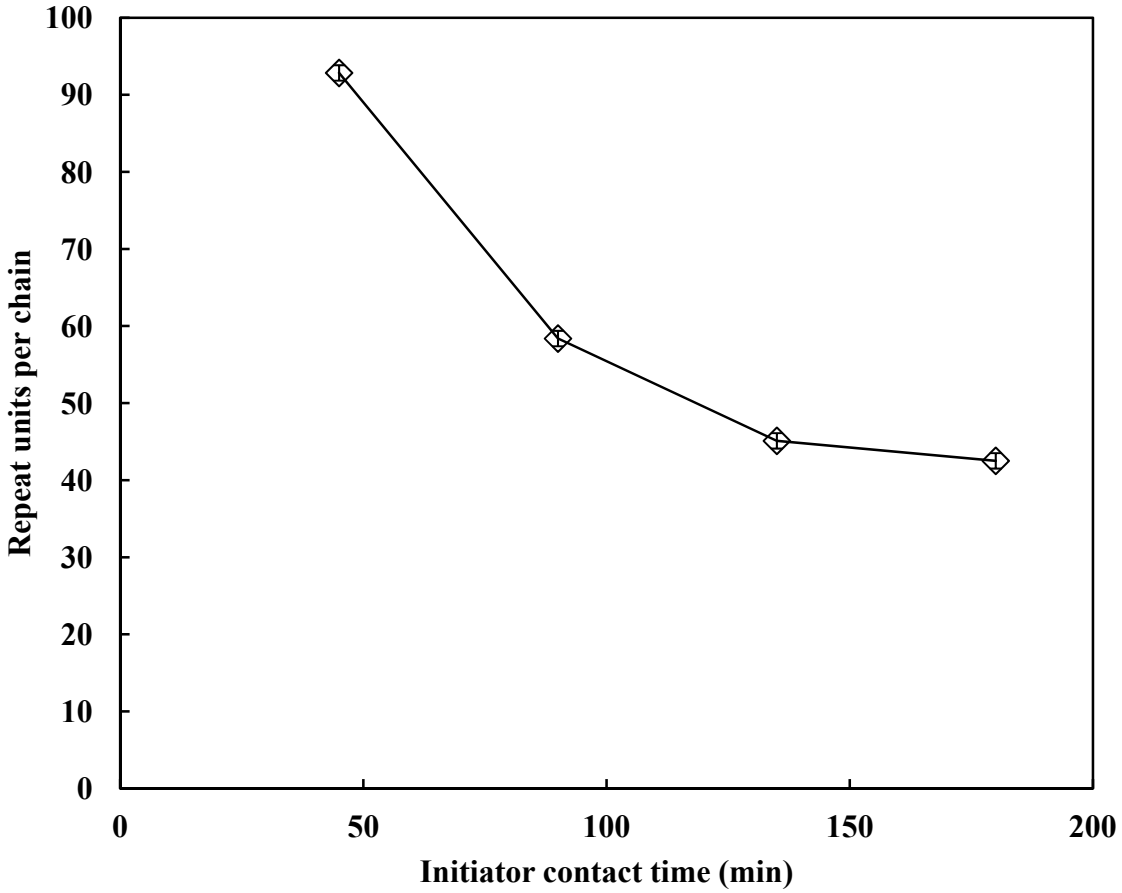

Figure 4-11. Effect of initiator reaction time on graft length.

4.2.7.6 Influence of initiator reaction time and monomer feed concentration on IEC

The membrane was first sulfonated at different initiator contact times. For each contact time the membrane was polymerized to form polystyrene grafts. After polymerization, the membrane was again sulfonated prior to measuring the IEC of the grafted membrane. Figure 4-12 shows the effect of initiator contact time on IEC (meq/g) of the grafted membrane. The polymerization reaction time was 120 minutes for all three monomer concentrations. The IEC value increased with increasing initiator contact time for all three monomer concentrations. For lower initiator contact time (50 and 100 minutes) the IEC increased linearly with increased monomer concentration. After 135 minutes of initiator reaction time the IEC approached a maximum where the initiator sites were saturated and no further change in IEC was observed. Thus, at lower initiator reaction times fewer grafts were formed and IEC was lower. At higher initiator contact times the number of initiator sites available for grafting was higher, more grafts were formed, and the IEC was higher. The IEC value was highest (4.9 meq/g) for 15% monomer concentration and 135 minutes of initiator reaction time. This corresponds to more than 350 times greater IEC than the raw membrane, and approximately 18 times greater than the sulfonated membrane. The IEC stayed constant for initiator contact times greater than 135 minutes, but it still showed linear dependency for changes in the monomer feed concentration. This indicated that both the reaction parameters have significant influence on IEC at lower initiator contact times. However, at higher initiator contact times, the monomer feed concentration dominated and had a more profound effect on IEC.

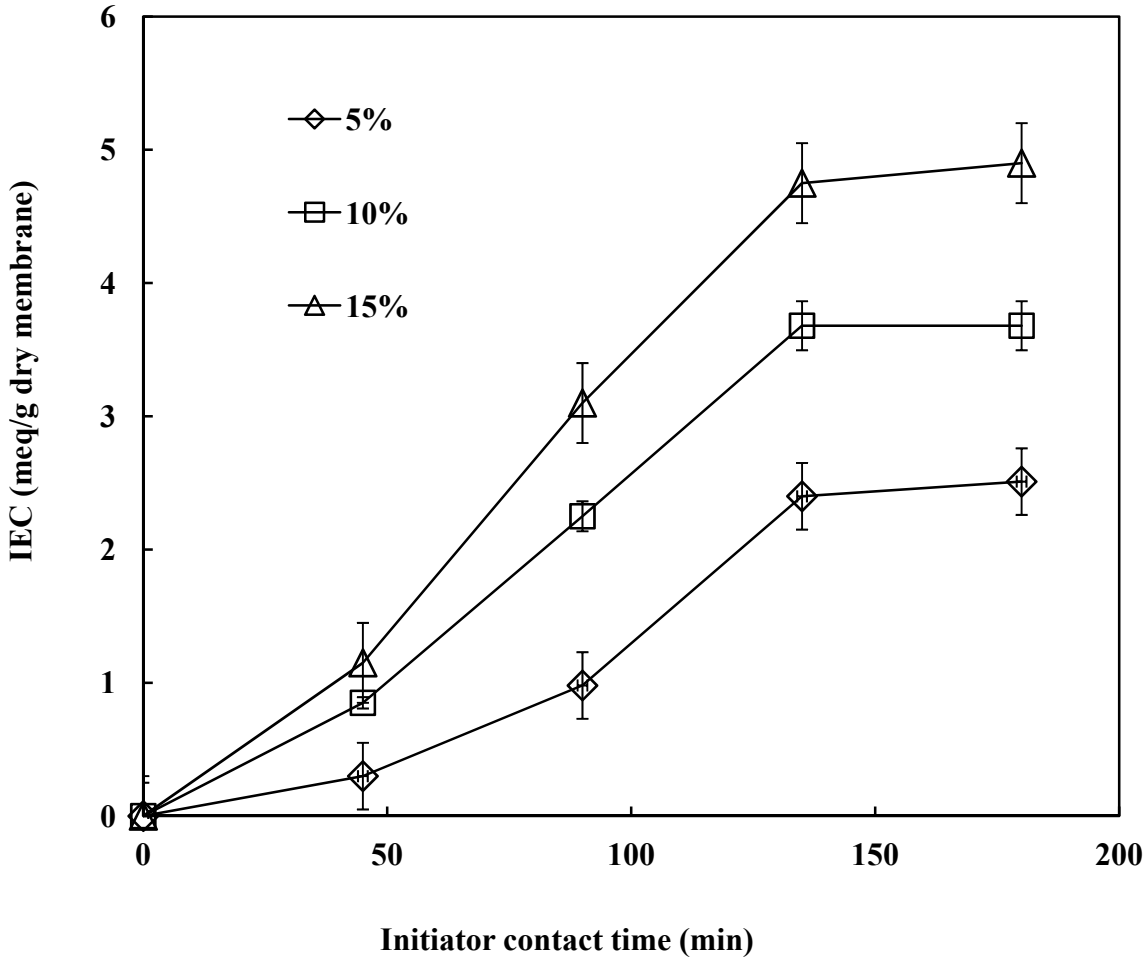

Figure 4-12. Effect of initiator reaction time and monomer feed concentration on IEC.

4.3 Phase 2: Development and characterization of functionalized membranes containing customized poly(styrene-co-HS) grafts and testing the performance of membranes for IgG adsorption

4.3.1 Functionalized membrane synthesis and characterization

Functionalized membranes were first sulfonated to immobilize sulfonic acid groups. The immobilization of initiator sulfonic acid groups in PES membrane pores has been well characterized in the literature [40, 137, 141] and therefore was not discussed in this study. The amounts of styrene and ES reacted were quantified by performing an overall material balance on feed and permeate solutions using gas chromatography. The material balance data showed that 0.63 mmol of styrene and 0.51 mmol of ES were reacted with the initiator to form poly(styrene-co-ES). Solutions containing the copolymer mixture of monomers (styrene and ES) were permeated through the raw membrane without immobilizing the initiator. However, no decrease in peak area was observed on the gas chromatogram for either monomer. This confirmed that monomers were neither adsorbed on the membrane surface nor absorbed. Additionally, the dry weight of the raw and modified membranes was measured. It was observed that the difference between dry mass of modified and the raw membrane and the amounts of each monomer measured from material balance using gas chromatography was less than 5 percent. This demonstrated the accuracy of the measurements and gave secondary verification of amount of each monomer reacted and retained in the membrane.

^{1}H NMR spectra at different stages of functionalization are shown in Figure 4-13. The NMR spectrum for raw PES membrane dissolved in a 1:1 ratio of mixture of deuterated dimethylsulfoxide and chloroform is shown in Figure 4-13(a). The peaks at 2.5 and 3.3 ppm were from solvent and water, respectively. The multiple peaks between 7 and 8 ppm correspond

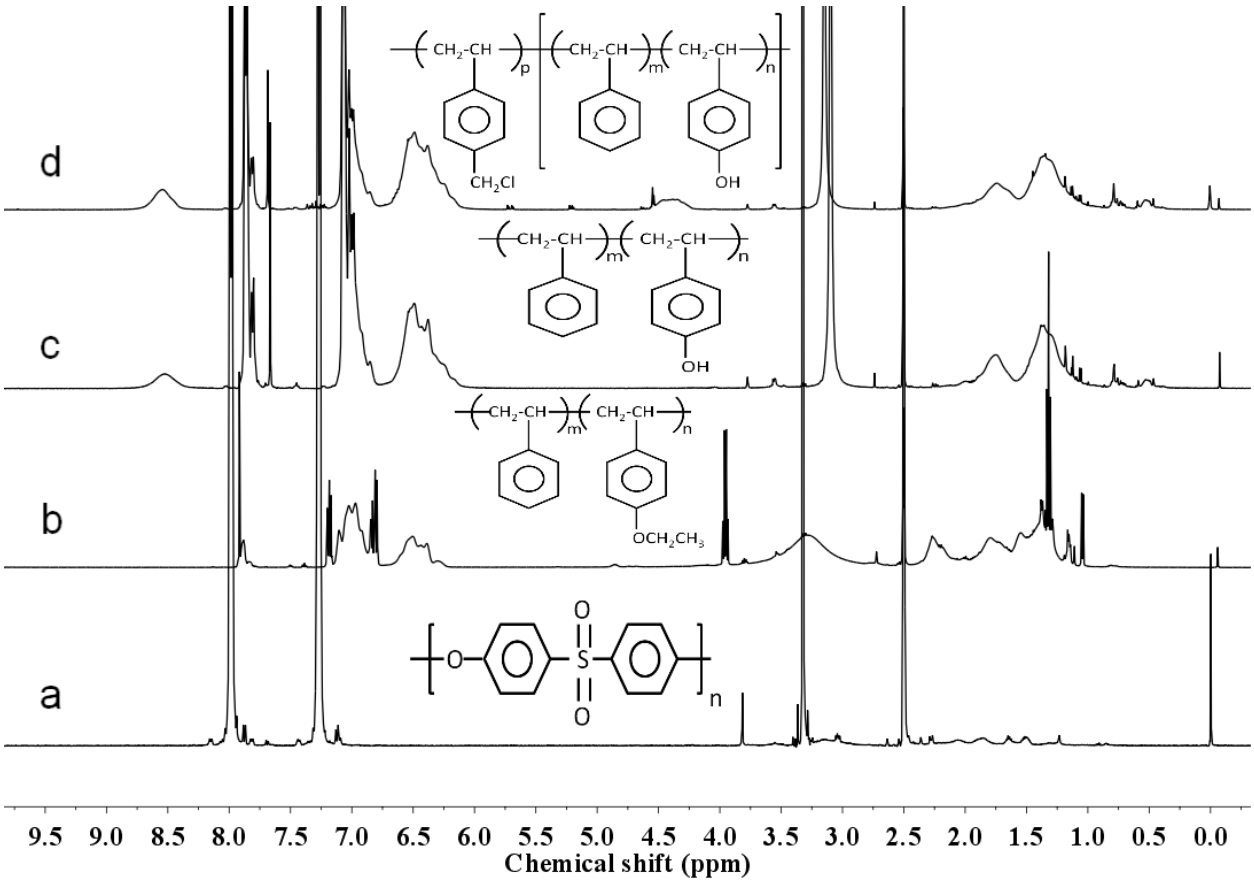

Figure 4-13. ^{1}H NMR spectra of (a) raw PES, (b) poly (styrene-co-ES), (c) poly (styrene-co-HS), and (d) poly ((styrene-co-HS)-b-CMS).

to aromatic protons on two phenyl rings of PES repeating unit [137, 141]. Figure 4-13(b) shows the spectrum for poly(styrene-co-ES) grafted membrane. Several new peaks appeared between chemical shifts 1 and 2 ppm. These peaks represent the methine and methylene protons on the backbone [136, 139]. If there was any unreacted monomer adsorbed on the membrane then the characteristic peaks for double bonded protons of ES monomer (i.e. =CH and $=CH_2$) would be seen between 5 and 6.5 ppm [144]. However, no evidence of these signals for unreacted vinyl protons was observed on the spectrum indicating breaking of double bond to single bond and formation of polymer. Additionally, two new sharp peaks appeared at 1.3 and 4 ppm. These were assigned to the protons on $–CH_3$ and $–CH_2–$ functional groups of the ethoxy pendant group. The assignment of peaks to protons on the ethoxy moiety was confirmed by analyzing the NMR spectrum of pure ES monomer in solvent. Additionally, new broad peaks can be seen on the spectrum between 6.25 and 7.25 ppm. These peaks are from protons on aromatic ring of styrene and ES. Therefore, NMR data confirms that poly(styrene-co-ES) was successfully synthesized in membrane pores.

Ritchie and coworkers have demonstrated that the silanol (silyl alcohol) groups on silica support were successfully reacted with methoxy group on 3-glycidoxypropyltrimethoxysilane in o-xylene solvent [128]. This line of reasoning forms the basis for hydrolyzing the ethoxy moiety on 4-ethoxystyrene using 0.5N NaOH base. Poly(styrene-co-ES) grafts in this work were subsequently hydrolyzed to create customized structures (poly(styrene-co-HS)) mimicking side chain functionalities of Phe-132/Tyr-133 dipeptide structure of ligand protein A. This trend was represented in Figure 4-13(c). The breaking of ethoxy moiety and incorporation of hydroxyl moiety can be explained by two experimental evidences. First, it was observed from the spectrum that the characteristic peaks of protons on ethoxy moiety at 1.4 ($-CH_3$) and 4.1 ppm (-

CH_2-) disappeared. Second, a new signal appeared at 8.5 ppm which was the characteristic of protons on the hydroxyl group attached to the phenyl ring [145]. Control experiments to give further evidence of hydrolysis of ethoxy moiety are described in the future work section of this manuscript.

Figure 4-13(d) shows the incorporation of poly(chloromethylstyrene) grafts into poly(styrene-co-HS) brush. The broad peak at 4.5 ppm is the characteristic signal of the chloromethyl pendant group [139]. If chloromethyl moiety was hydrolyzed then a peak should have appeared at 2.3 on spectrum "d" that represents characteristic of protons on -OH of -CH_2OH (NIST standard reference data). However, no such peak was observed on the spectrum which confirms that chloromethyl moiety was stable without undergoing any side reactions. These data confirmed the synthesis of poly((styrene-co-HS)-b-CMS) while still keeping other functional groups stable without any side reactions.

The chloromethyl groups were reacted with glycine to impart an overall negative charge to the grafted chain. The purpose of introducing negative charge to the adsorption sites was to selectively adsorb IgG during competitive sorption in presence of BSA, a typical negatively charged protein. Glycine functionalization of chloromethyl groups was characterized as shown in Figure 4-14. It was observed from Figure 4-14(b) that the characteristic peak of chloromethyl moiety at 4.5 ppm disappeared indicating the breaking of the chloromethyl bond. Additionally, three new signals were detected at 4, 8.4, and 12.5 ppm. The standard range of chemical shifts for protons on the hydroxyl group of a carboxylic acid is between 10.5-13 ppm. Therefore, the broad peak (zoomed in) at 12.5 ppm was assigned to the proton on carboxylic acid group (-COOH) of glycine. Similarly the range of chemical shifts for an amine group is 4-8.5 ppm. Hence, the peak at 8.4 was assigned to the proton on –NH– (secondary amine) group.

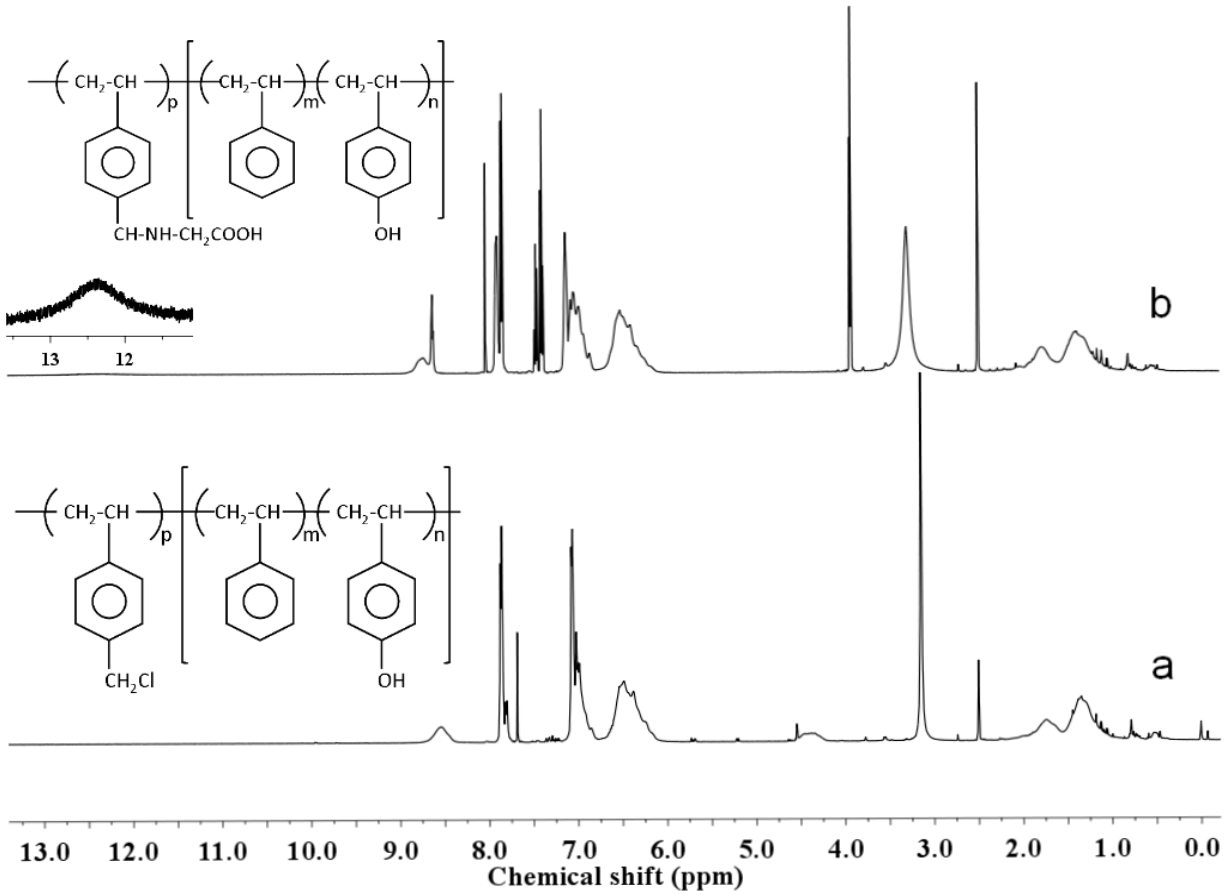

Figure 4-14. ^{1}H NMR spectra of (a) poly ((styrene-co-HS)-b-CMS), and (b) glycine functionalized poly ((styrene-co-HS)-b-CMS).

The presence of adjacent electronegative hydroxyl pendant group in the copolymer might have shifted the –NH– functional to the downfield region. Additionally, the integration of peaks at 4 and 8.4 yields a ratio of 2:1, indicating that the signals corresponded to the -CH_2 group of glycine and the –NH– functional group, respectively. These results demonstrated that glycine was successfully introduced by reacting with the chloromethyl pendant group while still keeping other moieties intact without any side reactions.

4.3.2 Functionalized membrane performance testing

4.3.2.1 Breakthrough curve

Breakthrough curves were generated to determine the dynamic binding capacities of modified membranes. Figure 4-15 shows the breakthrough curve for binding of IgG (3 mg/ml) to the poly(styrene-co-HS) grafted functionalized membrane. The data was obtained by measuring IgG concentration in permeates at different volumes. Initially, as IgG was permeated through the membrane bed, IgG was adsorbed and this continued as long as the binding sites were available for adsorption. When breakthrough started to approach, then IgG was detected in the permeate and the concentration increased until no further adsorption takes place and the concentration of feed was equal to concentration of permeate. The relative steepness of a breakthrough curve is indicative of mass transfer efficiency within the pores of membrane. In an ideal system, the breakthrough curve would be a step function indicative of high mass transfer efficiency. However, the breakthrough in this case was skewed being sharper at the beginning of the curve. This may be attributed to heterogeneity within the membrane bed, in terms of density of adsorption sites distributed over the membrane pore surface area, steric hindrance and membrane pore size distribution. The polymer graft length in some pores might be very high as compared to other pores resulting in inaccessibility of IgG molecules to the binding sites due to

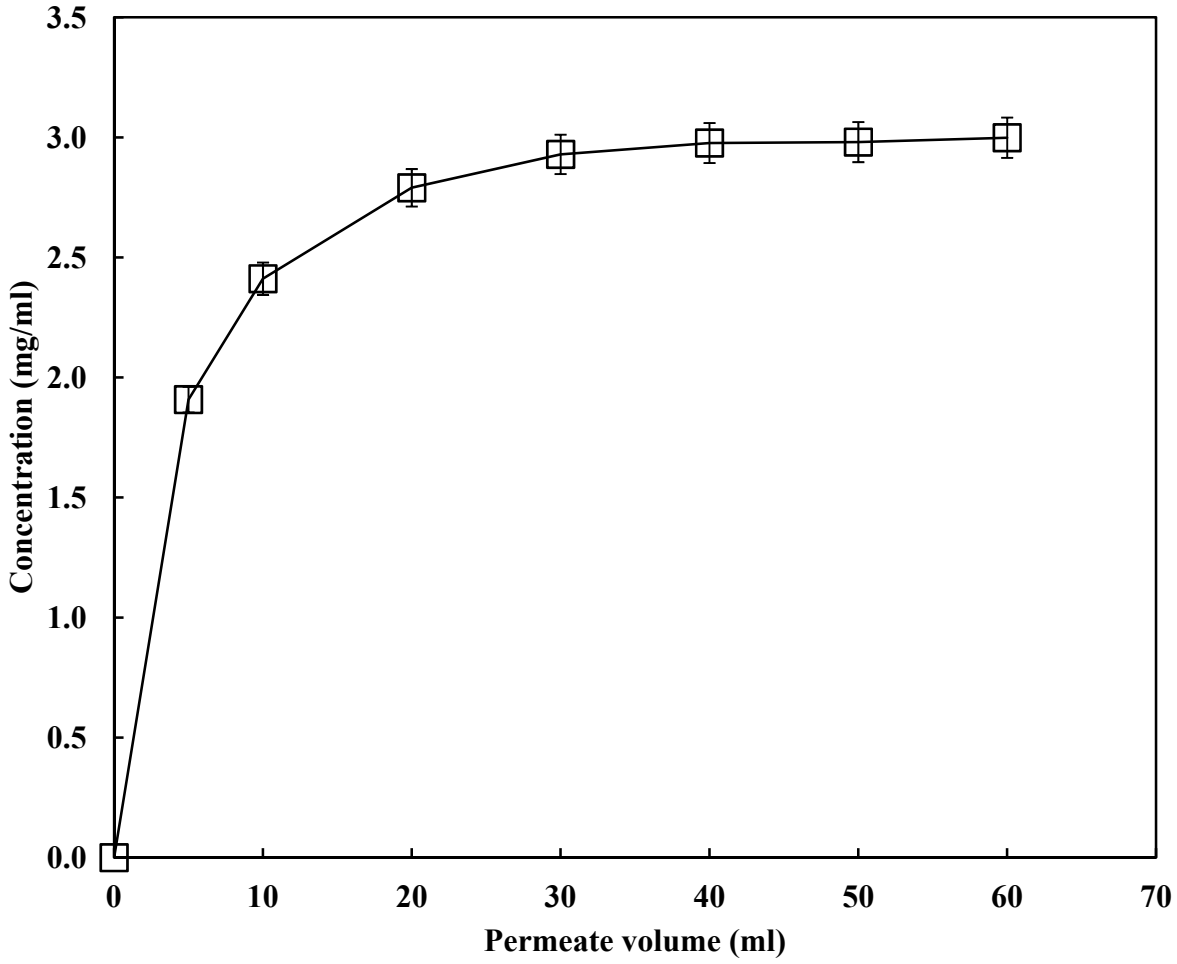

Figure 4-15. Breakthrough curve for adsorption of 3 mg/ml of IgG in functionalized membrane containing poly (styrene-co-HS) grafts. The curve was obtained using 50 mM sodium phosphate binding buffer, pH 7.4 and the flow rate was maintained at 1 ml/min.

steric hindrance. Finally, as the membrane bed approached saturation, mass transfer of IgG molecules may slow or cease in small pores and will persist in larger pores, leading to a decrease in gradient of the breakthrough curve. The breakthrough observed was immediate and fast due to thin membrane (165 μm), high flow rates, and dominance of convective mass transfer rates. However, the breakthrough can be delayed using a stack of membranes.

The IgG binding capacity was obtained by integrating the difference between feed and permeate concentrations on the breakthrough curve. The measured binding capacity was approximately 95 mg/ml of chromatographic media. This value was more than 9 times higher than commercially available Sartobind® and Ultrabind® membranes functionalized with protein A ligand, and more than 2 times higher than MabSelect® SuRe, a protein A coupled bioprocess medium used in affinity chromatography. The high DBC was most likely due to multiple complementary binding sites along each graft available for adsorption. Buffer solution was permeated through the saturated functionalized membrane and the permeate was analyzed for polymer graft loss using UV-vis spectrometry. However, no evidence of graft loss (aromatic peaks) was observed on the UV spectrum. Furthermore, the antibody solution was permeated through raw membrane and poly (styrene-co-ES) grafted membrane. However, no significant adsorption (< 2 mg/ml) of IgG was observed in either case, which further confirms that binding of IgG molecules was because of specific interaction sites formed post hydrolysis of poly (styrene-co-ES). The error bars represent standard deviation from the average of measurements taken for three experiments.

4.3.2.2 Adsorption isotherm

The adsorption isotherm represents the equilibrium sorption of IgG in the membrane and is a function of the concentration of IgG in buffer solution. Figure 4-16 shows the dependence of

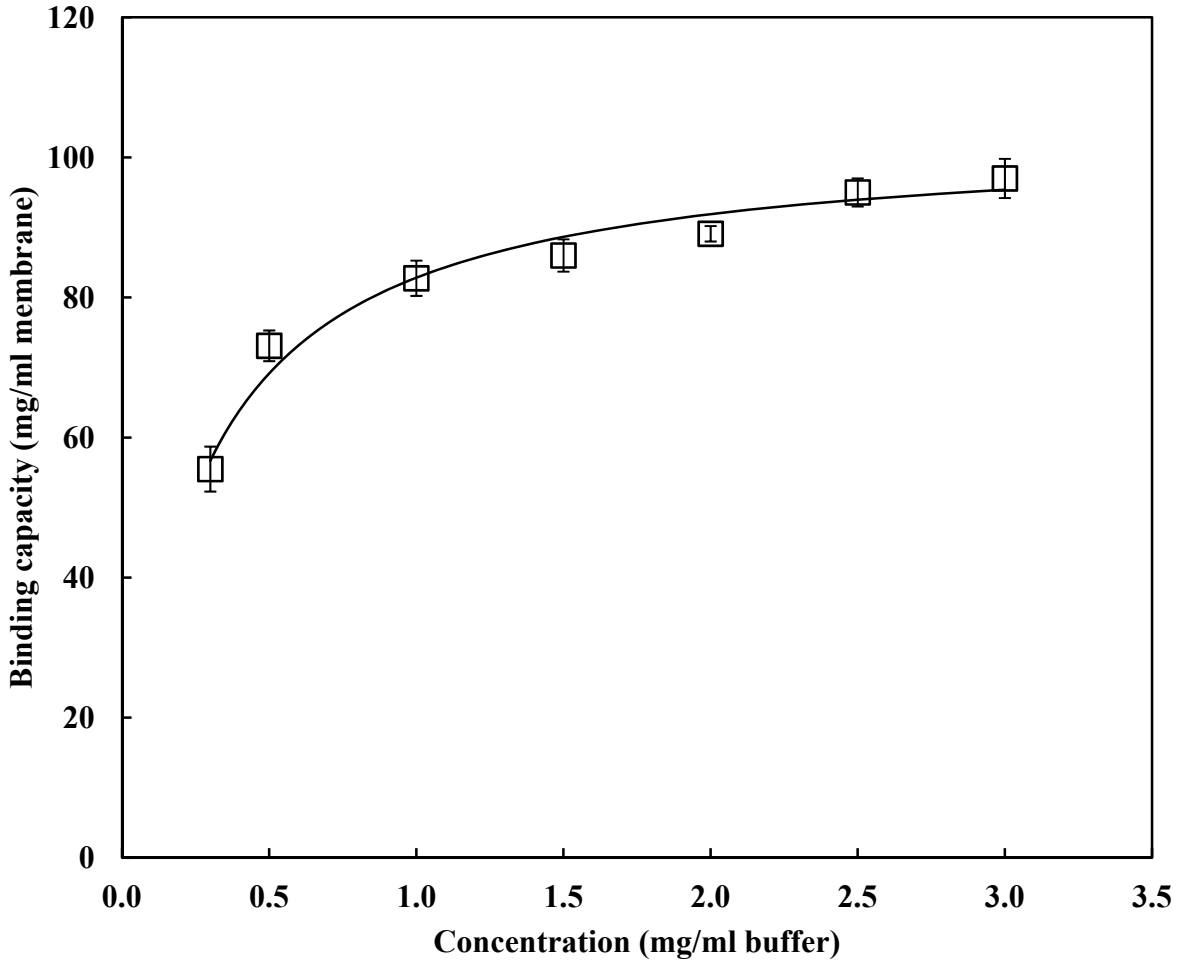

Figure 4-16. IgG adsorption isotherm (pH 7.4). The smooth curve represents the Langmuir isotherm fit and the data points represent experimental observation.

binding capacity of IgG to the functionalized membrane with respect to concentration of IgG in feed. The equilibrium binding capacity increased with an increase in solution concentration until saturation at 3 mg/ml. The experimental adsorption data were fit with the Langmuir adsorption isotherm model (Equation 2),

$$q = q_m C / (K_d + C) \tag{2}$$

where q is the amount of antibody bound per unit membrane volume (mg/ml), q_m is the maximum antibody binding capacity (mg/ml), K_d (mg/ml) is the dissociation constant which represents the affinity between antibody molecule and adsorbent, and C (mg/ml) is antibody equilibrium concentration in liquid phase [12, 136-137]. The correlation coefficient and thermodynamic parameters were obtained by regression analysis using the method of least squares. A correlation coefficient of 0.99 indicated excellent fitting of the model with the experimental data.

The Langmuir parameters of maximum binding capacity and dissociation constant were estimated to be 103.2 mg/ml of membrane and 0.24 mg/ml (6×10^{-7} M), respectively. The maximum binding capacity was approximately 8% higher than experimental data. The dissociation constant is the measure of affinity between the antibody molecule and chromatographic media. It is inversely proportional to the concentration of antibody-chromatographic media complex and therefore a smaller value indicates strong binding. The value of the dissociation constant was consistent with those reported in literature. For example, regenerated cellulose membrane immobilized with synthetic A2P ligand (protein A mimetic) for adsorption of IgG has a dissociation constant in the range of 10^{-7} – 10^{-6} M [12]. K_d values reported in literature for solution phase IgG-protein A binding were approximately 2.9×10^{-6} M [146]. The values of dissociation constants for commercially available Sartobind® and

Ultrabind® membranes for IgG are in the order of 10^{-6} M [49]. The value of parameter K_d for functionalized membranes in this study were one order of magnitude lower (10^{-7} M) indicating better performance as compared to commercially available protein A affinity membranes. The lower values of dissociation constant, and therefore high binding affinity, may be due to complementary synthetic binding sites incorporated multiple times along each polymeric graft immobilized in the membrane pore.

4.3.2.3 Effect of polymerization reaction time on binding capacity

The performance of modified membranes exposed to different polymerization times was tested in terms of binding capacity. Figure 4-17 shows that with an increase in polymerization reaction time, the DBC initially increases until approximately 120 minutes. After 120 minutes the binding capacity decreased at longer polymerization reaction times (120-180 minutes). The initial increase in binding capacity was attributed to an increase in the amount of each monomer reacted and hence an increased number of complementary binding sites available for antibody adsorption. However, after 120 minutes of polymerization reaction time, the binding sites may be less accessible due to crowding effects. Additionally, at longer polymerization times the smaller pores might be blocked due to long and entangled polymer grafts and therefore a decrease in binding capacity was reasonable. The breakthrough curves for longer polymerization times (beyond 120 minutes) were sharper and faster as compared to shorter polymerization times (<120 minutes). For polymerization times beyond 180 minutes the DBC reached a plateau and no further decrease in binding capacity was observed. Similar observations have been reported in the literature. For instance, nylon membranes containing a poly(2-(methacryloyloxy)ethyl succinate) brush showed a sharp drop in lysozyme binding capacity at polymerization times

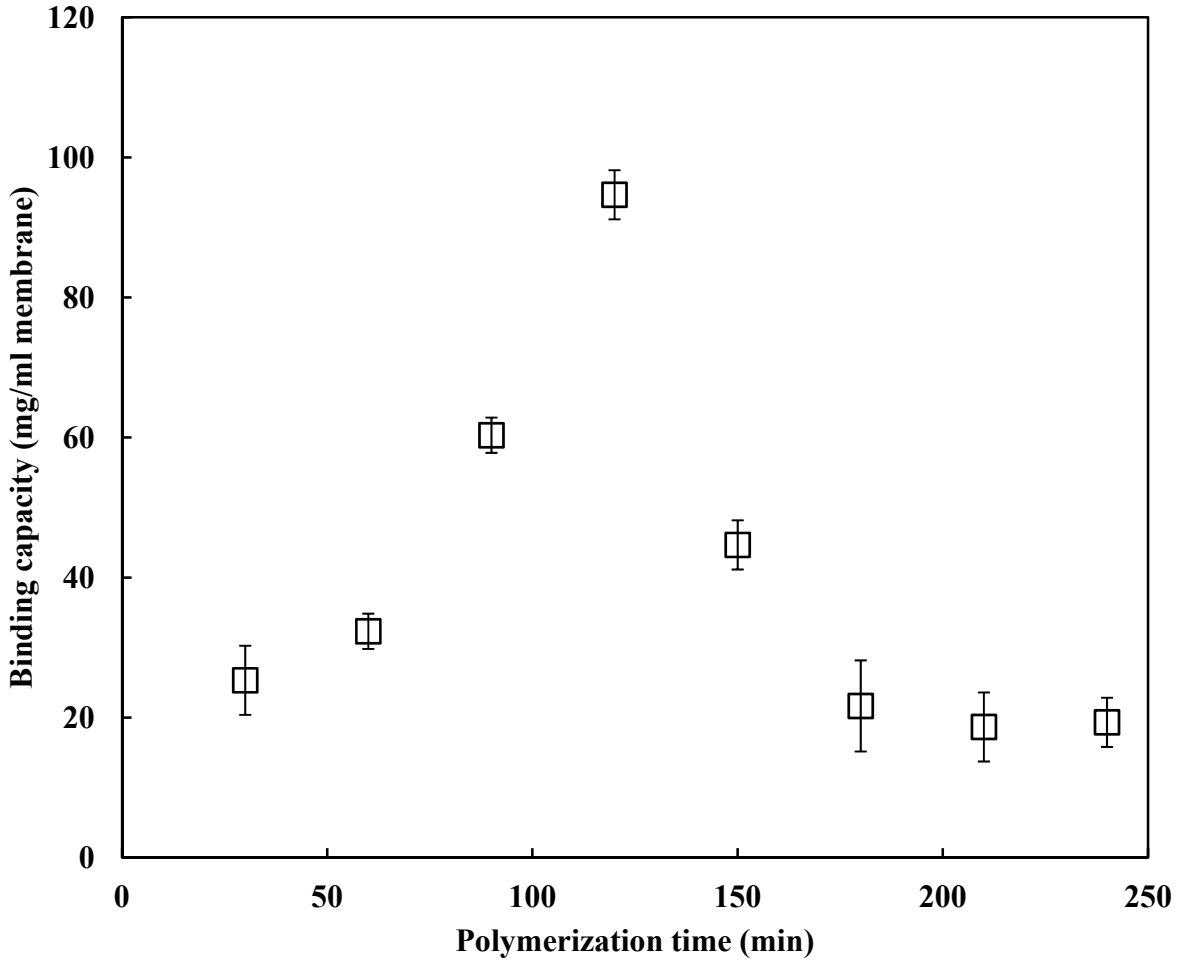

Figure 4-17. IgG binding capacities of poly (styrene-co-HS) grafted membranes as a function of polymerization reaction time.

greater than 1 hour [22, 147]. The drop in binding capacity was attributed to long polymer brushes blocking the pores and decreasing the binding capacity.

4.3.2.4 Influence of flow rate on binding capacity

The DBC for IgG was determined at various flow rates ranging from 1-50 ml/min. The equivalent range of linear velocities corresponding to these flow rates were 4.6-230 cm/h, and residence times of 12 and 0.25 s at the end points of the range, respectively. The linear velocities were calculated based on an effective membrane area of 13.2 cm^2. The linear velocities were about 50% higher than commercial gels at the higher end of range of flow rates [26, 147]. However, the linear velocities were still 2.5 times lower compared to typical values for membranes (570 cm/h) [147]. This was due to the presence of polymer grafts in the flow path that constrict the pores and reduce flow rate. Figure 4-18 shows that DBC is a weak function and independent of flow rate within the experimental error (<5%). Therefore, transport of IgG molecules to the adsorption sites was predominantly by convection and not diffusion as in the case of packed bed chromatography. Additionally, it was observed that for flow rates beyond 50 ml/min, mechanical strength of the membrane was severely compromised as significant cracking was observed. These data confirm that membrane chromatography allows high flow rates to be used, increasing throughput and decreasing cycle times. These results are in sharp contrast with packed bed chromatography where the binding capacity decreases with an increase in flow rate [148]. This is because in resin column the mass transport is predominantly diffusion-controlled.

The Peclet number (Pe) is a dimensionless number that characterizes the convective transport of solute molecules through the membrane pores. It is defined as the ratio of convective flux to diffusion flux. At Pe values greater or equal to 40, the effect of axial diffusion is

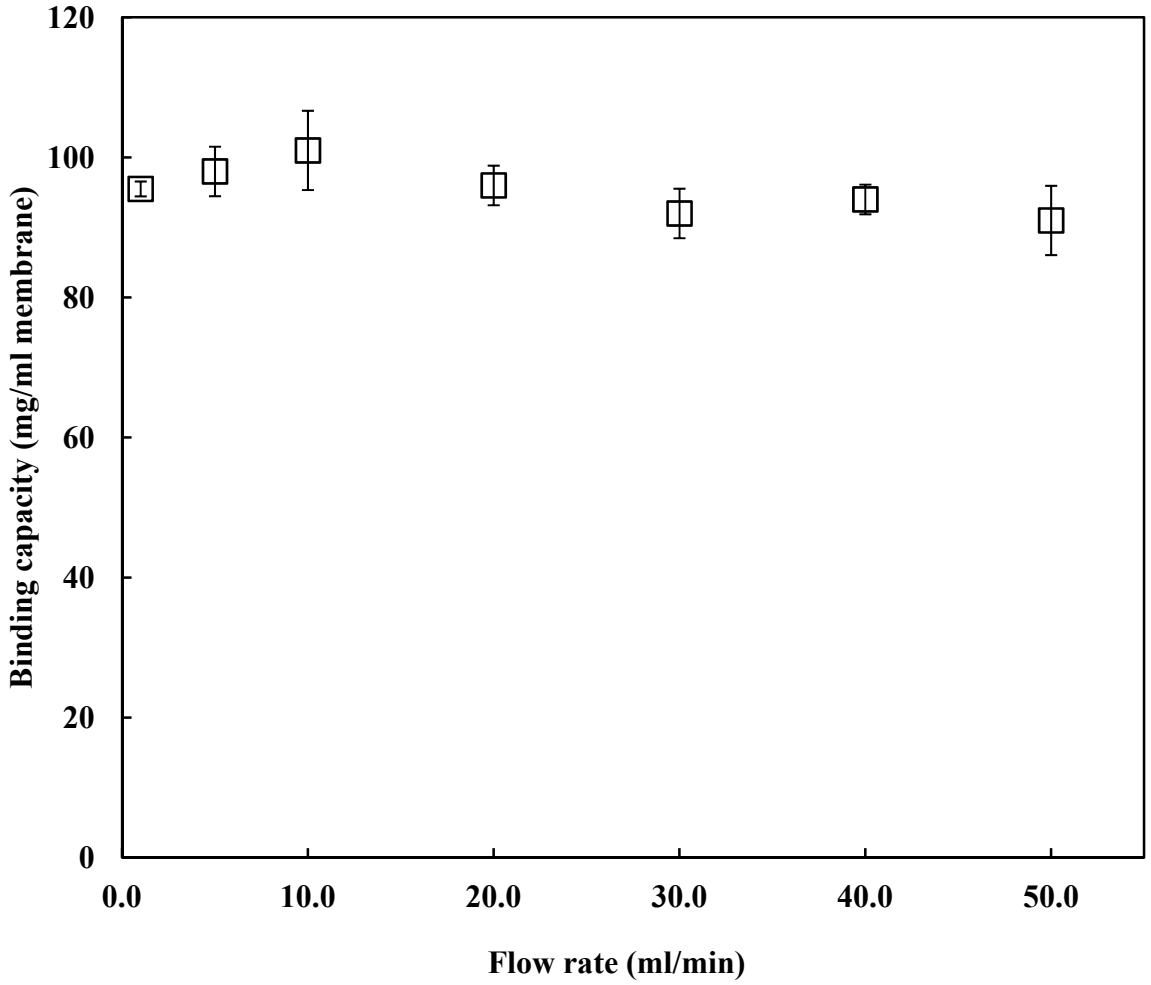

Figure 4-18. Effect of flow rate on IgG binding capacity. Polymerization reaction time and initiator contact times were 120 and 180 minutes, respectively. Antibody feed concentration was 3 mg/ml.

negligible and the transport of solute molecules is governed by convection [116]. The Pe was calculated using Equation 3,

$$P_e = \frac{UL\tau}{D} \tag{3}$$

where U is linear velocity (cm/s), L is the membrane thickness (cm), τ is the tortuosity, and D is the diffusion coefficient (cm^2/s) of IgG. The parameters D and τ were obtained from literature and are 3.89 x 10^{-7} (cm^2/s) and 2.1, respectively [41, 116, 149]. The membrane thickness (L) is 165 x 10^{-4} (cm). Peclet number values for linear velocities ranging from 4.6-230 cm/h were calculated to be 113-5,682. These data validate that even at low linear velocities, the flow of antibody molecules through the functionalized membrane was primarily by convection.

4.3.2.5 Bind and elute method

Multiple experiments of binding, elution and regeneration were performed on the functionalized membrane to determine elution efficiencies, loss of capacity, and give secondary confirmation of DBC. Figure 4-19 shows results of average recovery and measured DBC (adsorbed/eluted) over a period of five cycles. It was observed that there was no significant loss in DBC over a period of five cycles. Additionally, the average recovery, which is the percentage ratio of amount eluted to amount adsorbed, was more than 94%, indicating that the interaction between IgG molecule and the functionalized membrane was reversible and almost all the adsorbed antibody was eluted. The membranes were stable up to five repeated cycles of adsorption, elution and regeneration. However, the membrane undergoes significant cracking beyond five cycles of adsorption and elution, which may be due to prolonged exposure to low pH phosphoric acid solution during the regeneration step. The regeneration step was included to remove any tightly bound antibody into the membrane pores.

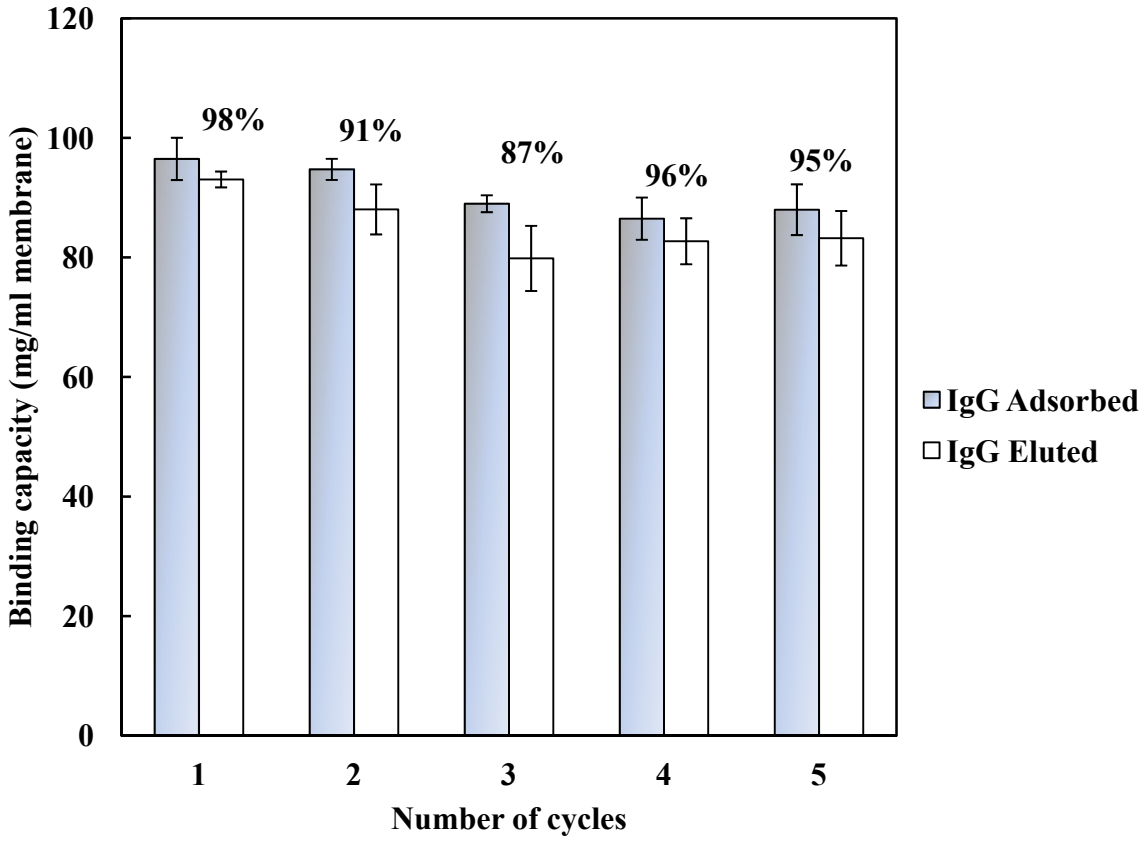

Figure 4-19. Binding capacity and recovery for multiple cycles of IgG adsorption, elution, and regeneration.

4.3.2.6 Competitive sorption

Competitive sorption in presence of BSA was performed to show the selectivity of the membrane. Membranes tailored with poly(styrene-co-HS) and a block of negatively charged glycine functionalized poly(CMS) grafts were used to selectively adsorb IgG in the presence of BSA. Figure 4-20 shows the breakthrough curves using IgG and BSA in the binding buffer to test the selectivity of the negatively charged functionalized membrane under convective flow conditions. The DBCs calculated by integrating the differences between feed and permeate on each breakthrough curve for IgG and BSA were 115 and 10 mg/ml, respectively.

Selectivity, which is measured as the ratio of binding capacity of IgG to BSA, was approximately 11. Isoelectric point (pI) is the pH at which the molecule carries no net electrical charge. Above the pI the molecule carries the negative charge and vice versa. The pI for BSA is 4.7 [14] and thus the protein was negatively charged at pH 7.4. This explains the inhibition of BSA sorption by the negatively charged functionalized membrane. DBC for IgG in presence of BSA using membrane containing negatively charged spacer arms (CMS functionalized with glycine) was 22% more as compared to without spacer arms. This can be attributed to three reasons. First, the isoelectric point of IgG is 7.3 +/- 1.2 [150], therefore at running conditions (pH 7.4) IgG is either slightly positively or negatively charged. Hence some IgG was adsorbed due to charge interaction with negatively charged spacer arms on the grafted chain. Second, the adsorption of IgG was due to specific interaction sites built into the polymer brush immobilized in the membrane pores. Third, IgG adsorption was most likely due to the negative charge stretching the grafted chains away from each other, reducing the steric hindrance, and improving the accessibility of antibody molecules to the binding sites. Therefore, higher binding capacity

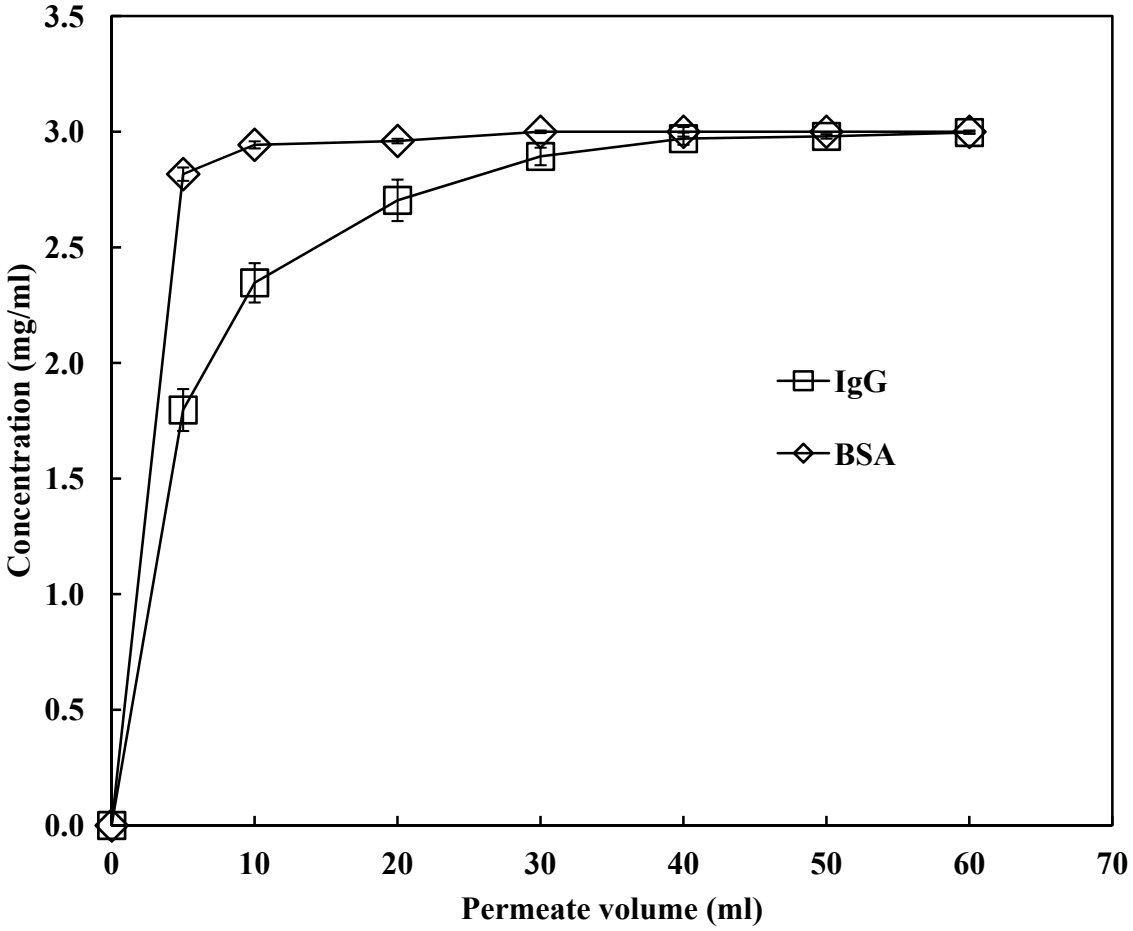

Figure 4-20. Breakthrough curves showing competitive adsorption of IgG (3 mg/ml) and BSA (3 mg/ml) in binding buffer (50 mM, pH 7.4).

was attributed to the combined effects of charge, complementary binding sites, and improved accessibility.

CHAPTER 5
CONCLUSIONS

A novel, high capacity, highly selective synthetic functionalized membrane containing poly(styrene-co-HS) grafts mimicking the Phe-132/Tyr-133 dipeptide structure of protein A ligand has been developed via surface-initiated living cationic polymerization for adsorption of IgG. Phase 1 studies clearly showed grafting of homopolymer and block copolymer brushes in the pores of microfiltration PES membrane. The quantitative information from the analytical experiments and material balances showed that the membrane has a very high IEC of (4.9 meq/g) with roughly 125 repeat units per chain. This represents roughly 92% of theoretical maximum (5.3 meq/g) IEC of an ion-exchange resin. Synthesis of homopolymer and block copolymer brushes has been confirmed by UV-visible spectroscopy and gas chromatography analysis of the feed and permeate solutions. Permeability studies at each step were performed. The results revealed that there is an order of magnitude decrease in pure water permeability from raw to sulfonated to styrene grafted and finally styrene-b-ES grafted membrane. This result gave secondary evidence of the presence of grafted polymer in the membrane.

Reaction kinetics of each monomer during formation of homopolymer brush were studied. A pseudo-first-order kinetic expression correlated well with the experimental data for each monomer reacted. It was observed that CMS was the least reactive; styrene and ES showed similar reactivity during formation of homopolymer. CMS reacted approximately 25% slower as compared to styrene and ES. The low reactivity of CMS is due to the presence of the strong electron-withdrawing chloromethyl pendent group. The ethoxy moiety in the ES monomer is an electron-donor substituent which makes it more reactive relative to CMS. Similar observations were reported during formation of block copolymers poly(styrene-b-CMS) and poly(styrene-b-ES). CMS reacted approximately 22% slower than ES after polymerization with styrene. Both

Monomers showed lower reactivity during formation of block copolymers. This was due to the diffusion barrier by polystyrene grafts already present in the membrane pores.

Controlled polymer growth of styrene monomer was studied to understand the process and control of the polymerization reactions. This was done by studying the effects of monomer concentration and initiator reaction time on polymer growth aspects like kinetics, amount of styrene reacted, IEC, and graft length. At lower initiator surface density, graft length and IEC were impacted by both monomer feed concentration and initiator contact time. However, for higher initiator surface density the monomer feed concentration parameter dominates.

In phase 2 it was demonstrated that the functionalized membrane has very high binding capacity of 95 mg IgG per ml of membrane. The Langmuir model showed good correlation (R^2 = 0.99) with the experimental adsorption isotherm, and the dissociation constant (~10^{-7}M) indicated strong affinity between the functionalized membrane and IgG. Experiments performed to understand the influence of polymerization time and flow rate on DBC led to two important conclusions. First, DBC reached a maximum at 120 minutes of polymerization reaction time and then decreased at longer polymerization times suggesting that binding sites are less accessible to antibody molecules due to long polymer brushes. Second, DBC is a weak function of flow rate at high linear velocities indicating that the transport of molecules to the binding sites was predominantly by convection. The residence times of functionalized membranes (0.25 s) developed in this research was several orders of magnitude lower than affinity resin (6 min).

The selectivity of the functionalized membrane for adsorption of IgG was demonstrated by performing antibody binding at different stages of preparation of functionalized membrane. The membrane only showed IgG binding when customized poly(styrene-co-HS) grafts were immobilized in the membrane pores. ^{1}H NMR data clearly demonstrated incorporation of

poly(styrene-co-HS) and subsequent addition of negatively charged glycine functionalized poly(chloromethylstyrene) spacer units. Competitive sorption studies in presence of BSA using negatively charged functionalized membrane showed that the membrane was highly selective (11 times) towards IgG and inhibited the sorption of BSA. The higher DBC of the functionalized membrane with negatively charged spacer arms was most likely due to the spacer arms which kept the grafted chains apart and improved the accessibility of binding sites. Finally, bind and elute experiments verified that more than 94% of bound IgG was recovered and the membrane was stable without any significant loss in DBC over a period of five cycles of binding, washing, elution, and regeneration. The results demonstrate that these functionalized membranes have a great potential to be used as membrane adsorbers in membrane chromatography for high throughput and cost effective production of IgG.

CHAPTER 6
FUTURE WORK

Functionalized membranes developed in this research show a great deal of promise for low cost and large scale purification of monoclonal antibodies. Copolymers formed in this work will have applications to mimic the dipeptide structure of phenylalanine/tyrosine in protein A ligand which is crucial for interaction with IgG. This will further result in understanding the formation of synthetic affinity ligand membrane adsorbers for protein and antibody separation. It is recommended that future work as an extension of this research should be focused on: control experiments for hydrolysis of ES, control experiments to show that the CH_2Cl moiety is not hydrolyzed, understanding pore size distribution, optimizing binding capacity with respect to pore size and initiator surface density, improving long term stability of the membrane, sequencing the grafts, and testing the performance of the membrane for an actual feed used in affinity chromatography.

One of the critical aspects of this research is hydrolysis of the ethoxy moiety to mimic tyrosine. NMR results clearly demonstrated breaking of the ethoxy moiety and incorporation of hydroxyl groups. However, control experiments need to be performed to give secondary evidence and more detailed understanding of this phenomenon. One experiment is to perform partial hydrolysis of the ethoxy moiety. This can be done by performing time based degradation, where 0.5N NaOH is reacted for different time intervals. The shrinking of ethoxy peaks (4.1 and 1.4 ppm) and a corresponding increase in the hydroxyl peak (8.5 ppm) will be monitored on NMR spectra.

CMS was reacted with glycine in order to incorporate an overall negative charge on the grafted chain. Control experiments showing that chloromethyl moiety was not hydrolyzed and all the chloromethyl styrene reacted with glycine should be performed. Glycine in PBS buffer was

used to react with CMS. Therefore, PBS buffer without glycine should be permeated through the poly(styrene-co-HS)-b-CMS) grafted membrane. The membrane will then be dissolved in a 1:1 mixture of deuterated DMSO and $CDCL_3$. If CH_2Cl group hydrolyzes then a new peak at 2.3 ppm, which is the characteristic of –OH on -CH_2OH, should appear on the spectra.

Microfiltration membranes normally have a very wide pore size distribution. As a result, the feed flow is favored through larger pores relative to smaller pores reducing the efficiency of the membrane adsorber. In this research, steric hindrance will eventually limit the formation of polymeric grafts in the membrane pores. Formation of polymeric grafts will be inhibited in smaller pores but still continue in the larger pores leading to a gradual narrowing of the pore size distribution. Future research efforts should be focused on determination of the membrane pore size distribution. Functionalized membranes can be sputter-coated with gold and SEM micrographs can be analyzed for image analysis. ImageJ software (open source software provided by National Institutes of Health) can be used to determine the average pore diameter and characterize narrowing of pore size distribution by using the "Thresholding" and "Analyze Particles" feature of this software. The pore size distribution will be determined for the top and bottom surfaces. The membrane is asymmetric, so more detailed understanding of the cross-section of the membrane will be needed. The membranes can be freeze fractured with liquid nitrogen and then SEM micrographs would be analyzed for pore size distribution. Additionally, the pores are not cylindrical but follow a tortuous path and the grafts are fanning from the surface. Understanding the pore morphology before and after functionalization will give a better understanding of the increase in DBC with incorporation of spacer arms.

In phase 1 of this research, it was observed that the polymer grafting density increased with an increase in the initiator surface density. Optimizing the initiator surface density while

keeping the polymerization reaction time constant would maximize the binding capacity. To test this hypothesis, membranes with different initiator densities should be synthesized by altering sulfonation time or sulfuric acid concentration. Next the membranes should be functionalized by the normal method to synthesize customized structures mimicking the Phe-132/Tyr-133 dipeptide structure of ligand protein A. Finally, the performance of the membrane should be tested for antibody binding capacity.

While studying the influence of polymerization time on antibody binding capacity, it was observed that binding capacity peaks at 2 hours of polymerization time. This is due to long polymeric brushes leading to inaccessibility of antibodies to the binding sites. However, the binding capacity can be increased beyond what is reported in this contribution by using a membrane with a larger pore diameter. This is because a larger pore diameter might improve the accessibility of molecules to the binding sites. However, there needs to be a trade-off between polymerization time and pore diameter so that the molecules do not pass through without coming in contact with binding sites.

PES material has shown excellent chemical and mechanical stability under the operating conditions of this research. However, it was observed that the mechanical stability of the membrane was compromised at high monomer feed concentration (>15%), high flow rates (>50 ml/min), and more than five cycles of binding-elution-regeneration. The membrane showed severe cracks under these conditions. Therefore, improving the long term stability of the membrane beyond the operating conditions in this research will not only have a potential to increase the binding capacity, but will improve throughput and increase life span leading to less number of membranes required over a period of time.

The highly structured polymeric grafts should be sequenced to determine the exact number of binding sites (styrene-co-HS). If the customized grafts can be extracted and analyzed to determine the number of repeat units of each block copolymer ((styrene-co-HS)-CMS), then this would be a significant leap towards truly developing synthetic affinity membranes. Finally, a set of experiments to test the performance of functionalized membrane using an actual feed sample of protein aggregates used in protein A chromatography would increase the practicability of using synthetic functionalized membranes for large scale and low cost production of monoclonal antibodies. Selectivity of the membrane should also be tested in presence of a positively charged protein like lysozyme.

REFERENCES

[1] D.S. Hage, "Affinity chromatography: A review of clinical applications," Clinical Chemistry, 45 (1999) 593-615.

[2] J. Hubbuch, T. Linden, E. Knieps, J. Thommes, M.R. Kula, "Dynamics of protein uptake within the adsorbent particle during packed bed chromatography," Biotechnology and Bioengineering, 80 (2002) 359-368.

[3] K. Huse, H.J. Bohme, G.H. Scholz, "Purification of antibodies by affinity chromatography," Journal of Biochemical and Biophysical Methods, 51 (2002) 217-231.

[4] B.V. Ayyar, S. Arora, C. Murphy, R. O'Kennedy, "Affinity chromatography as a tool for antibody purification," Methods, 56 (2012) 116-129.

[5] P. Gagnon, "Technology trends in antibody purification," Journal of Chromatography A, 1221 (2012) 57-70.

[6] T. Ishihara, N. Nakajima, T. Kadoya, "Evaluation of new affinity chromatography resins for polyclonal, oligoclonal and monoclonal antibody pharmaceuticals," Journal of Chromatography B-Analytical Technologies in the Biomedical and Life Sciences, 878 (2010) 2141-2144.

[7] S. Katoh, M. Imada, N. Takeda, T. Katsuda, H. Miyahara, M. Inoue, S. Nakamura, "Optimization of silica-based media for antibody purification by protein A affinity chromatography," Journal of Chromatography A, 1161 (2007) 36-40.

[8] P.S. Wierling, R. Bogumil, E. Knieps-Grunhagen, J. Hubbuchl, "High-throughput screening of packed-bed chromatography coupled with SELDI-TOF MS analysis: Monoclonal antibodies versus host cell protein," Biotechnology and Bioengineering, 98 (2007) 440-450.

[9] A. Saxena, B.P. Tripathi, M. Kumar, V.K. Shahi, "Membrane-based techniques for the separation and purification of proteins: An overview," Advances in Colloid and Interface Science, 145 (2009) 1-22.

[10] A.A. Shukla, B. Hubbard, T. Tressel, S. Guhan, D. Low, "Downstream processing of monoclonal antibodies—Application of platform approaches," Journal of Chromatography B-Analytical Technologies in the Biomedical and Life Sciences, 848 (2007) 28-39.

[11] A.A. Shukla, J. Thommes, "Recent advances in large-scale production of monoclonal antibodies and related proteins," Trends in Biotechnology, 28 (2010) 253-261.

[12] C. Boi, V. Busini, M. Salvalaglio, C. Cavallotti, G.C. Sarti, "Understanding ligand-protein interactions in affinity membrane chromatography for antibody purification," Journal of Chromatography A, 1216 (2009) 8687-8696.

[13] R. Ghosh, "Protein separation using membrane chromatography: Opportunities and challenges," Journal of Chromatography A, 952 (2002) 13-27.

[14] B.V. Bhut, S.M. Husson, "Dramatic performance improvement of weak anion-exchange membranes for chromatographic bioseparations," Journal of Membrane Science, 337 (2009) 215-223.

[15] B.V. Bhut, S.R. Wickramasinghe, S.M. Husson, "Preparation of high-capacity, weak anion-exchange membranes for protein separations using surface-initiated atom transfer radical polymerization," Journal of Membrane Science, 325 (2008) 176-183.

[16] C. Charcosset, "2.43 - Membrane systems and technology," Comprehensive Biotechnology (Second Edition), 2 (2011) 603-618.

[17] C. Charcosset, "5 - Membrane chromatography," in: Membrane Processes in Biotechnologies and Pharmaceutics, Elsevier, Amsterdam, 2012, pp. 169-212.

[18] S.M. Cramer, M.A. Holstein, "Downstream bioprocessing: Recent advances and future promise," Current Opinion in Chemical Engineering, 1 (2011) 27-37.

[19] H.E. Cutler, S.M. Husson, S.R. Wickramasinghe, "Prefiltration to suppress protein fouling of microfiltration membranes," Separation and Purification Technology, 89 (2012) 329-336.

[20] L. Wang, R. Ghosh, "Fractionation of monoclonal antibody aggregates using membrane chromatography," Journal of Membrane Science, 318 (2008) 311-316.

[21] A.L. Zydney, R. van Reis, "5.4 - Bioseparations: Membrane processes," Comprehensive Biotechnology (Second Edition), 5 (2011) 499-520.

[22] P. Jain, M.K. Vyas, J.H. Geiger, G.L. Baker, M.L. Bruening, "Protein purification with polymeric affinity membranes containing functionalized poly(acid) brushes," Biomacromolecules, 11 (2010) 1019-1026.

[23] F.T. Sarfert, M.R. Etzel, "Mass transfer limitations in protein separations using ion-exchange membranes," Journal of Chromatography A, 764 (1997) 3-20.

[24] M.B. Tennikov, N.V. Gazdina, T.B. Tennikova, F. Svec, "Effect of porous structure of macroporous polymer supports on resolution in high-performance membrane chromatography of proteins," Journal of Chromatography A, 798 (1998) 55-64.

[25] T.N. Warner, S. Nochumson, "Rethinking the economics of chromatography. New technologies and hidden costs," Biopharm International : The Applied Technologies of Biopharmaceutical Development, 16 (2003) 58-60.

[26] P. Jain, L. Sun, J.H. Dai, G.L. Baker, M.L. Bruening, "High-capacity purification of his-tagged proteins by affinity membranes containing functionalized polymer brushes," Biomacromolecules, 8 (2007) 3102-3107.

[27] J.H. Dai, Z.Y. Bao, L. Sun, S.U. Hong, G.L. Baker, M.L. Bruening, "High-capacity binding of proteins by poly(acrylic acid) brushes and their derivatives," Langmuir, 22 (2006) 4274-4281.

[28] J.E. Gautrot, W.T.S. Huck, M. Welch, M. Ramstedt, "Protein-resistant NTA-functionalized polymer brushes for selective and stable immobilization of histidine-tagged proteins," Applied Materials and Interfaces, 2 (2010) 193-202.

[29] W. Muller, "New ion-exchangers for the chromatography of biopolymers," Journal of Chromatography A, 510 (1990) 133-140.

[30] N. Singh, J. Wang, M. Ulbricht, S.R. Wickramasinghe, S.M. Husson, "Surface-initiated atom transfer radical polymerization: A new method for preparation of polymeric membrane adsorbers," Journal of Membrane Science, 309 (2008) 64-72.

[31] L. Sun, J.H. Dai, G.L. Baker, M.L. Bruening, "High-capacity, protein-binding membranes based on polymer brushes grown in porous substrates," Chemistry of Materials, 18 (2006) 4033-4039.

[32] M. Ulbricht, H. Yang, "Porous polypropylene membranes with different carboxyl polymer brush layers for reversible protein binding via surface-initiated graft copolymerization," Chemistry of Materials, 17 (2005) 2622-2631.

[33] A.H.M. Yusof, M. Ulbricht, "Structure variations of the grafted functional polymer brush enhance membrane adsorber performance," Desalination, 236 (2009) 16-22.

[34] S. Cowan, S. Ritchie, "Modified polyethersulfone (PES) ultrafiltration membranes for enhanced filtration of whey proteins," Separation Science and Technology, 42 (2007) 2405-2418.

[35] N. Singh, S.M. Husson, B. Zdyrko, I. Luzinov, "Surface modification of microporous PVDF membranes by ATRP," Journal of Membrane Science, 262 (2005) 81-90.

[36] Y.J. Choi, T. Yamaguchi, S. Nakao, "A novel separation system using porous thermosensitive membranes," Industrial & Engineering Chemistry Research, 39 (2000) 2491-2495.

[37] J. Hautojarvi, K. Kontturi, J.H. Nasman, B.L. Svarfvar, P. Viinikka, M. Vuoristo, "Characterization of graft-modified porous polymer membranes," Industrial & Engineering Chemistry Research, 35 (1996) 450-457.

[38] A.M. Hollman, D. Bhattacharyya, "Controlled permeability and ion exclusion in microporous membranes functionalized with poly(L-glutamic acid)," Langmuir, 18 (2002) 5946-5952.

[39] S.M.C. Ritchie, "Polymer grafted membranes," in: D. Bhattacharyya, D.A. Butterfield (Eds.) New Insights into Membrane Science and Technology: Polymeric and Biofunctional Membranes, Elsevier, New York, 2003, pp. 299-327.

[40] T.N. Shah, J.C. Goodwin, S.M.C. Ritchie, "Development and characterization of a microfiltration membrane catalyst containing sulfonated polystyrene grafts," Journal of Membrane Science, 251 (2005) 81-89.

[41] T.N. Shah, S.M.C. Ritchie, "Esterification catalysis using functionalized membranes," Applied Catalysis A: General, 296 (2005) 12-20.

[42] T. Yamaguchi, S. Nakao, S. Kimura, "Plasma-graft filling polymerization: Preparation of a new type of pervaporation membrane for organic liquid mixtures," Macromolecules, 24 (1991) 5522-5527.

[43] M. Yanagioka, H. Kurita, T. Yamaguchi, S. Nakao, "Development of a molecular recognition separation membrane using cyclodextrin complexation controlled by thermosensitive polymer chains," Industrial & Engineering Chemistry Research, 42 (2003) 380-385.

[44] D. He, M. Ulbricht, "Preparation and characterization of porous anion-exchange membrane adsorbers with high protein-binding capacity," Journal of Membrane Science, 315 (2008) 155-163.

[45] K. Hagiwara, S. Yonedu, K. Saito, T. Shiraishi, T. Sugo, T. Tojyo, E. Katayama, "High-performance purification of gelsolin from plasma using anion-exchange porous hollow-fiber membrane," Journal of Chromatography B-Analytical Technologies in the Biomedical and Life Sciences, 821 (2005) 153-158.

[46] A.R. Newcombe, C. Cresswell, S. Davies, K. Watson, G. Harris, K. O'Donovan, R. Francis, "Optimised affinity purification of polyclonal antibodies from hyper immunised ovine serum using a synthetic protein A adsorbent, MAbsorbento (R) A2P," Journal of Chromatography B-Analytical Technologies in the Biomedical and Life Sciences, 814 (2005) 209-215.

[47] K. Sproule, P. Morrill, J.C. Pearson, S.J. Burton, K.R. Hejnaes, H. Valore, S. Ludvigsen, C.R. Lowe, "New strategy for the design of ligands for the purification of pharmaceutical proteins by affinity chromatography," Journal of Chromatography B-Analytical Technologies in the Biomedical and Life Sciences, 740 (2000) 17-33.

[48] A. Verdoliva, G. Cassani, G. Fassina, "Affinity purification of polyclonal antibodies using immobilized multimeric peptides," Journal of Chromatography B Biomedical Applications, 664 (1995) 175-183.

[49] L.R. Castilho, F.B. Anspach, W.D. Deckwer, "Comparison of affinity membranes for the purification of immunoglobulins," Journal of Membrane Science, 207 (2002) 253-264.

[50] S. Hober, K. Nord, M. Linhult, "Protein A chromatography for antibody purification," Journal of Chromatography B-Analytical Technologies in the Biomedical and Life Sciences, 848 (2007) 40-47.

[51] L. Yang, M.E. Biswas, P. Chen, "Study of binding between protein A and immunoglobulin G using a surface tension probe," Biophysical Journal, 84 (2003) 509-522.

[52] E.N. Lightfoot, J.L. Coffman, F. Lode, Q.S. Yuan, T.W. Perkins, T.W. Root, "Refining the description of protein chromatography," Journal of Chromatography A, 760 (1997) 139-149.

[53] H. Hamada, T. Tsuruo, "Determination of membrane-antigens by a covalent cross-linking method with monoclonal-antibodies," Analytical Biochemistry, 160 (1987) 483-488.

[54] T.R. Chaudhuri, K.R. Zinn, J.S. Morris, G.A. McDonald, A.S. Llorens, T.K. Chaudhuri, "Human monoclonal-antibody developed against ovarian-cancer cell-surface antigen," Cancer, 73 (1994) 1098-1104.

[55] D.R.J. Kuypers, Y.F.C. Vanrenterghem, "Monoclonal antibodies in renal transplantation: Old and new," Nephrology Dialysis Transplantation, 19 (2004) 297-300.

[56] D. Josic, Y.P. Lim, "Analytical and preparative methods for purification of antibodies," Food Technology and Biotechnology, 39 (2001) 215-226.

[57] T.M. Przybycien, N.S. Pujar, L.M. Steele, "Alternative bioseparation operations: Life beyond packed-bed chromatography," Current Opinion in Biotechnology, 15 (2004) 469-478.

[58] M.R. Schure, R.S. Maier, D.M. Kroll, H.T. Davis, "Simulation of packed-bed chromatography utilizing high-resolution flow fields: Comparison with models," Analytical Chemistry, 74 (2002) 6006-6016.

[59] R. van Reis, A. Zydney, "Membrane separations in biotechnology," Current Opinion in Biotechnology, 12 (2001) 208-211.

[60] W.H. Scouten, "Affinity chromatography: Bioselective adsorption on inert matrices," Wiley, New York, 1981.

[61] G. Fassina, M. Ruvo, G. Palombo, A. Verdoliva, M. Marino, "Novel ligands for the affinity-chromatographic purification of antibodies," Journal of Biochemical and Biophysical Methods, 49 (2001) 481-490.

[62] S. Kabir, "Immunoglobulin purification by affinity chromatography using protein A mimetic ligands prepared by combinatorial chemical synthesis," Immunological Investigations, 31 (2002) 263-278.

[63] S.F. Teng, K. Sproule, A. Husain, C.R. Lowe, "Affinity chromatography on immobilized "biomimetic" ligands synthesis, immobilization and chromatographic assessment of an immunoglobulin G-binding ligand," Journal of Chromatography B, 740 (2000) 1-15.

[64] B.V. Torres, D.F. Smith, "Purification of forssman and human blood group A glycolipids by affinity chromatography on immobilized helix pomatia lectin," Analytical Biochemistry, 170 (1988) 209-219.

[65] A.F. Aubry, "Applications of affinity chromatography to the study of drug-melanin binding interactions," Journal of Chromatography B-Analytical Technologies in the Biomedical and Life Sciences, 768 (2002) 67-74.

[66] G. Fassina, A. Verdoliva, G. Palombo, M. Ruvo, G. Cassani, "Immunoglobulin specificity of TG19318: A novel synthetic ligand for antibody affinity purification," Journal of Molecular Recognition, 11 (1998) 128-133.

[67] R.A. Houghten, C. Pinilla, S.E. Blondelle, J.R. Appel, C.T. Dooley, J.H. Cuervo, "Generation and use of synthetic peptide combinatorial libraries for basic research and drug discovery," Nature, 354 (1991) 84-86.

[68] K.S. Lam, S.E. Salmon, E.M. Hersh, V.J. Hruby, W.M. Kazmeierski, R.J. Knapp, "A new type of synthetic peptide library for identifying ligand-binding activity," Nature, 360 (1992) 768-768.

[69] E. Evensen, D. Joseph-McCarthy, G.A. Weiss, S.L. Schreiber, M. Karplus, "Ligand design by a combinatorial approach based on modeling and experiment: application to HLA-DR4," Journal of Computer-Aided Molecular Design, 21 (2007) 395-418.

[70] P. Fuglistaller, "Comparison of immunoglobulin binding capacities and ligand leakage using 8 different protein A affinity chromatography matrices," Journal of Immunological Methods, 124 (1989) 171-177.

[71] P.F. Zatta, "A new bioluminescent assay for studies of protein G and protein A binding to IgG and IgM," Journal of Biochemical and Biophysical Methods, 32 (1996) 7-13.

[72] M.A. Scott, J.M. Davis, K.A. Schwartz, "Staphylococcal protein A binding to canine IgG and IgM," Veterinary Immunology and Immunopathology, 59 (1997) 205-212.

[73] J.R. Nevens, A.K. Mallia, M.W. Wendt, P.K. Smith, "Affinity chromatographic purification of immunoglobulin M antibodies utilizing immobilized mannan binding protein," Faseb Journal, 6 (1992) A1451-A1451.

[74] H. Khayambashi, R.M. Blanken, C.L. Schwartz, "Chromatographic separation and purification of secretory IgA from human milk," Preparative Biochemistry, 7 (1977) 225-241.

[75] R.H. Waldman, J.P. Mach, M.M. Stella, D.S. Rowe, "Secretory IgA in human serum," Journal of Immunology, 105 (1970) 43-47.

[76] G.W. Litman, R.A. Good, "Rapid purification of IgA from normal human serum," Biochimica et Biophysica Acta (BBA) - Protein Structure, 263 (1972) 89-93.

[77] S.B. Lehrer, "Isolation of IgE from normal mouse serum," Immunology, 36 (1979) 103-109.

[78] H. Vonschenck, R.H. Unger, "Ligand leakage from immunoaffinity column," Scandinavian Journal of Clinical & Laboratory Investigation, 43 (1983) 527-531.

[79] S. Ikeyama, S. Nakagawa, M. Arakawa, H. Sugino, A. Kakinuma, "Purification and characterization of IgE produced by human myeloma cell line, U266," Molecular Immunology, 23 (1986) 159-167.

[80] Z.K. Peng, A.B. Becker, F.E.R. Simons, "Binding properties of protein A and protein G for Human IgE," International Archives of Allergy and Immunology, 104 (1994) 204-206.

[81] G. Kronvall, U.S. Seal, S. Svensson, R.C. Williams, "Phylogenetic aspects of staphylococcal protein A-reactive serum globulins in birds and mammals," Acta Pathologica Et Microbiologica Scandinavica Section B-Microbiology, 82B (1974) 12-18.

[82] A.I. Taylor, R.L. Beavil, B.J. Sutton, R.A. Calvert, "A monomeric chicken IgY receptor binds IgY with 2:1 stoichiometry," Journal of Biological Chemistry, 284 (2009) 24168-24175.

[83] L.N. Lund, P.E. Gustavsson, R. Michael, J. Lindgren, L. Norskov-Lauritsen, M. Lund, G. Houen, A. Staby, P.M. St Hilaire, "Novel peptide ligand with high binding capacity for antibody purification," Journal of Chromatography A, 1225 (2012) 158-167.

[84] C.R. Lowe, S.J. Burton, N.P. Burton, W.K. Alderton, J.M. Pitts, J.A. Thomas, "Designer dyes: Biomimetic ligands for the purification of pharmaceutical proteins by affinity chromatography," Trends in Biotechnology, 10 (1992) 442-448.

[85] C.R. Lowe, A.R. Lowe, G. Gupta, "New developments in affinity chromatography with potential application in the production of biopharmaceuticals," Journal of Biochemical and Biophysical Methods, 49 (2001) 561-574.

[86] C.R. Lowe, S.J. Burton, N. Burton, D.J. Stewart, D.R. Purvis, I. Pitfield, S. Eapen, "New developments in affinity chromatography," Journal of Molecular Recognition, 3 (1990) 117-122.

[87] R.X. Li, V. Dowd, D.J. Stewart, S.J. Burton, C.R. Lowe, "Design, synthesis, and application of a protein A mimetic," Nature Biotechnology, 16 (1998) 190-195.

[88] C.A. Orengo, A.D. Michie, S. Jones, D.T. Jones, M.B. Swindells, J.M. Thornton, "CATH - a hierarchic classification of protein domain structures," Structure, 5 (1997) 1093-1108.

[89] S.F. Teng, K. Sproule, A. Hussain, C.R. Lowe, "A strategy for the generation of biomimetic ligands for affinity chromatography. Combinatorial synthesis and biological evaluation of an IgG binding ligand," Journal of Molecular Recognition, 12 (1999) 67-75.

[90] G. Fassina, A. Verdoliva, M.R. Odierna, M. Ruvo, G. Cassini, "Protein A mimetic peptide ligand for affinity purification of antibodies," Journal of Molecular Recognition, 9 (1996) 564-569.

[91] G. Palombo, M. Rossi, G. Cassani, G. Fassina, "Affinity purification of mouse monoclonal IgE using a protein A mimetic ligand (TG19318) immobilized on solid supports," Journal of Molecular Recognition, 11 (1998) 247-249.

[92] G. Palombo, A. Verdoliva, G. Fassina, "Affinity purification of immunoglobulin M using a novel synthetic ligand," Journal of Chromatography B, 715 (1998) 137-145.

[93] J. Deisenhofer, "Crystallographic refinement and atomic models of a human Fc fragment and its complex with fragment B of protein A from Staphylococcus aureus at 2.9-A and 2.8-A resolution," Biochemistry, 20 (1981) 2361-2370.

[94] Z. Buday, J.C. Linden, M.N. Karim, "Improved acetone-butanol fermentation analysis using subambient HPLC column temperature," Enzyme and Microbial Technology, 12 (1990) 24-27.

[95] D.K. Schisla, P.W. Carr, E.L. Cussler, "Hollow fiber array affinity chromatography," Biotechnology Progress, 11 (1995) 651-658.

[96] R. Ghosh, L. Wang, "Purification of humanized monoclonal antibody by hydrophobic interaction membrane chromatography," Journal of Chromatography A, 1107 (2006) 104-109.

[97] H.L. Knudsen, R.L. Fahrner, Y. Xu, L.A. Norling, G.S. Blank, "Membrane ion-exchange chromatography for process-scale antibody purification," Journal of Chromatography A, 907 (2001) 145-154.

[98] D. Lutkemeyer, M. Bretschneider, H. Buntemeyer, J. Lehmann, "Membrane chromatography for rapid purification of recombinant antithrombin III and monoclonal antibodies from cell culture supernatant," Journal of Chromatography, 639 (1993) 57-66.

[99] K.G. Briefs, M.R. Kula, "Fast protein chromatography on analytical and preparative scale using modified microporous membranes," Chemical Engineering Science, 47 (1992) 141-149.

[100] B. Champluvier, M.R. Kula, "Microfiltration membranes as pseudo-affinity adsorbents: Modification and comparison with gel beads," Journal of Chromatography, 539 (1991) 315-325.

[101] B. Champluvier, M.R. Kula, "Dye-ligand membranes as selective adsorbents for rapid purification of enzymes: A case-study," Biotechnology and Bioengineering, 40 (1992) 33-40.

[102] S. Kiyohara, M. Kim, Y. Toida, K. Saito, K. Sugita, T. Sugo, "Selection of a precursor monomer for the introduction of affinity ligands onto a porous membrane by radiation-induced graft polymerization," Journal of Chromatography A, 758 (1997) 209-215.

[103] S.M.C. Ritchie, D. Bhattacharyya, "Polymeric ligand-based functionalized materials and membranes for ion exchange," in: A.K. SenGupta (Ed.) Ion Exchange and Solvent Extraction, Marcel Dekker, Inc., New York, 2001, pp. 81-118.

[104] W.C. Mcgregor, D.P. Szesko, R.M. Mandaro, V.R. Rai, "Practicum: High performance isolation of a recombinant protein on composite ion exchange media," Bio/Technology, 4 (1986) 526-527.

[105] C. Boi, "Membrane adsorbers as purification tools for monoclonal antibody purification," Journal of Chromatography B-Analytical Technologies in the Biomedical and Life Sciences, 848 (2007) 19-27.

[106] C. Charcosset, Z.G. Su, S. Karoor, G. Daun, C.K. Colton, "Protein A immunoaffinity hollow fiber membranes for immunoglobulin G purification: Experimental characterization," Biotechnology and Bioengineering, 48 (1995) 415-427.

[107] S. Krause, K.H. Kroner, W.D. Deckwer, "Comparison of affinity membranes and conventional affinity matrices with regard to protein purification," Biotechnology Techniques, 5 (1991) 199-204.

[108] J. Luksa, V. Menart, S. Milicic, B. Kus, V. Gabercporekar, D. Josic, "Purification of human tumor necrosis factor by membrane chromatography," Journal of Chromatography A, 661 (1994) 161-168.

[109] T.B. Tennikova, M. Bleha, F. Svec, T.V. Almazova, B.G. Belenkii, "High-performance membrane chromatography of proteins, a novel method of protein separation," Journal of Chromatography, 555 (1991) 97-107.

[110] H.W. Yang, C. Viera, J. Fischer, M.R. Etzel, "Purification of a large protein using ion-exchange membranes," Industrial & Engineering Chemistry Research, 41 (2002) 1597-1602.

[111] M. Kim, K. Saito, S. Furusaki, T. Sato, T. Sugo, I. Ishigaki, "Adsorption and elution of bovine gamma-globulin using an affinity membrane containing hydrophobic amino acids as ligands," Journal of Chromatography, 585 (1991) 45-51.

[112] S. Kiyohara, M. Sasaki, K. Saito, K. Sugita, T. Sugo, "Amino acid addition to epoxy-group-containing polymer chain grafted onto a porous membrane," Journal of Membrane Science, 109 (1996) 87-92.

[113] A. Malakian, M. Golebiowska, J. Bellefeuille, "Purification of monoclonal and polyclonal IgG with affinity membrane matrix coupled with protein A and protein G," American Laboratory, 25 (1993) 40P-40V.

[114] S.M.A. Bueno, K. Haupt, M.A. Vijayalakshmi, "In vitro removal of human IgG by pseudobiospecific affinity membrane filtration on a large scale. A Preliminary report," International Journal of Artificial Organs, 18 (1995) 392-398.

[115] R. Woker, B. Champluvier, M.R. Kula, "Purification of s-oxynitrilase from sorghum bicolor by immobilized metal ion affinity chromatography on different carrier materials," Journal of Chromatography-Biomedical Applications, 584 (1992) 85-92.

[116] S.-Y. Suen, M.R. Etzel, "A mathematical analysis of affinity membrane bioseparations," Chemical Engineering Science, 47 (1992) 1355-1364.

[117] A. Halperin, M. Tirrell, T.P. Lodge, "Tethered chains in polymer microstructures," Advances in Polymer Science, 100 (1992) 31-71.

[118] S.T. Milner, "Polymer brushes," Science, 251 (1991) 905-914.

[119] I. Szleifer, M.A. Carignano, "Tethered polymer layers," Advances in Chemical Physics, 94 (1996) 165-260.

[120] K.G. Soga, M.J. Zuckermann, H. Guo, "Binary polymer brush in a solvent," Macromolecules, 29 (1996) 1998-2005.

[121] P. Mansky, Y. Liu, E. Huang, T.P. Russell, C.J. Hawker, "Controlling polymer-surface interactions with random copolymer brushes," Science, 275 (1997) 1458-1460.

[122] B. Zhao, W.J. Brittain, "Synthesis of tethered polystyrene-block-poly(methyl methacrylate) monolayer on a silicate substrate by sequential carbocationic polymerization and atom transfer radical polymerization," Journal of the American Chemical Society, 121 (1999) 3557-3558.

[123] B. Zhao, W.J. Brittain, "Polymer brushes: surface-immobilized macromolecules," Progress in Polymer Science, 25 (2000) 677-710.

[124] R. Faust, J.P. Kennedy, "Living carbocationic polymerization of styrene," Polymer Bulletin, 19 (1988) 21-28.

[125] M. Hayashi, S. Nakahama, A. Hirao, "Synthesis of end-functionalized polymers by means of living anionic polymerization. Reactions of living anionic polymers with halopropylstyrene derivatives," Macromolecules, 32 (1999) 1325-1331.

[126] A. Hirao, H. Nagahama, T. Ishizone, S. Nakahama, "Synthesis of polymers with carboxy end groups by reaction of polystyryl anions with 4-bromo-1,1,1-trimethoxybutane," Macromolecules, 26 (1993) 2145-2150.

[127] R.P. Quirk, L.F. Zhu, "Anionic synthesis of chain-end functionalized polymers using 1,1-diphenylethylene derivatives. Preparation of 4-hydroxyphenyl terminated polystyrenes," Makromolekulare Chemie-Macromolecular Chemistry and Physics, 190 (1989) 487-493.

[128] S.M.C. Ritchie, L.G. Bachas, T. Olin, S.K. Sikdar, D. Bhattacharyya, "Surface modification of silica- and cellulose-based microfiltration membranes with functional polyamino acids for heavy metal sorption," Langmuir, 15 (1999) 6346-6357.

[129] S.M.C. Ritchie, K.E. Kissick, L.G. Bachas, S.K. Sikdar, C. Parikh, D. Bhattacharyya, "Polycysteine and other polyamino acid functionalized microfiltration membranes for heavy metal capture," Environmental Science & Technology, 35 (2001) 3252-3258.

[130] Y. Ishihama, M. Sawamoto, T. Higashimura, "Living cationic polymerization of styrene by the methanesulfonic acid/tin tetrachloride initiating system in the presence of tetra-n-butylammonium chloride," Polymer Bulletin, 23 (1990) 361-366.

[131] S.V. Kostjuk, F.N. Kapytsky, V.P. Mardykin, L.M.V. Gaponik, L.M. Antipin, "Living cationic polymerization of styrene with 1-phenylethyl chloride/TiCl4/BU2O," Polymer Bulletin, 49 (2002) 251-256.

[132] J.F. Blanco, Q.T. Nguyen, P. Schaetzel, "Novel hydrophilic membrane materials: sulfonated polyethersulfone Cardo," Journal of Membrane Science, 186 (2001) 267-279.

[133] M.D. Guiver, S. Croteau, J.D. Hazlett, O. Kutowy, "Synthesis and characterization of carboxylated polysulfones," British Polymer Journal, 23 (1990) 29-39.

[134] H.R. Allcock, R.J. Fitzpatrick, L. Salvati, "Sulfonation of (aryloxy)phosphazenes and (arylamino)phosphazenes - Small-molecule compounds, polymers and surfaces," Chemistry of Materials, 3 (1991) 1120-1132.

[135] A.M. Hollman, N.T. Scherrer, A. Cammers-Goodwin, D. Bhattacharyya, "Separation of dilute electrolytes in poly(amino acid) functionalized microporous membranes: Model evaluation and experimental results," Journal of Membrane Science, 239 (2004) 65-79.

[136] M. Kamigaito, J. Nakashima, K. Satoh, M. Sawamoto, "Controlled cationic polymerization of p-(chloromethyl)styrene: BF3-catalyzed selective activation of a C-O terminal from alcohol," Macromolecules, 36 (2003) 3540-3544.

[137] Q.Y. Li, Y.X. Wu, W.Y. Ma, R.W. Xu, G.Y. Wu, W.T. Yang, "Synthesis of graft copolymers with polyisobutylene branch chains," Chinese Journal of Polymer Science, 28 (2010) 449-456.

[138] Y.T. Goh, R. Patel, S.J. Im, J.H. Kim, B.R. Min, "Synthesis and characterization of poly(ether sulfone) grafted poly(styrene sulfonic acid) for proton conducting membranes," Korean Journal of Chemical Engineering, 26 (2009) 518-522.

[139] J. Shin, G. Fei, S.A. Kang, B.S. Ko, P.H. Kang, Y.C. Nho, "Simultaneous radiation grafting of vinylbenzyl chloride onto poly(tetrafluoroethylene-co-hexafluoropropylene) films," Journal of Applied Polymer Science, 113 (2009) 2858-2862.

[140] C. Klaysom, B.P. Ladewig, G.Q.M. Lu, L.Z. Wang, "Preparation and characterization of sulfonated polyethersulfone for cation-exchange membranes," Journal of Membrane Science, 368 (2011) 48-53.

[141] D.P. Lu, H. Zou, R. Guan, H. Dai, L. Lu, "Sulfonation of polyethersulfone by chlorosulfonic acid," Polymer Bulletin, 54 (2005) 21-28.

[142] A. Ozcan, A.S. Ozcan, "Adsorption of acid red 57 from aqueous solutions onto surfactant-modified sepiolite," Journal of Hazardous Materials, 125 (2005) 252-259.

[143] F. Zermane, O. Bouras, M. Baudu, J.P. Basly, "Cooperative coadsorption of 4-nitrophenol and basic yellow 28 dye onto an iron organo-inorgano pillared montmorillonite clay," Journal of Colloid and Interface Science, 350 (2010) 315-319.

[144] M.L. Xiang, M. Jiang, L.X. Feng, "A novel synthesis of linear high-molecular-weight poly(4-vinylphenol) and poly[styrene-co-(4-vinylphenol)]," Macromolecular Rapid Communications, 16 (1995) 477-481.

[145] K. Satoh, M. Kamigaito, M. Sawamoto, "Direct synthesis of amphiphilic random and block copolymers of p-hydroxystyrene and p-methoxystyrene via living cationic polymerization with BF3OEt2/ROH systems," Macromolecules, 33 (2000) 5830-5835.

[146] K. Saha, F. Bender, E. Gizeli, "Comparative study of IgG binding to proteins G and A: Nonequilibrium kinetic and binding constant determination with the acoustic waveguide device," Analytical Chemistry, 75 (2003) 835-842.

[147] N. Anuraj, S. Bhattacharjee, J.H. Geiger, G.L. Baker, M.L. Bruening, "An all-aqueous route to polymer brush-modified membranes with remarkable permeabilites and protein capture rates," Journal of Membrane Science, 389 (2012) 117-125.

[148] F.B. Anspach, D. Curbelo, R. Hartmann, G. Garke, W.D. Deckwer, "Expanded-bed chromatography in primary protein purification," Journal of Chromatography A, 865 (1999) 129-144.

[149] T. Jossang, J. Feder, E. Rosenqvist, "Photon correlation spectroscopy of human IgG," Journal of Protein Chemistry, 7 (1988) 165-171.

[150] A. Danielsson, A. Ljunglof, H. Lindblom, "One-step purification of monoclonal IgG antibodies from mouse ascites. An evaluation of different adsorption techniques using high performance liquid chromatography," Journal of Immunological Methods, 115 (1988) 79-88.